2018

# Harnessing Interfacial Phenomena Involving Macromolecules For Emulsion Processing

Gang Duan
*University of Pennsylvania*, 1084175748@qq.com

# Harnessing Interfacial Phenomena Involving Macromolecules For Emulsion Processing

**Abstract**
An emulsion is a mixture of two immiscible solutions, one dispersed in the other. Intrinsically, most emulsions are thermodynamically unstable and thus active agents called surfactant are added to the mixture to stabilize the interface. The surfactant lowers the interfacial tension and provides steric and/or electrostatic repulsion at the fluid interfaces to enhance the stability of emulsions. Macromolecules, either intrinsically surface active or not, have attracted lots of attention for emulsion processing. On one hand, advances in polymeric synthesis technique present various polymeric surfactants waiting to be exploited. On the other hand, macromolecules present the platform for versatile modification that can result in assemblies with special properties. Various natural materials are also macromolecules, waiting to be exploited as replacements for synthetic surfactants of petrochemical origins. In this thesis, ion pairing and microfluidic techniques are used to expand the macromolecules' application and to investigate the composition effect of polymeric surfactants in emulsion processing. Polyelectrolyte is extracted into an organic phase via ion pairing with an oppositely charged surfactant. The formed ion pair retain the polyelectrolyte's capability to form complexes. It complexes with oppositely charged polyelectrolyte and is exploited for one-step polyelectrolyte microcapsules generation. Meanwhile, the composition effect of a set of polymeric surfactants, Pluronics, on flow-induced phase inversion emulsification (FIPIE) is studied. Through microfluidic technology, emulsion phase inversion process at the single droplet level is monitored. We find strong correlation between the molecular weight (MW) and the lengths of individual blocks of the Pluronics and the tendency of droplets to undergo (FIPIE). In Chapter 4, dynamic ion pairing between polyelectrolyte and surfactant is used to induce phase inversion emulsification (PIE). The ion pair formation is controlled as a function of the solution pH and surfactant concentration. Both oil-in-water (O/W) and water-in-oil (W/O) emulsions are formed and PIE from W/O to O/W emulsion is demonstrated. In summary, macromolecules possess rich behaviors at the emulsion interfaces. The macromolecule and surfactant association, such as ion pairing, form assemblies with distinct properties, expanding common materials' application for versatile emulsion processing.

**Degree Type**
Dissertation

**Degree Name**
Doctor of Philosophy (PhD)

**Graduate Group**
Chemical and Biomolecular Engineering

**First Advisor**
Daeyeon Lee

**Keywords**
Emulsion, Macromolecule

# HARNESSING INTERFACIAL PHENOMENA INVOLVING MACROMOLECULES FOR EMULSION PROCESSING

Gang Duan

A DISSERTATION

in

Chemical and Biomolecular Engineering

Presented to the Faculties of the University of Pennsylvania

in

Partial Fulfillment of the Requirements for the

Degree of Doctor of Philosophy

2018

Supervisor of Dissertation

_____

Daeyeon Lee, Professor, Chemical and Biomolecular Engineering

Graduate Group Chairperson

_____

John C. Crocker, Professor, Chemical and Biomolecular Engineering

Dissertation Committee

Chinedum Osuji, Professor, Chemical and Biomolecular Engineering

Robert A. Riggleman, Associate Professor, Chemical and Biomolecular Engineering

Kathleen J. Stebe, Professor, Chemical and Biomolecular Engineering

**HARNESSING INTERFACIAL PHENOMENA INVOLVING MACROMOLECULES FOR EMULSION PROCESSING**

To my family

# Acknowledgements

First of all, I want to thank my advisor, Professor Daeyeon Lee. It is under his guidance, I set myself in the path to develop my critical thinking and become an independent researcher. His optimism and industrious personality inspire me to always challenge myself and become better for not only myself, but also for the people around me.

I would like to thank my thesis committee members, Professor Chinedum Osuji, Professor Robert A. Riggleman, and Professor Kathleen J. Stebe. I also really enjoyed the Advanced Molecular Thermodynamics course taught by Professor Riggleman, and the Interfacial Phenomena course taught by Professor Stebe. I also want to express my gratitude to Dr. Shigeng Li and Dr. Chieh-Min Cheng from Xerox. Thank them for the monthly discussions we have on research, and for the hospitality they showed me during my visit at Xerox.

My PhD life would not be the same without the members in the Lee lab. I really appreciate the encouragements, teachings, discussions, and friendships shared with the Lee group members, especially Woo-Sik Jang. Yang Lan, Xu Zhang, Danny Strickland, Rajarshi Chattaraj, Tim Murdoch, Yun Kee Jo, David Ring, Zhiwei Liao, Neha Manohar, Giuseppe Di Vitantonio, Syung Hun Han, Renjing Huang, Katie Rose, Wilfredo Mendez Ortiz, Jingyu Wu, Bharath Venkatesh, Yiwei Qiang, Tiancheng Wang, Je Choi, Shizhao Lu, Haoyang Li, Yankai Jia, Zhuo Chen, Yupan Wu, Yuanchi Ma, Jyo Lyn Hor, Katherine W. Pulsipher, Jiayi Deng, Laura Bradley, Sarah Hann, Tagbo H. R. Niepa,

Harim Jeon, Heon-Ho Jeong, Martin Haase, Ankit Kumar, Sanghak Cha, Miju Kim, Likai Hou, Tae Soup Shim, Yeongseon Jang, Jacob Prosser, Fuquan Tu, Rohini Gupta, Dongkyu Roh, Seongchol Park, Abhishek Ravva, Teresa Brugarolas, Francesco Elio Angile, and Yun-Ru Huang.

I want to thank my parents, for always supporting me and being understanding. They taught me the value of giving, and the meaning of family. I also want to thank Ms. Zhuangyuan Fan, for always accompanying me, and keeping me fed.

In the end, I would like to thank the funding from National Science Foundation GOALI program that made my project possible.

# ABSTRACT


**HARNESSING INTERFACIAL PHENOMENA INVOLVING MACROMOLECULES FOR EMULSION PROCESSING**

Gang Duan

Daeyeon Lee

An emulsion is a mixture of two immiscible solutions, one dispersed in the other. Intrinsically, most emulsions are thermodynamically unstable and thus active agents called surfactant are added to the mixture to stabilize the interface. The surfactant lowers the interfacial tension and provides steric and/or electrostatic repulsion at the fluid interfaces to enhance the stability of emulsions. Macromolecules, either intrinsically surface active or not, have attracted lots of attention for emulsion processing. On one hand, advances in polymeric synthesis technique present various polymeric surfactants waiting to be exploited. On the other hand, macromolecules present the platform for versatile modification that can result in assemblies with special properties. Various natural materials are also macromolecules, waiting to be exploited as replacements for synthetic surfactants of petrochemical origins. In this thesis, ion pairing and microfluidic techniques are used to expand the macromolecules' application and to investigate the composition effect of polymeric surfactants in emulsion processing. Polyelectrolyte is extracted into an organic phase via ion pairing with an oppositely charged surfactant. The formed ion pair retain the polyelectrolyte's capability to form complexes. It complexes

with oppositely charged polyelectrolyte and is exploited for one-step polyelectrolyte microcapsules generation. Meanwhile, the composition effect of a set of polymeric surfactants, Pluronics, on flow-induced phase inversion emulsification (FIPIE) is studied. Through microfluidic technology, emulsion phase inversion process at the single droplet level is monitored. We find strong correlation between the molecular weight (MW) and the lengths of individual blocks of the Pluronics and the tendency of droplets to undergo (FIPIE). In Chapter 4, dynamic ion pairing between polyelectrolyte and surfactant is used to induce phase inversion emulsification (PIE). The ion pair formation is controlled as a function of the solution pH and surfactant concentration. Both oil-in-water (O/W) and water-in-oil (W/O) emulsions are formed and PIE from W/O to O/W emulsion is demonstrated. In summary, macromolecules possess rich behaviors at the emulsion interfaces. The macromolecule and surfactant association, such as ion pairing, form assemblies with distinct properties, expanding common materials' application for versatile emulsion processing.

# Table of Contents

# List of Tables

# List of Figures

# Chapter 1. Introduction

## 1.1 Background and Motivation

### 1.1.1 Emulsion

Emulsion are mixtures of two immiscible liquids, one dispersed in the other, typically in the form of droplets. It is ubiquitous in our daily lives, from various chemical processes to oil fields, and to our own kitchens.[1-2] Many of our food ingredients are made of emulsions; for example, the cream we add to coffee, the mayonnaise to salad, and the butter on bread. The cream is an oil-in-water (O/W) emulsion, whereas the butter is a water-in-oil (W/O) emulsion. The list of the applications and products that rely on and contain emulsions is continuously growing.

During the production of emulsions, surface active agents are added to stabilize the oil-water interface. The stability of the emulsion can be determined based on the total free energy the system.[3]

$$\Delta G_{formation} = \Delta G_I - T\Delta S_{config} \qquad (1\text{-}1)$$

where $\Delta G_{formation}$ is the total free energy change upon emulsion formation, $\Delta G_I$ is the interfacial free energy term, and ( $-T\Delta S_{config}$) is the configuration entropy term of the dispersed droplets.

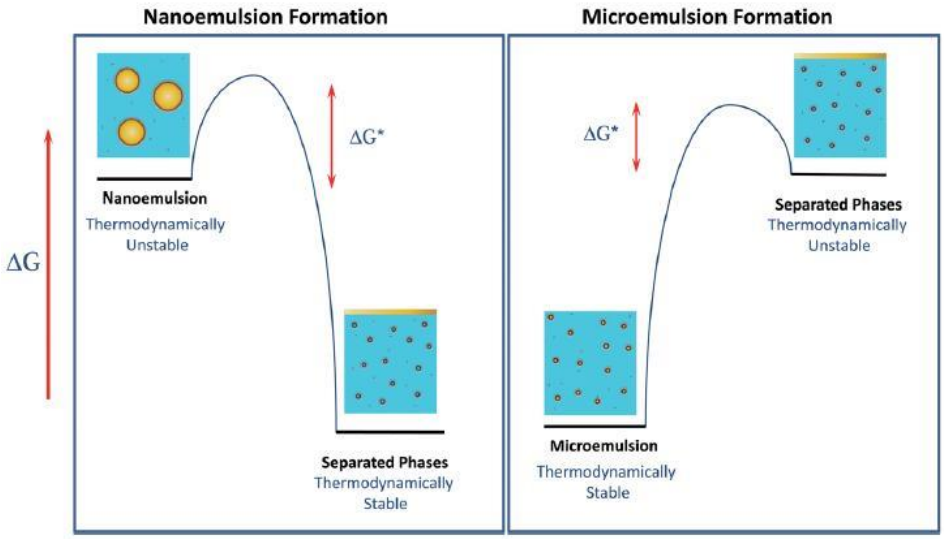


**Figure 1.1** Schematics of the free energy of microemulsion and nanoemulsion systems compare to the phase separated state. Reprinted with permission from reference 3.

Depending on the size and thermodynamic stability of the dispersed droplets, emulsions can be classified into three major types: microemulsions, nanoemulsions, and macroemulsions.[3-4] Microemulsions are emulsions with dispersed droplet size varying from 1 nm to 100 nm. It is isotropic and thermodynamically stable. This is usually results from the specific geometry and packing of the added surface active agents at the interface.[5-6] Nanoemulsions have dispersed phase of similar size as that of the microemulsions, yet they are not thermodynamically stable. Macroemulsions, in contrast, have droplet size larger than 100 nm and are also thermodynamically unstable. Their origin can be traced back to the second century with the emulsification of beeswax.[7] Most, if not all, of the practical applications of emulsions are based on macroemulsions. They can be easily observed under a microscope and are usually presented in the form of a turbid, milky liquid mixture.

For macroemulsions, the major emulsion destabilization mechanisms include creaming, flocculation, coagulation, and coalescence, which eventually lead to phase separation between the water and oil phases.[8-9] Multiple emulsions, which are systems with its dispersed phase containing another phase of droplets, have also been produced.[10]

Most macroemulsions in industry today are generated through mechanical shearing, which has been used to prepare products for both industrial and household use. Although mechanical shearing has proven to be a very effective way of preparing emulsions at large scales, there are several aspects of such a process that is non-ideal. One of them is its demand for a large energy input.[11]

Energy is required to generate new oil-water interface when dispersing one phase into the other.[12] This is a fundamental requirement for emulsion formation. Yet in the shearing process, a large amount of energy input is dissipated via viscous dissipation, which not only increases the cost of energy, but also may have negative impact in the quality of the products. For example, such energy dissipation can lead to temperature increase in the mixture, causing recoalescence of the droplets as well as degradation of active components. Recent studies have shown benefits of using smaller size droplets; for example, the absorption of drugs in gastrointestinal tract has reported to be correlated with the size of the emulsion droplets.[13] Consequently, with more emulsion-based products adopting smaller droplets, the power input as well as the cost to ensure safe operation of the related emulsification facilities likely are increasing as well.

The pressure jump at the droplet interface is governed by the Young-Laplace equation, which states:[14]

$$\Delta p = \frac{2\gamma}{r} \qquad (1\text{-}2)$$

for spherical droplets. To continuously break droplets into smaller sizes, the pressure gradient the emulsification system needs to provide can be expressed as: [14]

$$\frac{\Delta P}{\Delta x} \approx \frac{2\gamma}{r^2} \qquad (1\text{-}3)$$

It scales with the power of -2 with respect to the size of the droplets, indicating an increasing energy demand as the droplet size becomes smaller. In addition, the droplets created in this manner are also intrinsically heterogeneous, as the pressure gradient created by mechanical shearing is not homogenous throughout the mixture and the mixing vessel.

### 1.1.2 Surfactant

As discussed above, macroemulsions are thermodynamically unstable. Surface active agents (surfactants) are thus added to the emulsion to enhance its stability.[4] Adsorption of surfactant to the fluid interface lowers the interfacial energy between the different fluids, thus lowers the barrier for emulsion formation. The processing requirement to generate emulsion with smaller sizes is thus lowered upon the addition of surfactants. Moreover, surfactants at the oil-water interface of emulsion droplets prolong the lifetime of

emulsions; that is, the surfactants enhance the emulsion stability.[15-16] The stability of the emulsions is enhanced due to steric repulsion and/or electrostatic repulsion between the polar groups of the surfactants. It is important to remember, however, macro/nanoemulsions stay only kinetically stable even after they have been stabilized with surfactants. Meanwhile, the kinetics of the adsorption of surfactants is also important. Surfactants that can rapidly adsorb to the oil-water interface is more effective in the stabilization of emulsions, especially those with small droplets. These are normally the surfactants that have high diffusion coefficients and flexibly to change their conformation upon adsorption, facilitating their adsorption. [17]

To evaluate what type of macroemulsions a surfactant would prefer to form, two parameters can be used, its hydrophilic-lipophilic balance (HLB) number, and its packing parameter.[14] The HLB number represents the degree of a surfactant's hydrophilicity or hydrophobicity. While there are different ways to define HLB number for a given surfactant, the definition given by Evans et al. states that with HLB number ranging from 4 -8 typically stabilize W/O emulsions, whereas those with HLB number from 12-16 stabilize O/W emulsions. The packing parameter, on the other hand, provide the general information on the molecular structure of a surfactant. It is defined as the ratio between the surfactant's tail volume and the product of its effective head group's area and its tail length:

$$N = \frac{v}{la_o} \qquad (1\text{-}4)$$

Surfactants with N >1 would normally have higher solubility in oil. According to the Bancroft's rule, the phase in which an emulsifier is more soluble constitutes the continuous phase.[18] Consequently, the emulsions they stabilize would be W/O emulsions. With N< 1, the opposite is true, surfactant would preferably in the aqueous phase, and the emulsions they stabilized are likely to be O/W emulsions. The packing parameter is also used for estimating the curvature of the aggregates form by the surfactants.

### 1.1.3 Macromolecules at emulsion interface

The versatility and complexity of synthetic polymers have been expanded significantly since the introduction of controlled radical polymerization methods. Polymeric surfactants, a group of macromolecules synthesized for the modification of fluid interfaces, has shown to have drastically different behaviors compare to their small molecular counterparts, as their interactions with each other and with the interface differ in time, length, and magnitude scales.[19]

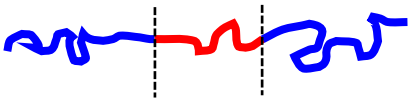

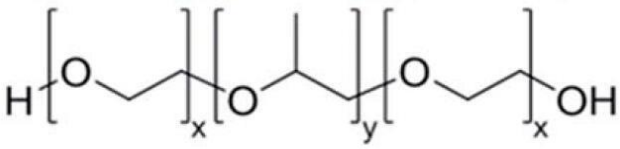

**Figure 1.2 (Top)** Schematic and (bottom) molecular structure of Pluronics triblock copolymer. Figure reproduced with from reference 21.

Due to polymeric surfactants' varying MW, composition, and structure, it usually takes time for their full potential to be discovered. One of the most well-known sets of polymeric surfactants is called Pluronic surfactants (Figure 1.2).[20] It is a set of ABA triblock copolymer composed of poly(ethylene oxide) (PEO) and hydrophobic poly(propylene oxide) (PPO) (A=PEO, B=PPO), and was first used as industrial detergents. Yet, its application quickly expanded into various areas including biomedical fields. Multiple Pluronics have been used to form drug carriers and to interfere with metabolism of cancer cells. Pluronics have now been widely accepted as emulsifying agents for pharmaceutical formulations and are listed in the U.S. pharmacopoeias.[21] Thus, with the advancement of polymerization techniques, analyzing and understanding the properties of synthetic polymeric surfactants have become extremely important, and will provide guidance for synthesis of new surfactants.

Macromolecules also present a platform for versatile modifications. By controlling the composition, structure, and ratio of the side chain/small molecules attached to a macromolecule, the resulting macromolecular entity can have rich emulsification behaviors, accompanied by responsiveness.[19, 22] Chitosan, for example, is a weak polyelectrolyte of weak surface activity. By associating aldehyde to its amine group via Schiff base reaction, the resulting chitosan complex has been reported to have enhanced surface activity and can stabilize O/W emulsions for an extended period of time.[23]

Another important reason to study the behavior of macromolecules at emulsion interface is the recent demand and interest in using non-petrochemical based materials. A significant number of such materials are macromolecules, such as proteins and polysaccharides.[1, 24] Being of natural origin, they are considered to be more compatible with the human body, and also to be environmentally friendly, and sustainable. Various industries are trying to meet the surging demand for the application of these biologically derived ingredients, especially in the food, cosmetics, and pharmaceutical sectors. The emulsifier market for food industry in U.S. is estimated to around $2.1 billion in 2012, and a large portion of the synthetic surfactants have been replaced.[25-26]

## 1.2 Challenges

While macromolecules provide a versatile material system to control emulsion processing and impart functionality to emulsions, their high molecular weight, slow dynamics (e.g., diffusion and relaxation) and entropy-dominated behavior of such molecules can complicate their application in emulsion-involving processes. For example, while polyelectrolytes offer several functionalities such as stimuli-responsiveness, they do not dissolve well in highly non-polar media. Chemical modification have been conducted to increase macromolecules' solubility in specific solvents. However, such modifications can bring side effects, for example, creating mutation and toxicity in proteins.[27] Enabling the application of macromolecules without drastically changing their original chemical

and physical properties would bring much benefits to their adoption across different sectors and applications.

Meanwhile, there are also some technical challenges to be addressed to study macromolecules behavior at the emulsion interface. The effect of polymeric surfactants on emulsion interface is difficult to probe in bulk media.[28] With heterogeneous droplet size distribution, and different continuous film thickness due to possible creaming or flocculation of the dispersed droplets, the macroscale properties of the emulsions, such as its rheology, can vary quite differently among different measurements; thus it can be very difficult to derive a convincing analysis on the effect of the polymeric surfactants on the behavior and properties of emulsions. To be able to conduct reliable characterization, close monitoring and testing of the effect of macromolecules, especially at monodispersed single droplet level is required.

To address these challenges, we exploited the following two approaches: microfluidics and ion pairing.

## 1.3 Approaches: Ion pairing and microfluidic

### 1.3.1 Ion pairing

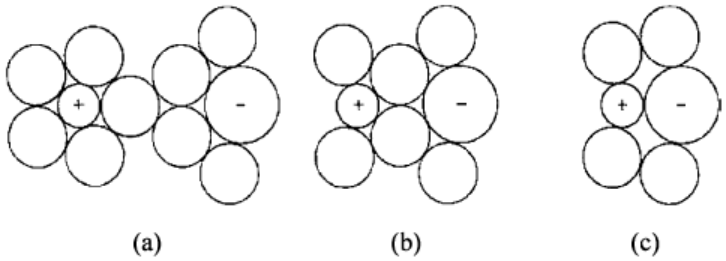


(a) (b) (c)

**Figure 1.3** Schematic representation of ion pair. Reprinted with permission from reference 29.

Ion pairs are the chemical species formed by electrostatic interaction between electrolytes of opposite charges (Figure 1.3). In 1926, Bjerrum was first to develop the concept of ion pairing of strong electrolytes.[29] The model he developed describe ion pairs formed under Coulomb's law. The interaction between the electrolytes is strengthened by the magnitude of their charges, and attenuated by the permittivity of the solvents that they are dissolved in.

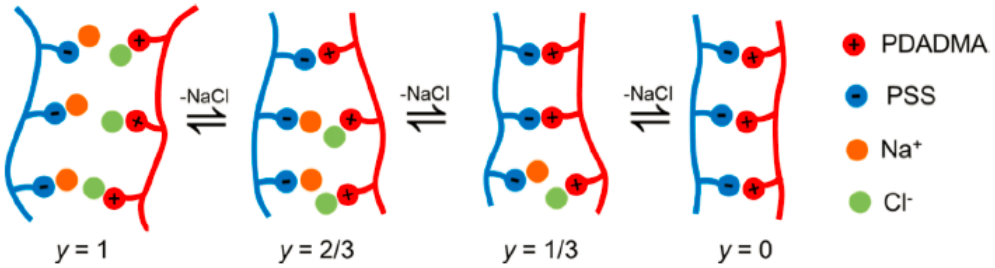


**Figure 1.4** Schematics of a polyelectrolyte complex by poly-(diallyldimethylammonium chloride) (PDADMAC) and poly(styrenesulfonate, sodium salt) (PSS). Reprinted with permission from reference 30.

Later with further development in the field, especially for the purpose of describing charged assemblies of macromolecules such as polyelectrolytes, the concept of ion pairing and its associated driving force for formation broadens. Arguing that the original continuum electrostatics model is no longer accurate when describing polyelectrolytes

that introduce concentrated ions in small regions, it was proposed that the entropic contribution associated with the release of counter ions is the major driving force for the formation of the ion pairs.[30] Ion pairs form within polyelectrolyte complexes, and are classified as either intrinsic or extrinsic ion pairs, depending on whether they form between the oppositely charged polyelectrolytes or between polyelectrolyte and free counter ions (Figure 1.4).[31]

Many applications have been developed based on ion pairing, leveraging its capability to extract ions into organic solvents. Phase-transfer catalysis is a set of processes developed based on transferring ionic species from water to an organic phase, where it retains high reactivity. A representative reaction is the synthesis of polycarbonates from diphenols, where diphenols form ion pairs with quaternary ammonium cations.[32] For polyelectrolyte extraction, both synthetic and biological polyelectrolytes have been reported to be successfully extracted into organic phases via ion pairing. Poly (styrene sulfonate) has been reported to precipitate when ion paired with cetyltrimethylammonium chloride in water. The precipitate can be dissolved in polar organic solvents including 2-butanol with its polyelectrolyte properties retained.[33] Insulin, a positively charged protein, can be extracted into an organic solvent, isooctane, by ion pairing with a negatively charged surfactant, sodium dodecyl sulfate (SDS). The solubility of insulin-SDS ion pair in isooctane can increase by 10 folds compared to its solubility in water while the native structure of insulin is retained.[34]

## 1.3.2 Microfluidics

Microfluidics is a set of technologies that manipulate fluids at micro- and nano-scale using engineered microchannels and chambers. Capillary forces become significant when fluids are operating in these confined geometries.[35] The inertial force that dominates the fluid behavior at the macroscopic scale becomes negligible compared to the viscous forces of the fluids, and most fluids operating in microfluidic devices transports as laminar flows with low Reynolds numbers.[36-37]

Since being introduced two decades ago, microfluidics has attracted tremendous interests, which led to the enthusiastic development of materials and processes for microfluidic chip fabrication. The five major materials for microfluidic device fabrication are glass and silicon, elastomer, plastic, hydrogel, and paper.[38] The glass and silicon, and elastomer, mostly polydimethylsiloxane (PDMS), are mostly used to fabricate microfluidic deices for research purposes. The glass and silicon microfluidic devices are normally fabricated through photolithography or through assembly of glass capillaries.[39-40] Their advantages lie in their mechanical rigidity as well as compatibility with various kinds of organic solutions. The PDMS devices are typically fabricated through soft lithography.[41] They normally possess complicated channel geometry with high resolution. Due to their flexibility, functional units, such as “Quake valve”, can be integrated into PDMS devices, enriching the operations of the device.[42-43] The plastic and paper devices were later developed for commercial purposes, and hydrogel devices have their unique advantages in biological studies.[44-45]

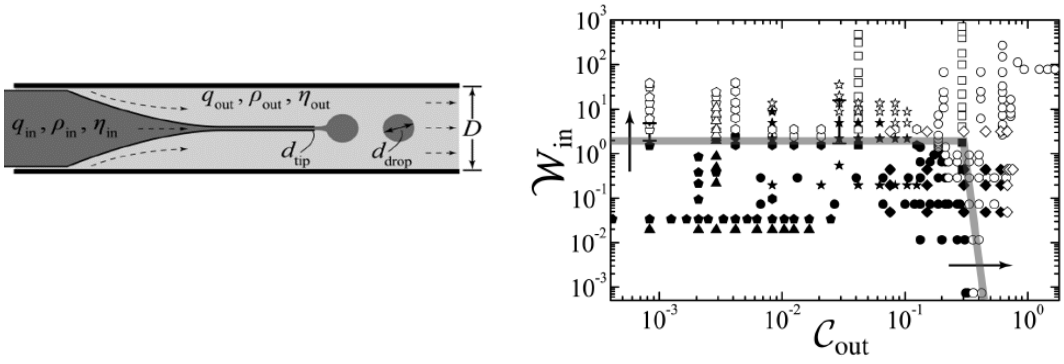


**Figure 1.5** (Left) Schematic of droplet formation in microfluidic; (right) the state diagram of dripping to jetting transition as a function of Ca and We number, the filled symbols represent dripping while the open symbols represent jetting. Reprinted with permission from reference 46.

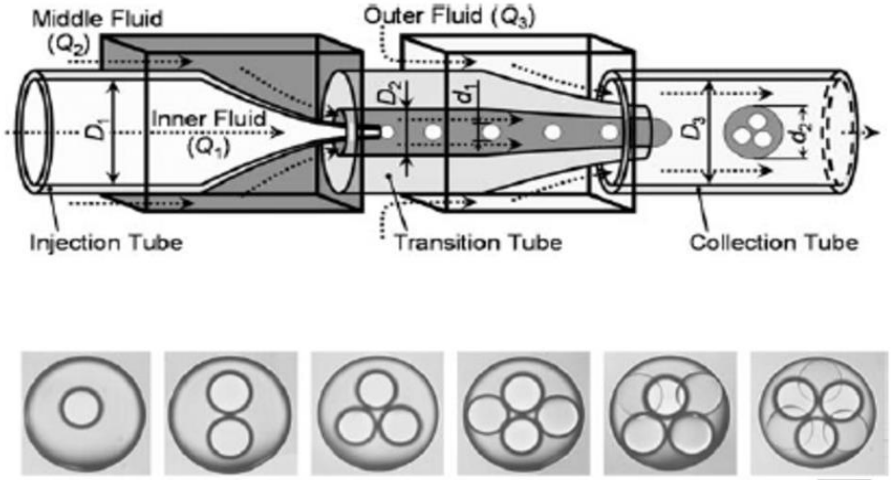


**Figure 1.6** (Top) Schematic of multiple emulsion generation via hieratical microfluid device design and (bottom) multiple emulsion droplets generated with various number of inner droplets. Reprinted with permission from reference 47.

The many benefits of microfluidics cannot be summarized in one brief paragraph. One significant advance that microfluidics has enabled is in the area of emulsion processing. On one hand, the microfluidics technology offers precise control over the size and structure of the emulsions they generate. By injecting one fluid into the second one and balancing the interfacial tension with the shear stress at the interface and the inertial force of the injected dispersed phase, highly uniform emulsion droplets can be produced one at a time. The comparison between these three parameters are normally presented as the Capillary number (Ca) and the Weber number (We) (Figure 1.5).[46] The Capillary number compares the relative importance between shear stress and the interfacial tension while the Weber compares the inertial force and interfacial tension. When Ca and We $\leq$ O (1), it implies the domination of the interfacial tension in the system, droplet formation occurs in the so-called dripping region. In this region, highly monodisperse droplets periodically pinch-off from the tip where it is first introduced. Through hierarchical design, the dripping process can be synchronized among different fluids to produce multiple emulsions with complex structure, such as controllable number of inner droplets (Figure 1.6).[47]

On the other hand, microfluidic techniques have also been applied to probe various emulsion phenomena at the single droplet level, for example, testing the stability of an emulsion under flow. Patterns and barriers in microfluidic devices have been used to induce coalescence of emulsions.[48] The droplet break-up behaviors when flowing through constricted channel also have been presented quantitatively as a function of the emulsion flow conditions and geometries of the channel.[49-50] The high interfacial area to volume

ratio at the small scale is exploited in coated microfluidic devices to induce phase separation, even phase inversion, of a precursor emulsion. In summary, in addition to emulsion generation, the microfluidic technology represents a powerful platform for comprehensively and quantitatively uncovering of various mechanisms related to emulsion processing/phenomena.[51-52]

## 1.4 Thesis Objectives and Outline

With the increasing application of emulsions, and with the surging demand to study and exploit macromolecules, in this thesis, we intend to harness the interfacial phenomena of macromolecules at fluid interfaces for emulsion processing via ion pairing and microfluidics techniques. The main questions we want to explore in this thesis are:

- How can ion pairing be harnessed to enable one step polyelectrolyte microcapsule generation?
- How does flow induced phase inversion emulsification depend on the composition of the macromolecular surfactants?
- Can ion pairing be used to produce new "surfactant systems" that induce phase inversion emulsification?

Chapter 2 presents a microfluidic polyelectrolyte microcapsule generation process aided by ion pairing between a polyelectrolyte and a surfactant. One limitation of one-step

generation of polyelectrolyte microcapsules using water-in-oil-in-water (W/O/W) double emulsion templates generated by microfluidic device is that one of the polyelectrolytes used needs to be oil-soluble. In this study, a polyelectrolyte is extracted into an organic phase via ion pairing. Complexation between polyelectrolytes at oil-water interface is successfully induced, which leads to the formation of the polyelectrolyte microcapsules. These microcapsules show adjustable hydrophobicity and release their cargo upon changes in the ionic strength of the solution.

Chapter 3 presents a thorough study on the composition effect of a polymeric surfactant on flow induced phase inversion emulsification (FIPIE). The FIPIE tendency of emulsion flowing through a tapered microchannel is shown to depend strongly on the molecular weight of Pluronics as well as the lengths of their individual blocks. The steric repulsion pressure provided by the Pluronics at the fluid interface is estimated to increase with the length of PEO blocks, and the dilatational elasticity measurement shows that Pluronics with long PPO block provide high dilatational elasticity at the fluid interface, inhibiting FIPIE.

Chapter 4 demonstrates phase inversion emulsification (PIE) via ion pairing between a weak polyelectrolyte and a surfactant. Emulsions are made by homogenizing equal volumes of aqueous and toluene solutions. When either the polyelectrolyte or surfactant is used alone, emulsions formed are O/W type. When both of them are present, however, W/O emulsions can be formed under certain conditions. To comprehensively understand how different factors affect the type of emulsions produced upon ion pairing, we vary two parameters: pH of the aqueous solution and the surfactant concentration in the oil

phase. Multiple emulsion droplets are also formed near the PIE compositions. The sizes of O/W and W/O emulsion droplets are at their minima near the PIE compositions. Emulsions are pH responsive. W/O-to-O/W PIE is demonstrated.

The dissertation concludes with chapter 5, which gives a brief summary of the projects carried out based on ion pairing and/or microfluidics. Recommendations are given for the continuous exploration of macromolecules' application for emulsion processing via ion pairing.

# Chapter 2. One-Step Generation of Salt-Responsive Polyelectrolyte Microcapsules via Surfactant Organized Nanoscale Interfacial Complexation in Emulsions (SO NICE)



## 2.1 Introduction

Microcapsules that encapsulate and release active agents are widely used in numerous fields including pharmaceutical,[53-55] agriculture[56-57] and cosmetics.[58-60] Enabling triggered (active) release of molecules such as drugs,[61-64] herbicides,[65] and pesticides[66-67] from microcapsules could be especially advantageous for various applications. Polyelectrolyte complexation (i.e., association of oppositely charged polymers) provides a powerful platform to prepare microcapsules with excellent triggered release properties, because they can be dissociated via various external stimuli such as salt and pH.[68-71] However, the conventional methods of polyelectrolyte microcapsule preparation typically require multiple steps or has very low encapsulation efficiency.

One emerging approach for one-step polyelectrolyte microcapsule generation is to exploit complexation at interfaces between two immiscible phases.[72-73] For example, by dissolving a polyelectrolyte of one charge in an aqueous phase and an oppositely charged polyelectrolyte in an organic phase, the two polymers can be induced to form complex layers at the interfaces between the two phases. Introducing one liquid phase as droplets

into the second phase would lead to membranes that encapsulate liquid cores. In particular, by placing two oppositely charged polyelectrolytes in the middle organic and inner water phases of a water-in-oil-in-water (W/O/W) double emulsion, multifunctional polyelectrolyte microcapsules can be prepared via nanoscale interfacial complexation in emulsions (NICE).[74-75] This method overcomes fabrication challenges that are posed by conventional methods of polyelectrolyte microcapsule preparation.[76-78] Furthermore, the use of microfluidics for double emulsion generation ensures high encapsulation (Figure 2.1b, i).[39, 79]

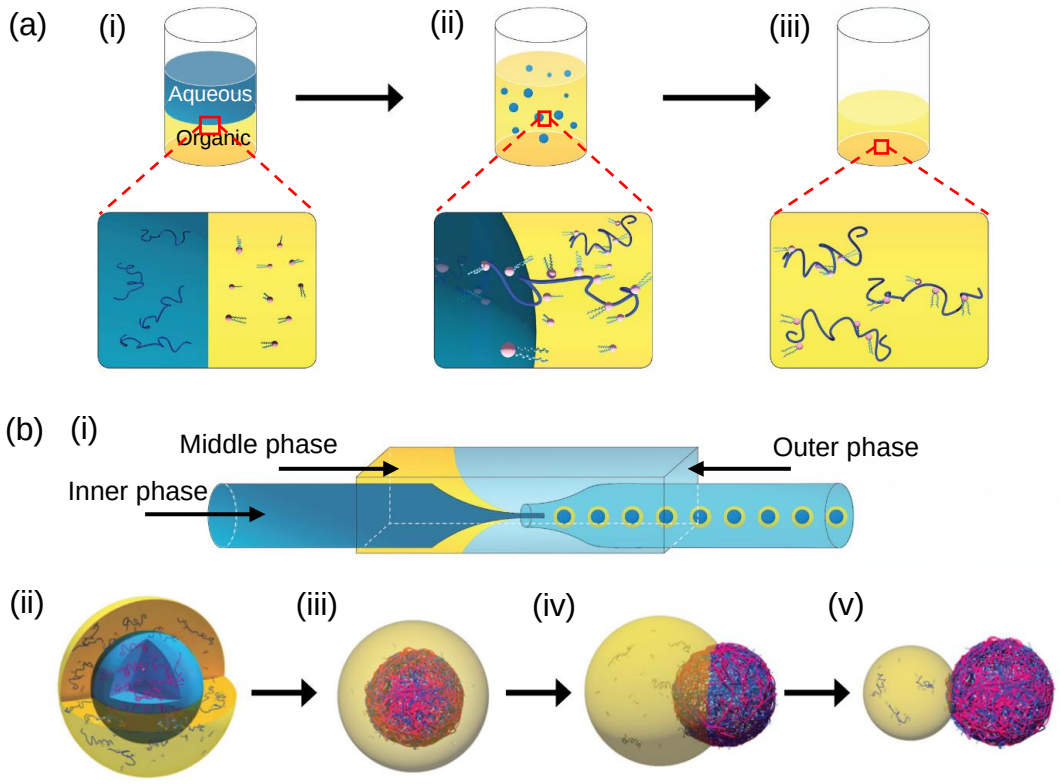

**Figure 2.1** (a) Schematics depicting PSS extraction from aqueous phase (blue) into organic phase (yellow), both procedure and illustration of interfacial ion-pairing between PSS and a double-chain surfactant DDAB are presented. (i) The aqueous and organic phases are introduced into the same container; (ii) The aqueous phase is emulsified into the organic phase; (iii) Organic phase with PSS-DDAB ion-pairs retrieved after phase separation. (b) Schematics of SO NICE microcapsule formation process (i) W/O/W double emulsion droplets generated via microfluidic technique (ii) W/O/W double emulsion droplets with PDADMAC in the inner water droplet and PSS-DDAB ion-pairs in the organic shell. (iii) Interfacial complexation of PDADMAC and PSS-DDAB at the inner water/oil interface. (iii-v) Dewetting of the polyelectrolyte shell from the oil droplet to form a water-filled SO NICE microcapsule.

One major challenge in using interfacial complexation for the fabrication of polyelectrolyte microcapsules or membranes is the insolubility of many polyelectrolytes in organic solvents.[33] Because of the low permittivity of organic solvents, counter-ions of polyelectrolytes do not dissociate readily in such media. Because of this limitation, a relatively limited number of polymers (e.g., copolymers of charged and hydrophobic repeat units or un-ionized polymers that can acquire charge such as weak polyamines) with specific structures and compositions can be used to induce microcapsule formation when oil-water based emulsions are used for polyelectrolyte microcapsule preparation.[74, 80] Thus, a new approach is needed to enable the use of a broad variety of polyelectrolytes, both synthetic and natural, to widen significantly the applicability of interfacial complexation for the preparation of functional polyelectrolyte microcapsules.

In this chapter, we introduce surfactant organized nanoscale interfacial complexation in emulsions (SO NICE) to generate salt-responsive microcapsules. The microcapsules are made of two strong polyelectrolytes. Solubilization of one polyelectrolyte in the organic phase is induced via ion pairing with hydrophobic surfactants. We show that these SO

NICE microcapsules can be induced to release the encapsulated materials via changes in the ionic strength of the solution. The SO NICE method broadens the pallet of polyelectrolytes that can be used for one-step generation of multifunctional polyelectrolyte microcapsules. Moreover, the combination of ion pairing[81-82] and interfacial complexation can be exploited for a number of other applications that will lead to formation of functional polyelectrolyte membranes.

## 2.2 Experimental Section

### 2.2.1 Formation and characterization of poly(sodium 4-styrenesulfonate) (PSS)-didecyldimethylammonium bromide (DDAB) ion-pairs

The PSS-DDAB ion-pairs are generated through mixing and stirring of aqueous and organic phases containing PSS and DDAB, respectively. 1 wt% PSS is dissolved in DI water. The aqueous phase is then added to chloroform with 1:1.5 volume ratio. DDAB is dissolved in chloroform with 0.6: 1, 0.8: 1, 1:1, 1.2: 1, and 1.5: 1 DDAB:SS molar ratio. The mixture is vortexed vigorously and subsequently stirred with a stirring bar for 1 hour. The solution is then centrifuged for 1 hour at 4500 rpm to induce complete phase separation between the aqueous and organic phases.

The concentration of residual PSS in the aqueous solution is determined using UV Vis spectroscopy. The fraction of PSS extracted into chloroform is subsequently inferred from the concentration of residual PSS in the water phase. Each data point presented in Figure 2.2 is average of three independent measurements.

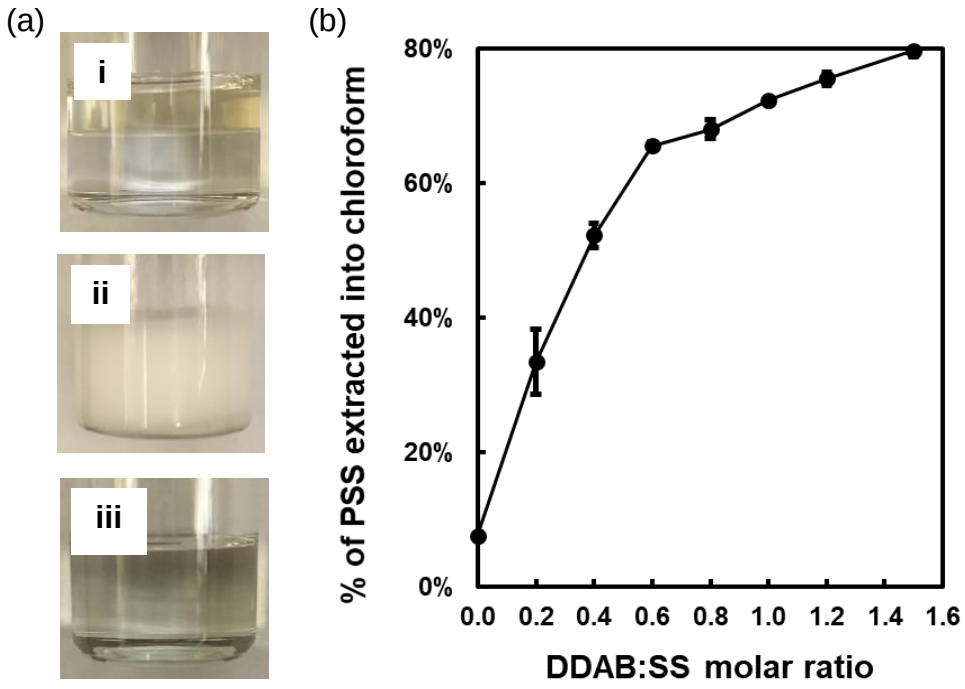


**Figure 2.2** (a) PSS extraction. (i) Aqueous phase is placed on top of the chloroform phase containing DDAB; (ii) aqueous phase is emulsified into fine droplets; (iii) emulsion is broken to form two macroscopic phases of organic and water. (b) Percentage of PSS that extracted into chloroform under different DDAB:SS molar ratio.

### 2.2.2 Generation and characterization of SO NICE microcapsules

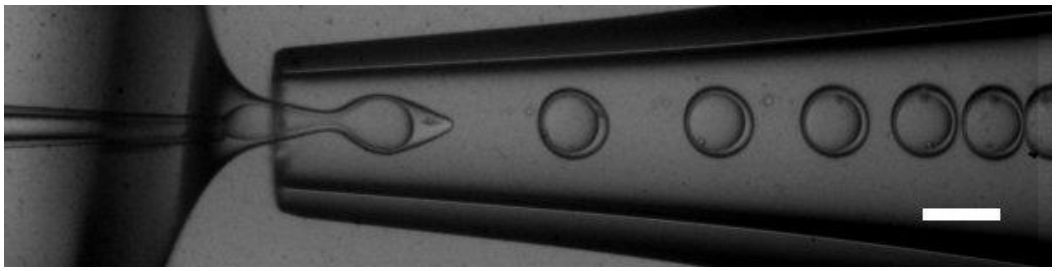

**Figure 2.3** Formation of double emulsion in a glass capillary microfluidic device. Scale bar = 100 μm.

SO NICE microcapsules are generated using microfluidic technique as previously reported.[74] The microfluidic device is made of glass capillaries with combination of flow-focusing and co-flow geometries as shown in Figure 2.3.

Double emulsion generation within the microfluidic device is captured using an inverted microscope (Nikon Eclipse TE200) equipped with a high-speed camera (Phantom v 7.1). We use the upright microscope (Zeiss Axio Plan 2) equipped with a digital camera (AmScope MU 1003-CK 10 MP) for bright filed imaging. All images are analyzed using ImageJ.

The three liquid phases used are 1 wt% poly(diallyldimethylammonium chloride) (PDADMAC, 200,000 – 300,000 Mw, Sigma-Aldrich) and 0.001 M dodecyltrimethylammonium bromide (Sigma-Aldrich) dissolved in 0 – 0.45 M sodium chloride (NaCl, Fisher Scientific) aqueous solution as the inner phase, 0.63 wt% PSS-DDAB ion pairs in a 1:1 mixture of chloroform and butyl acetate as the middle phase, and 2 wt% polyvinyl alcohol (PVA, 13,000-23,000 Mw, 87%- 89% hydrolyzed, Sigma-Aldrich) in DI water as the outer phase. The size of the double emulsion droplets as well as the organic phase thickness are controlled by adjusting the flow rates of the inner, middle, and outer phases. Generated double emulsions are collected in 2 wt% PVA solution to allow for the complete evaporation of the solvents. The collecting container is coated with trichloro(1H,1H,2H,2H-perfluorooctyl) silane to avoid microcapsule attachment.

To characterize dried microcapsules via atomic force microscopy, microcapsules collected in 2 wt% PVA are washed with DI water for 4 to 5 times. Several drops of

solution containing microcapsules are then placed on top of a silicon wafer and left to air dry at room temperature (~ 25 $^{o}$C). The sample is further washed with a copious amount of DI water to make sure all residual PVA is removed. The thickness of dried microcapsules is then measured using Nano RTM AFM (Pacific Technology, Inc.) in tapping mode at room temperature. The AFM cantilever used has resonance frequency of 300 kHz under tapping mode and the scan rate is set at 1 Hz. Gwyddion (v 2.30), a scanning probe microscopy data visualization and processing software, is used for AFM image analysis. The thickness of microcapsule shell is estimated using average thickness measured over the entire microcapsule area.

To incorporate fluorescence dyes for confocal microscopy, 0.1 wt% Nile red (Sigma-Aldrich) is dissolved in the organic phase, and 0.001wt% fluorescein sodium salt (Mw 376 Da, Sigma-Aldrich) is dissolved in the inner phase.

Fluorescence images are captured using a confocal laser scanning microscope (Olymus Fluo View FV 1000). During salt responsiveness test, a circle with a radius of 30% of the microcapsules' radius is used to monitor the central region of the microcapsules. The mean values as well as the standard deviations of the fluorescence intensity over the selected area are measured using ImageJ.

## 2.3 Results and Discussions

We demonstrate the formation of SO NICE polyelectrolyte microcapsules with triggered release functionality using two strong polyelectrolytes, PSS and PDADMAC. Neither of these polyelectrolytes can be easily dissolved in an organic solvent. The dissolution of PSS in the organic phase is achieved by electrostatically associating (or ion pairing) PSS with DDAB in a two-phase medium. An aqueous phase containing PSS is dispersed in an organic phase with DDAB, inducing association between the two molecules at the oil-water interface and subsequent partitioning of PSS-DDAB complexes into the organic phase as schematically illustrated in Figure 2.1a. Subsequently, W/O/W double emulsions are generated with PDADMAC in the inner water droplet and the PSS-DDAB ion-pairs in the middle organic phase (Figure 2.1b). Our hypothesis is that PDADMAC and PSS-DDAB will undergo interfacial complexation at the inner water-oil interface of the W/O/W double emulsions to form microcapsules, potentially by dewetting from the organic droplets.

### 2.3.1 Transfer of PSS from aqueous to organic phases via hydrophobic ion-pairing with DDAB

In NICE, polyelectrolyte microcapsules are templated with W/O/W double emulsions by dissolving one of the two polyelectrolytes in the middle organic phase and the other in the inner aqueous phase. One limitation of this method is that many polyelectrolytes are highly insoluble in organic phase due to their inability to undergo dissociation in a low permittivity medium. To enable NICE with a widely studied strong polyelectrolyte pair

like PADAMAC and PSS, we test the possibility of extracting PSS into the organic phase by inducing its association with a hydrophobic cationic surfactant, DDAB.

Such a process of associating a charged polymer with an oppositely charged surfactant is known as ion pairing.[81-82] A unique aspect of this work is that ion pairing is performed in an emulsion (Figure 2.2a). We emulsify an aqueous solution of 1 wt% PSS in an organic phase (chloroform) with DDAB with a water-to-oil volume ratio of 1:1.5 (Figure 2.2a). The emulsion is vigorously stirred for 1 hour (Figure 2.2a, ii), and is broken by centrifuging for 1 hour to form two macroscopic phases of water (top) and organic (bottom). The organic phase appears yellow, suggesting the extraction of PSS into the organic phase presumably due to its association with DDAB. (Figure 2.2a, iii). We use UV Visible spectroscopy to determine the residual amount of PSS in the aqueous phase. A mass balance gives the fraction of PSS partitioned into the chloroform.

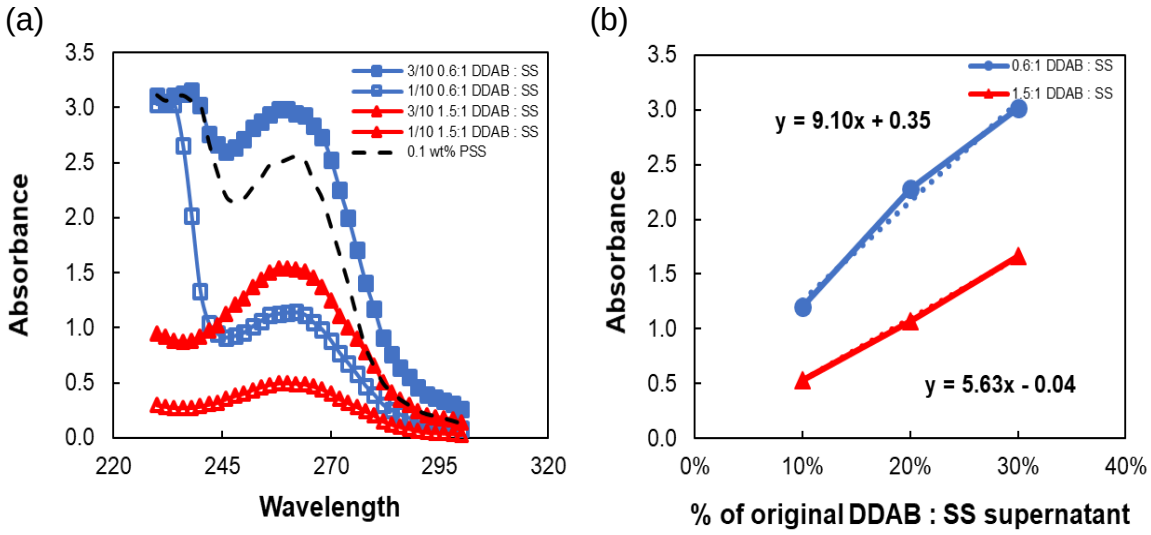


**Figure 2.4** UV Vis spectra of aqueous supernatant of 0.6 :1 and 1.5 :1 DDAB : SS molar ratio. (a) UV Vis spectra of PSS aqueous supernatant dilute to 1/10, 3/10 of original

concentration after extraction. (b) UV Vis spectra absorbance as a function of supernatant dilution.

$$C_p \times V_o = C_o \times V_a - C_s \times V_a \quad (2\text{-}1)$$

$$C_s = S + I \quad (2\text{-}2)$$

The amount of PSS extracted into the oil phase is calculated via subtracting the original amount of PSS with that of PSS remain in the aqueous phase after the ion-pairing extraction. Residual PSS in the aqueous phase is too concentrated for direct UV Vis spectroscopy. Consequently, the aqueous supernatant is diluted with DI water to enable UV Vis spectroscopy. The characteristic peak of PSS is at 262 nm. The Beers-Lambert linear correlation between concentration and absorbance is verified. The achieved values of slopes and intercepts are then used to calculate the concentration of PSS in the supernatant. The amount of the PSS remains in the supernatant and the amount of PSS extracted into the organic phase are then calculated based on mass balance. Equation (2-1) and (2-2) are used for the calculation. $C_o$ is the original PSS concentration in aqueous phase before extraction, $C_p$ is the PSS concentration in organic phase, $C_s$ is the PSS concentration in supernatant after extraction, S is slope of linear regression, I is the intercept of linear regression, $V_a$ is the volume of aqueous phase, $V_o$ is the volume of oil phase.

The fraction of PSS partitioned into chloroform can be controlled by changing the molar ratio of DDAB to sodium sulfate (SS) groups of PSS as shown in Figure 2.2b. This method of extracting polyelectrolytes into the organic phase via ion pairing can be useful in many applications where the dissolution of highly polar/charged polyelectrolytes in non-polar media is required.

The macroscopic film formation test is used to select the suitable organic phase for polyelectrolyte microcapsule generation. An aqueous phase (1 mL) is added on top of an organic phase (1 mL) (Figure 2.5). The aqueous phase is 5 wt% PDADMAC and the organic phase is the mixture of 0.5 mL chloroform made with different DDAB:SS molar ratios with 0.5 mL of butyl acetate. Interfacial films are formed with intermediate DDAB:SS molar ratios, 0.6: 1, 0.8:1, and not at the two extreme DDAB:SS molar ratios, 0:1 and 1.5:1. The film formed is further demonstrated by probing with a wooden rod as presented in Figure 2.5b. Organic phase made with 0.8:1 DDAB:SS molar ratio is selected and used for microcapsule generation.

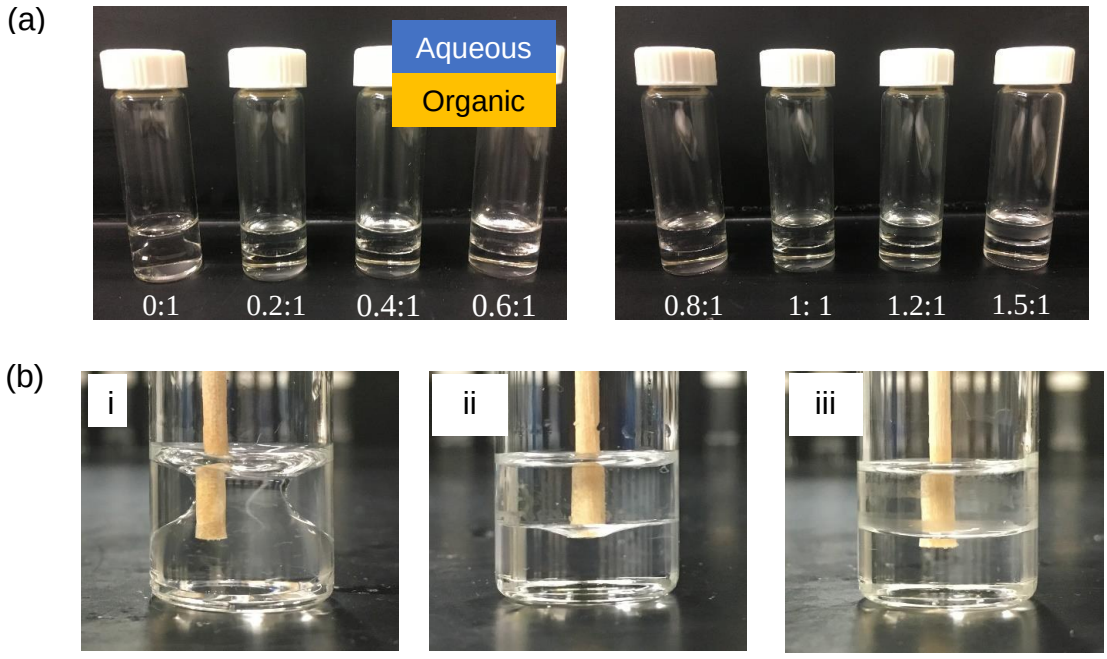


**Figure 2.5** (a) Macroscopic film formation at the aqueous and organic interface, using organic phase containing different DDAB:SS molar ratios. From left to right, the organic phases are made with DDAB:SS molar ratio of 0, 0.2, 0.4, 0.6, 0.8, 1, 1.2, 1.5 :1. (b) The aqueous organic interface is probed with a wooden rod, (i) DDAB:SS = 0:1; (ii) DDAB:SS = 0.8:1; (iii) DDAB:SS = 1.5:1.

This finding shows that PDADMAC and PSS-DDAB can undergo complexation at the water/oil interface and that the extent of PSS-DDAB association plays a critical role in enabling this complexation process. The fact that DDAB:SS molar ratios above 0.8 do not favor PDADMAC/PSS-DDAB interfacial complexation likely indicates that an appreciable number of free sulfonate groups (i.e., those that are not associated with DDAB) are necessary for PDADMAC and PSS to undergo complexation.

### 2.3.2 SO NICE microcapsule generation

To fabricate SO NICE microcapsules, we create water-in-oil-in-water (W/O/W) double emulsion droplets with a glass capillary microfluidic device, which enables the production of highly uniform droplets with perfect encapsulation efficiency.[39] PDADMAC is dissolved in the inner water phase and the PSS-DDAB ion pair is dissolved in the middle organic phase (see Table 2.1 for compositions). The outer continuous water phase contains 2 wt% PVA for double emulsion stabilization.

**Table 2.1** Composition of inner, middle and outer phases.

| | **Solvent** | **Solute** |
|---|---|---|
| **Inner** | DI water | 1 wt% PDADMAC, 0.001 M DTAB, 0.1 - 0.45 M NaCl |
| **Middle** | 1:1 vol Chloroform/Butyl acetate | 0.19 wt% PSS, 0.44 wt% DDAM |
| **Outer** | DI water | 2 wt% PVA |

We find that the presence of a sufficient amount of salt (NaCl) in the inner phase is crucial for stable formation of microcapsules from these double emulsions. When double

emulsion droplets without any salt are allowed to undergo solvent evaporation, unstable polyelectrolyte microcapsules are formed, as shown in Figure 2.6a (i-v). Such microcapsules collapse and lose their integrity upon solvent removal. However, stable microcapsule formation is observed when salt is added to the inner phase as seen in Figure 2.6b.

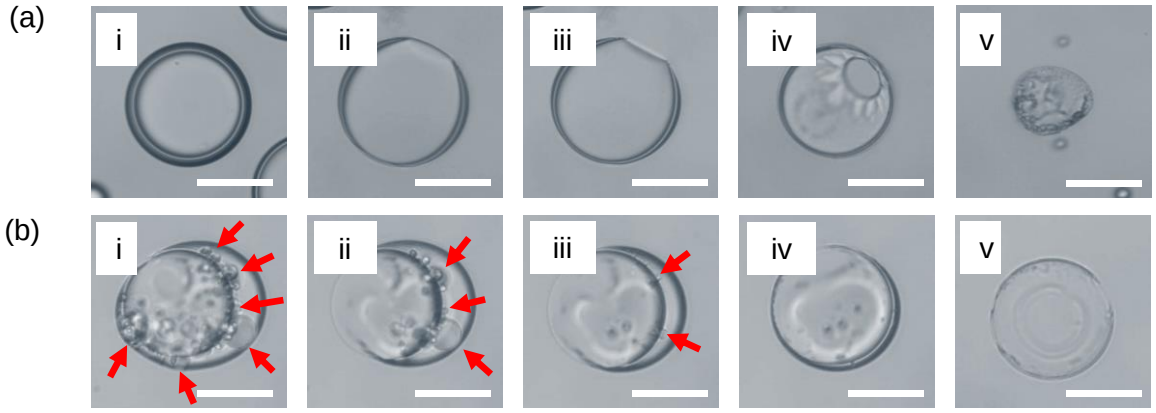


**Figure 2.6** (PDADMAC/PSS) SO NICE microcapsules formation from double emulsions. Inner phase with no NaCl: (a-i,ii,iii,iv,v) Unstable formation of polyelectrolyte microcapsules. Inner phase with 0.2 M NaCl: (b-i) Small water droplets spontaneously appear in the initial stage. (b-ii) Aqueous droplets coalesce as organic phase evaporates. (b-iii, iv) The microcapsule begins to dewet from the mother organic phase droplet. (b-v) A microcapsule is observed after complete organic phase evaporation. Scale bars = 50 µm.

The salt added to the inner aqueous phase of W/O/W double emulsions may facilitate the interfacial complexation between PDADMAC and PSS-DDAB by weakening interactions between PSS and DDAB via electrostatic screening.[81] Because of the

polyvalency of PDADMAC and PSS, the addition of salt favors the complexation of the diallyldimethylammonium groups of PDADMAC and the sulfate groups of PSS over the ion pairing between DDAB and the sulfate groups of PSS. Thus, the enhanced complexation between PSS and PDADMAC may lead to more robust interfacial complex layer and thus more stable microcapsule formation. In addition, salt addition would also induce screening of mirror charge-induced repulsion, promoting the adsorption of PDADMAC to the inner water-oil interface.[83-84] Interestingly, when 0.2 M NaCl is present in the inner aqueous phase of the W/O/W double emulsion, tiny droplets (indicated by red arrows in Figure 2.6b, i-v) are spontaneously formed in the middle organic phase as double emulsions become microcapsules. We do not fully understand the origin of these tiny droplets but they seem to be associated with auto-emulsification process akin to those that have been observed in amphiphilic block copolymer-containing oil-water emulsions.[85] We believe that PSS-DDAB ion pair is quite amphiphilic and therefore can induce auto-emulsification. These tiny droplets eventually undergo coalescence with the inner droplets, and subsequently the organic phase undergoes dewetting, resulting in the formation of polyelectrolyte microcapsules.

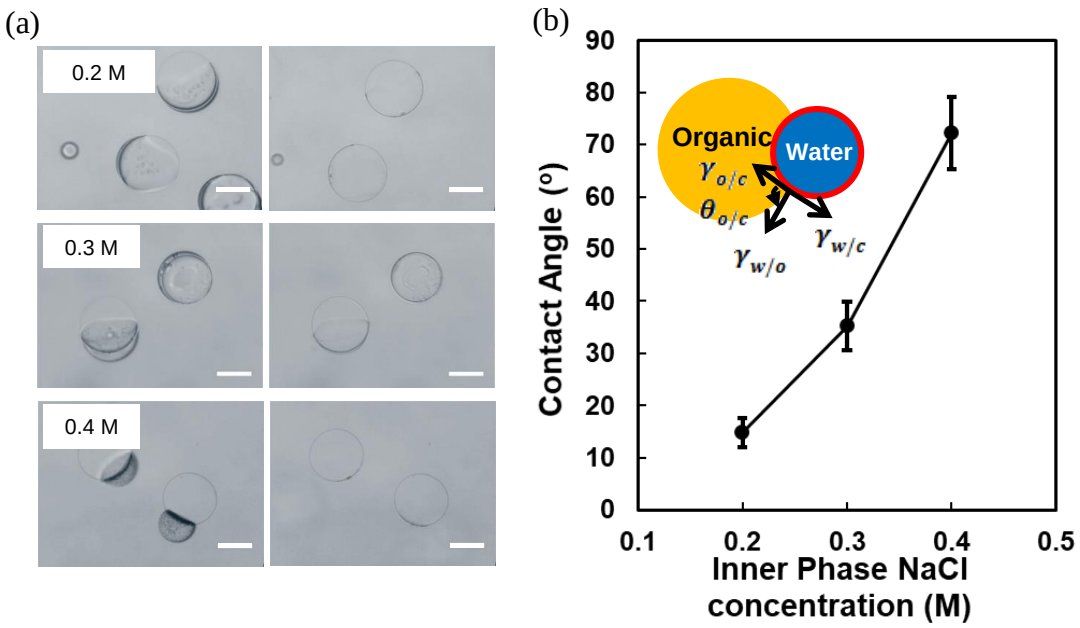


**Figure 2.7** (a) Optical microscopy images of (PDADMAC/PSS) SO NICE microcapsules upon (left column) dewetting and (right column) complete removal of the solvent. Data with inner phase NaCl concentration of 0.2 M, 0.3M and 0.4M presented. Scale bar = 50 μm. (b) Three phase contact angle between SO NICE microcapsules and mother organic phase droplets as a function of inner phase NaCl concentration. 10 double emulsions are analyzed to obtain the average values for each salt concentration. $\gamma_{w/o}$: interfacial tension between water and organic phase; $\gamma_{o/c}$ : interfacial tension between organic phase and complex; $\gamma_{w/c}$ : interfacial tension between water and complex; $\Theta_{o/c}$: three phase contact angle between SO NICE microcapsules and mother organic phase droplets.

Dewetting of the organic phase during the formation of polyelectrolyte microcapsules from double emulsions indicates that the shell formed via interfacial complexation is not fully compatible with the organic phase.[74, 86-87] The effect of salt on the dewetting phenomena in SO NICE is further probed by varying its concentration in the inner aqueous phase. An increase in the salt concentration leads to more significant dewetting, or higher three phase contact angles (Figure 2.7), which suggests that different salt

concentrations likely affect the composition of the polyelectrolyte complex shell. The low contact angles at low concentrations of NaCl (< 0.3 M), for example, indicates the polyelectrolyte complex is very hydrophobic, possibly due to thesignificant incorporation of hydrophobic DDAB in the polyelectrolyte complex film. In contrast, increasing NaCl concentrations make the polyelectrolyte film more hydrophilic, likely by inducing dissociation between DDAB and PSS. Thus, tuning the composition of the shell by changing the salt concentration could provide a powerful method of tailoring the properties of the SO NICE microcapsule. We have also observed that the polyelectrolyte microcapsules stick to the surface of glass slides but does not do so onto glass slides coated with PDADMAC. These observations strongly suggest that the surface of the microcapsules is positively charged.

### 2.3.3 Characterization of SO NICE microcapsules

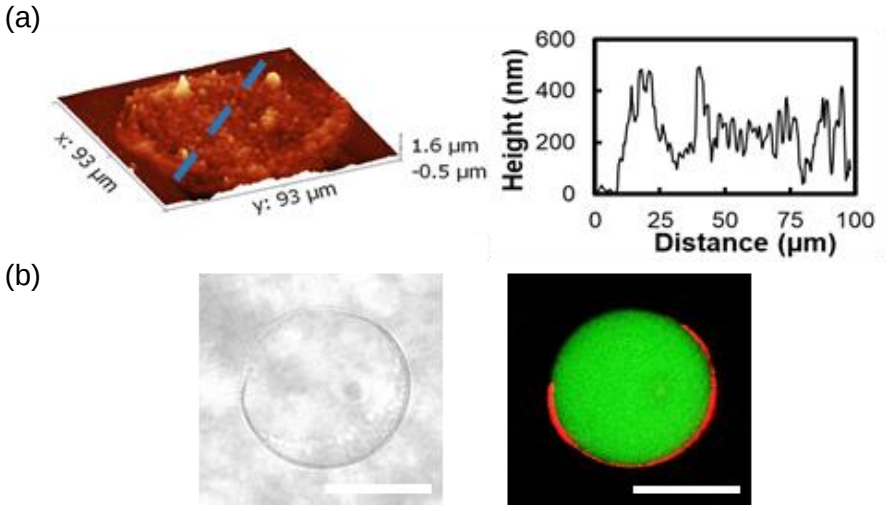


**Figure 2.8** (a) AFM image of dry-state $(PDADMAC/PSS)_{0.2}$ SO NICE microcapsule and height profile along the blue dashed line (subscript denotes the concentration of NaCl in

the inner aqueous phase). (b) Confocal laser scanning micrograph of a SO NICE microcapsule encapsulating fluorescein sodium salt (green) and Nile red (red) in the core and shell of the microcapsule, respectively. Scale bars = 50 µm.

The thickness of the SO NICE microcapsule shell made with 0.2M NaCl in the inner phase is approximately 127 ± 51 nm as determined by dry-state atomic force microscopy (Figure 2.8a). Estimation of the shell thickness assuming a uniform shell composed of PSS, PDADMAC and DDAB yields a thickness of 104 nm, in good agreement with the experimental measurement. Equation (2-3) and (2-4) are used for the estimation.

In the estimation, the diameter of both the oil phase and the aqueous phase of the double emulsion are measured right after its generation in microfluidic device. All images are analyzed using ImageJ. The diameters of 10 double emulsion droplets are measured and the average values are used for calculation. The calculation also takes account of double emulsion dilation due to osmosis imbalance. The density of the polyelectrolyte complex is assumed to be 1.1 g/cm$^3$.

$$V_{comp} = \left[\frac{4}{3}\pi {R_{in}}^3 \times \rho_{in} \times w_{PDADMAC} + \frac{4}{3}\pi\left({R_{out}}^3 - {R_{in}}^3\right) \times \rho_{middle} \times (w_{PSS} + w_{DDAB})\right] \Big/ \rho_{comp} \quad (2\text{-}3)$$

$$t = \left[{R_{in\_swollen}}^3 + \frac{3V_{comp}}{4\pi}\right]^{1/3} - R_{in\_swollen} \quad (2\text{-}4)$$

$R_{in}$ is the inner aqueous core radius of W/O/W double emulsion right after generation in device, $R_{out}$ is the outer radius of W/O/W double emulsion right after generation in device, $R_{in\_swollen}$ is the dilated microcapsule radius, $\rho_{in}$ is the inner aqueous phase density, $\rho_{middle}$ is the middle oil phase density, $\rho_{comp}$ is the complex structure density, w is the

weight percentage of specific compound in solution, $V_{comp}$ is the volume of the complex structure, t is the shell thickness.

Equation (2-3) calculates the total volume of the complex structure expected to form from a double emulsion droplet. Equation (2-4) takes into account dilation of double emulsions during solvent removal due osmosis imbalance between the microcapsule lumen and the surrounding. The shell thickness is calculated assuming uniform shell thickness composed of PSS, PDADMAC and DDAB.

A key advantage of NICE is that hydrophobic species can be incorporated into the shell by simply adding them to the organic phase of the double emulsion. We confirm that SO NICE also enables the incorporation of hydrophobic species in the shell, as evidenced by the retention of a hydrophobic dye (Nile red), which was added to the organic phase of the double emulsion, in the shell of resulting SO NICE microcapsules (Figure 2.8).

### 2.3.4 Triggered release of SO NICE microcapsule

Polyelectrolyte microcapsules are known to have stimuli-responsive properties, which enable their applications in triggered release of active agents. We show that triggered release of the model compound, fluorescein sodium salt, from SO NICE microcapsules can be induced by adding salt to the surrounding solution. When the concentration of NaCl is increased from 0.00 M to 0.06 M, the fluorescence intensity of the microcapsule lumen drops precipitously within 100 sec, as shown in Figure 2.9, indicating triggered release, likely due to substantial changes in the shell permeability rather than capsule

dissolution. The 100-sec induction time likely represents the time needed for salt diffusion after concentrated salt solution is added to the medium. Interestingly, the spherical shape of the microcapsule remains intact, as is observed in the confocal image of the shell, suggesting that substantial interactions between the two polyelectrolytes remain, thus maintaining the overall structure despite the significant change in the permeability of the shell. We also observe that under a high environmental NaCl concentration (2.0 M), polyelectrolyte microcapsules shrink dramatically within seconds. This is comparatively a much shorter time than the fluorescein release time shown in the Figure 2.9. Thus, we hypothesize that the release profile of the polyelectrolyte microcapsules will vary with NaCl concentration in the surrounding aqueous medium.

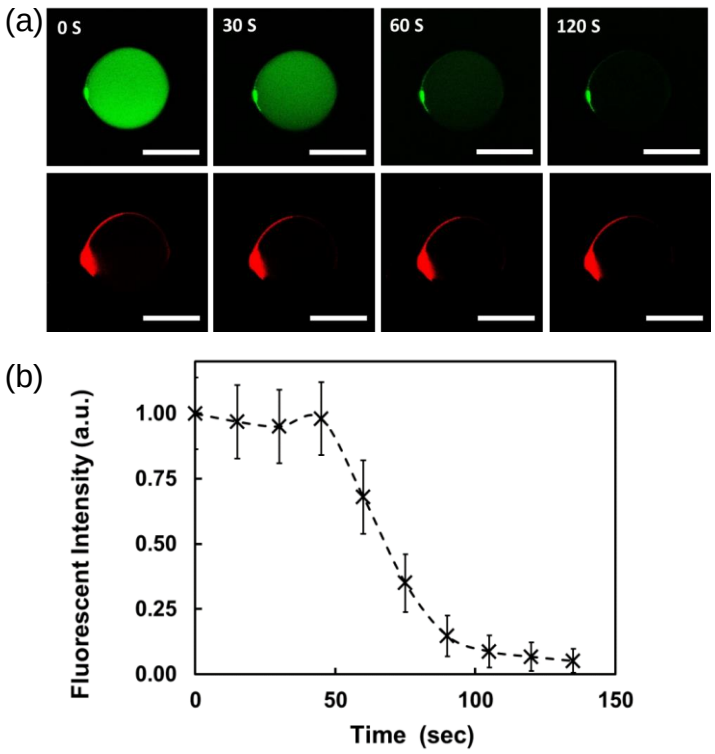

**Figure 2.9** Salt responsiveness of SO NICE microcapsules. (a) CLSM image of a $(PDADMAC/PSS)_{0.2}$ SO NICE microcapsule as a function of time after NaCl is added to the solution. NaCl concentration is raised from 0 M to 0.06 M. All scale bars= 40 μm. (b) Fluorescence intensity at the center of SO NICE microcapsule measured as a function of time. The mean and standard deviation value are normalized by initial mean fluorescent intensity.

## 2.4 Conclusions

In this chapter, we show that salt-responsive polyelectrolyte microcapsules can be generated in one step with strong polyelectrolytes using SO NICE. By dissolving a strong polyelectrolyte in an organic medium via ion pairing with an oppositely charged hydrophobic surfactant, W/O/W double emulsions can be used as templates for the generation of polyelectrolyte microcapsules with high encapsulation efficiency and salt responsive properties. This approach potentially widens the pallet of polyelectrolytes that can be used for functional microcapsules via SO NICE. We believe it will be possible to fabricate SO NICE microcapsules that response to other stimuli such as pH and temperature by using weak and temperature-responsive polyelectrolytes, respectively. Natural polyelectrolytes such as polysaccharides and DNA could also be used for SO NICE microcapsule generation. We hypothesize that the mechanical properties and the long-term release behaviors of SO NICE microcapsules could be controlled by changing the ratio of surfactant-PE. Moreover, by varying the structure of surfactants and their concentrations, the functionality and properties of SO NICE microcapsule could be potentially tailored for specific applications.

# Chapter 3 Effect of Triblock Copolymer Surfactant Composition on Flow-induced Phase Inversion Emulsification in a Tapered Channel

## 3.1 Introduction

Emulsions are mixtures of two immiscible fluids, one dispersed in the other and are present in countless products and manufacturing processes of pharmaceutics, cosmetics, and agriculture industries.[26, 88-89] Conventional methods of emulsion generation typically involve highly energy intensive processes such as mechanical stirring and sonication which can be expensive and can potentially damage the final products due to undesirable heat generation.[90-92]

Phase inversion emulsification (PIE) is a process that interconverts the dispersed and continuous phases of an emulsion and has been used to produce emulsions that are challenging to produce using conventional emulsification techniques.[93-97] Flow-induced phase inversion emulsification (FIPIE) is a process designed to achieve PIE by flowing a precursor emulsion through structured channels, potentially enabling continuous generation of target emulsions.[98] Prior reports have shown that an emulsion can undergo FIPIE as it flows through channels with barriers that promote the coalescence of the dispersed phase and encapsulation of the original continuous phase.[99-100] Other studies have demonstrated FIPIE by flowing emulsions through channels or membranes with preferable wettability towards the dispersed phases.[52, 101-103]

One of the key components that are added in the formation and stabilization of emulsions is a class of materials known as surface active agents (surfactants) such as amphiphilic molecules, copolymers, and solid particles.[104-106] Surfactants dwell at the interfaces between two immiscible fluids and lower the interfacial tension, facilitating the creation of interfaces and enhancing emulsion stability by providing electrostatic repulsion, steric repulsion, and/or increasing bulk and interfacial viscoelasticity.[107-109]

Although several reports have focused on the development of FIPIE processes for emulsion generation, the effect of surfactant composition on the FIPIE of emulsions is not clearly understood. In this study, we focus on investigating the composition effect of polymeric surfactant, Pluronics, on the tendency of emulsions to undergo FIPIE. Pluronics are commercially available ABA triblock copolymers composed of hydrophilic poly(ethylene oxide) (PEO) and hydrophobic poly(propylene oxide) (PPO) (A=PEO, B=PPO).[20-21, 110] Pluronics provide an ideal system to study the effect of surfactant composition because a homologous series of the triblock copolymer surfactants are commercially available and widely used in the industrial processes and products. The tendency of emulsions to undergo FIPIE is analyzed using a recently developed FIPIE process that uses a tapered microchannel.[111] When an oil-in-water (O/W) emulsion is flowed through a hydrophobically treated tapered microchannel, oil droplets deform and undergo coalescence with an oil film on the surface of the channel, inducing phase inversion from O/W to water-in-oil (W/O) emulsions. The draining and rupture of the aqueous film between the oil phases in the phase inversion channel (PIC) depends strongly on the flow conditions; emulsions tend to undergo FIPIE at a low velocity as

they pass through the PIC. The use of a single tapered channel also provides important advantages of *in situ* monitoring and thus enables single droplet-level understanding of the phenomenon. Based on this approach, in this chapter we find that the composition of the copolymer surfactants has a direct impact on the tendency of emulsions to undergo FIPIE and that the steric repulsion seems to be the major factor that influences the fate of emulsions flowing through PIC. Our findings on the effect of Pluronic composition on FIPIE provides guidance on surfactant selection for emulsion generation via FIPIE.

## 3.2 Experimental Section

### 3.2.1 Materials

10 Pluronics with different compositions are selected to make aqueous solutions with the concentration of 0.01M. Their interfacial tensions and viscosities are measured using pendant drop tensiometry and Ubbelohde viscometry, respectively. The concentration of L64 and P65 is 0.05M because emulsions formed with 0.01M L64 and P65 are not stable enough to be used for FIPIE investigation. Figure 3.1 shows the general steps involved in our study. An O/W precursor emulsion is first generated in a glass capillary device, and subsequently this emulsion is introduced into a hydrophobically modified polydimethylsiloxane (PDMS) PIC in which the precursor emulsion is flowed through a tapered channel. The channel width tapers from 250 μm to 40 μm, with an angle of 2.5$^{o}$. The channel height is kept constant at 200 μm. The FIPIE process is recorded with a high-speed camera.

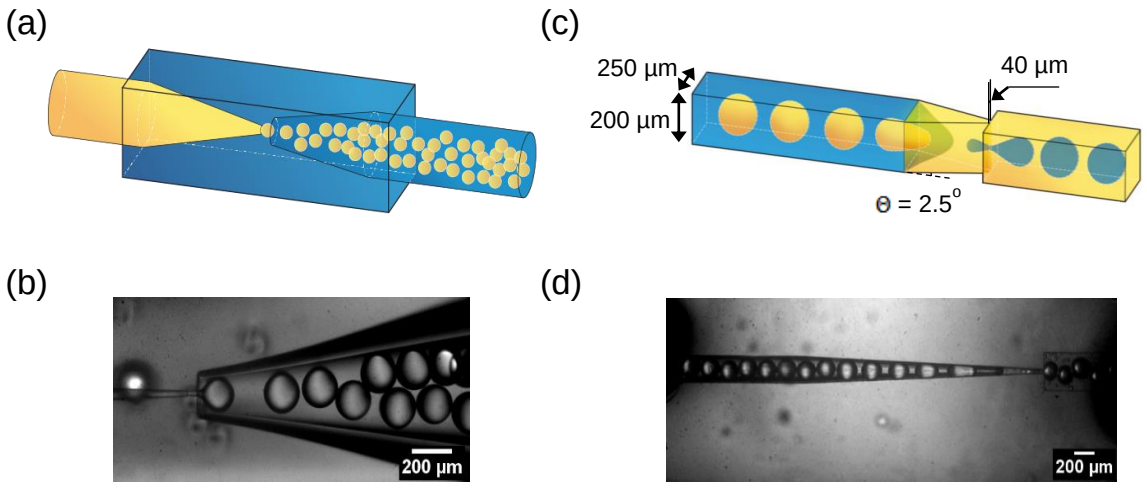


**Figure 3.1** Overview of precursor O/W emulsion generation and FIPIE processes. (a) Schematic illustration of precursor O/W emulsion generation in a glass capillary device. The aqueous and oil phases are presented in blue and yellow, respectively. (b) Optical microscope image of precursor O/W emulsion generation. (c) Schematic illustration of O/W to W/O FIPIE process in a tapered channel. The channel width tapers from 250 µm to 40 µm with an approach angle of $\Theta$ =2.5°. The channel height is 200 µm. (d) Optical microscope image of O/W to W/O FIPIE process in a tapered channel. The water phase contains methylene blue, imparting contrast between the two liquid phases.

### 3.2.2 Aqueous phase preparation and characterization

Aqueous solutions with Pluronics (BASF) are prepared by dissolving corresponding surfactants in deionized (DI) water (18.2 mΩ-cm, purified by Barnstead Nanopure System). Light mineral oil (LMO, Fisher) is used as the oil phase. Interfacial tensions (IFT) between aqueous solutions and LMO are measured by pendant drop tensiometry using an optical tensiometer (Attention Theta). A pendant drop of LMO is formed in the aqueous polymer solution using a U-shape dispensing needle. The curvature of the oil droplet is recoded and analyzed to obtain IFT (OneAttention). The interface is allowed to

equilibrate for an hour. The viscosities of the aqueous solutions of Pluronics are measured by using a Ubbelohde viscometer:

$$\mu = \frac{\mu_w t \rho}{t_w \rho_w} \qquad (3\text{-}1)$$

The viscosity of the Pluronic solutions are determined by measuring the time required for a defined volume of the solutions to flow pass through two measuring marks within a capillary tube. The efflux time of the Pluronic solutions are compared with that of water to calculate their viscosity. $\mu$ is the dynamic viscosity of the Pluronic solutions, $\mu_w$ is the dynamic viscosity of DI water, t is the efflux time of the Pluronic solutions, $t_w$ is the efflux time of DI water, $\rho$ is the density of the Pluronic solutions, and $\rho_w$ is the density of DI water.

### 3.2.3 Precursor oil-in-water emulsion preparation

Precursor O/W emulsions are prepared using a glass capillary device. Fabrication of the glass capillary device has been described elsewhere.[111-112] Briefly, aqueous and oil phases are introduced into the device using syringe pumps (Harvard Apparatus). The flow rates are kept at 100-500 µL/hr and 600-2000 µL/hr for the oil and aqueous phases, respectively. Uniform 200 µm diameter O/W emulsions are prepared with methylene blue added to the aqueous phase to facilitate visualization under an optical microscope (Figure 3.1).

### 3.2.4 Flow-induced phase inversion emulsification (FIPIE)

The precursor O/W emulsions are stored in vertically oriented polyethylene tubing for 1 hour. The creamed dispersed oil droplets are subsequently introduced into a PDMS PIC device to study FIPIE. Fabrication of the PDMS device has been described elsewhere.[111] The PIC channel height is 200 μm. The width of the PIC tapers from 250 μm to 40 μm with an approach angle of 2.5$^{o}$ (Figure 3.1). The channel surface is hydrophobically modified with octadecyltrichlorosilane (OTS, Sigma) and prewetted with LMO before injection of the precursor emulsions. The tubing with creamed precursor emulsions is reconnected to glass syringe (SGE Analytical Science, Trajan Scientific & Medical) containing corresponding aqueous phases, and the emulsions are injected into the PDMS devices at flow rates between 20 μL/hr and 2,000 μL/hr using a syringe pump (Harvard Apparatus). The velocity of each droplet is tracked by measuring the displacement of the oil droplet centroid, using images captured under an inverted microscope (Nikon Exlipse TE200) equipped with a high-speed camera (Phantom v7.1). Videos are recorded at the frame rates ranging between 10 and 100 frames per second. The ImageJ software package is used to process images and measure the distances traveled by droplets in the last 10 to 100 frames before their point of FIPIE or before they flow out of the tapered channel without FIPIE.

### 3.2.5 Interfacial dilatational elasticity measurement

The interfacial dilatational elasticity is measured using pendant drop tensiometry using the same set-up as that used in the aforementioned IFT measurement. The oil-water interface is created by dispensing a 5μL LMO droplet into an aqueous polymer solution using a U-shape dispensing needle. The droplet volume is sinusoidally oscillated to a maximum change of 10% of its original volume. The oscillating frequency is 0.01 Hz. The concentration of Pluronic solutions are 1 μM. The dynamic change in the shape of the LMO droplet is recorded and analyzed to obtain IFT and dilatation elasticity (OneAttention).

## 3.3 Results and Discussions

The effect of surfactant composition on FIPIE is investigated by examining the percentage of the precursor emulsion droplets that undergo FIPIE under a given set of conditions. The precursor emulsion is first generated in a glass capillary microfluidic device then introduced into a tapered PDMS channel as illustrated in Figure 3.1. The FIPIE of individual droplets is closely monitored under an inverted microscope.

To understand the effect of surfactant composition on the tendency of emulsion droplets to undergo FIPIE, we vary the molecular weight (MW) as well as the ratio of poly(ethylene oxide) (PEO) and poly(propylene oxide) (PPO) segments of the Pluronics. 10 Pluronics are selected which can be grouped in different ways to probe the effect of

various aspects of surfactant compositions and structures on FIPIE. The composition and molecular weight of the 10 Pluronics are summarized in Table 3.1.[20-21, 110]

**Table 3.1** Pluronics used in this work.

| Pluronic[a] | MW[b] | PEO%[c] | $n_{PEO}$[d] | $n_{PPO}$[e] |
|---|---|---|---|---|
| L64 | 2,900 | 40% | 2 ×13 | 30 |
| P65 | 3,400 | 50% | 2 × 18 | 29 |
| F68 | 8,400 | 80% | 2 × 76 | 29 |
| F77 | 6,600 | 70% | 2 × 53 | 34 |
| P84 | 4,200 | 40% | 2 × 19 | 43 |
| F88 | 11,400 | 80% | 2 × 103 | 39 |
| P104 | 5,900 | 40% | 2 × 27 | 61 |
| F108 | 14,600 | 80% | 2 × 132 | 50 |
| P123 | 5,750 | 30% | 2 × 19 | 69 |
| F127 | 12,600 | 70% | 2 × 100 | 65 |

[a]The nomenclature of Pluronics is composed of one letter followed by a 2 to 3-digit numeric code. The letter being either F, P, or L, stands for flakes, paste, or liquid. The one to two digits following the letter represent 1/300 of the molar mass of the PPO block of the Pluronics. The last digit represents one-tenth of the molar mass percentage of the

PEO blocks of the Pluronics. For example, the molar mass percentage of PEO in F108 is 80%, and its PPO block molar mass is around 10 × 300 = 3,000 (2,920) Da.[20, 110] [b,c]Molecular weight and PEO% are provided by the supplier, BASF. [d]$n_{PEO}$ represents the number of PEO units in a single PEO block. The average number of $n_{PEO}$ were calculated using the MW and PEO%. [e]$n_{PPO}$ represents the number of PPO units in the PPO block. The average number of $n_{PPO}$ were calculated using MW and PEO%.

Unless noted otherwise, we use aqueous solutions that have 0.01 M Pluronics, which is significantly higher than the critical micelle concentrations of the polymers. The tendency of emulsions to undergo FIPIE in the PIC channel is presented by plotting the frequency of FIPIE as a function of the product of Capillary number (Ca) and the ratio of the dynamic viscosities of the dispersed and continuous phases.

$$Ca = \frac{\mu_c \cdot v}{\gamma} \qquad (3\text{-}2)$$

Ca (Equation (3-2), $\mu_c$ is the dynamic viscosity of the continuous phase, v is the velocity of the emulsion extrapolated from droplet centroid displacement, and $\gamma$ is the interfacial tension between the continuous and dispersed phases) represents the relative importance of viscous force to the interfacial tension force and is widely used to understand dynamic fluid phenomena at small scales where the viscous forces dominate over the inertial forces.[113]

A recent study showed a strong correlation between break-up probability of a concentrated emulsion passing through a constricted channel and the product of Ca and

viscosity ratio ($\lambda$).[114] The viscosity ratio is defined as the dynamic viscosity ratio between that of the dispersed phase ($\mu_d$) and continuous phase ($\mu_c$):

$$\lambda = \frac{\mu_d}{\mu_c} \qquad (3\text{-}3)$$

The break-up profiles of the emulsions with different viscosity ratios collapse onto a single curve when $Ca \cdot \lambda$ is used as the variable. This indicates the viscosity of the droplet, which represents the resistance of the droplet against undergoing shape change under compression, is the determining factor for emulsion break-up. We adopt the product of Ca and $\lambda$ as the processing variable for our analysis.

The phase inversion frequency for an emulsion passing through the PIC is estimated based on the percentage of at least 30 droplets that undergo FIPIE:[111]

$$\text{FIPIE Frequency} = \frac{\text{\# of droplets that undergo FIPIE}}{\text{\# of droplets that pass through the PIC}} \qquad (3\text{-}4)$$

The frequency of FIPIE as a function of $Ca \cdot \lambda$ show profiles that can be described by a modified logistic function:

$$y(x) = \frac{(x)^k}{(x)^k + (x_o)^k} \qquad (3\text{-}5)$$

For each FIPIE profile, the coordinate of the measurement that is closest to 50% FIPIE frequency is used as the inflection point coordinate to fit the logistic function plot. The

coordinate of the inflection point of each curve ($x_o$, 50%) is included in the logistic function as shown in Equation (3-5). The exponent k is adjusted to have the minimum residual sum of squares between predicted values and the experimental measurements for each FIPIE profile.

The concentration of L64 and P65 is kept at 0.05M because the O/W emulsions formed with 0.01M L64 and P65 are not stable enough for the subsequent FIPIE investigation. In the meantime, such concentration change should not alter the original trend in Pluronics to be tested. The FIPIE profiles shift when Pluronic concentration is changed as shown in Figure 3.2 for P84, P104, and F127. Yet with a decrease of the Pluronic concentration, the FIPIE profiles shift rightwards. Thus, if the 0.01M L64 and 0.01M P65 FIPIE profile could be plotted, they likely will be located further to right than their current 0.05M profiles. As shown in Figure 3.3a and 3.4a, the L64 and P65 FIPIE profiles are already the rightmost profiles in the plots, respectively. Thus, the overall trends would have stayed consistent with our discussion if FIPIE experiments had been performed with 0.01M L64 and P65 stabilized emulsions.

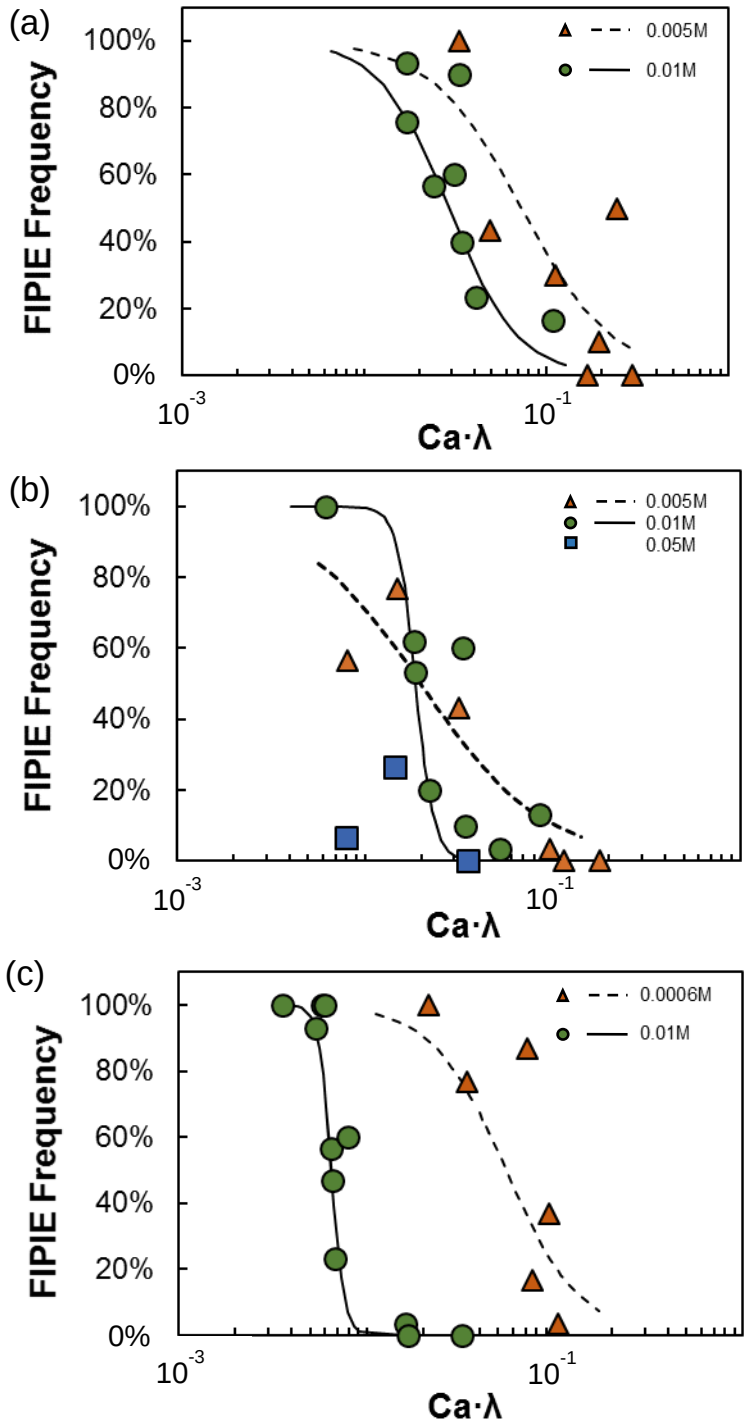


**Figure 3.2** Pluronics concentration effect on FIPIE. (a) P84, (b) P104, (c) F127.

### 3.3.1 Effect of molecular weight (MW) of triblock copolymers on FIPIE

To test the effect of molecular weight (MW) of the block copolymer, three sets of Pluronics at different PEO% with increasing MW are compared. In the increasing order of MW, Set 1-1 comprise MW = 2,900, 4,200, 5,900: L64< P84 < P104; Set 1-2: MW = 6,600, 12,600: F77 < F127; Set 1-3: MW= 8,400, 11,400, 14,600: F68 < F88 <F108 (Table 3.2). All FIPIE profiles have similar shapes that can be described by logistic functions, with FIPIE frequency decreasing from 1 to 0 with increasing $Ca \cdot \lambda$ as seen in Figure 3.3. Emulsions that can sustain lower $Ca \cdot \lambda$ without undergoing FIPIE are more resistant to FIPIE. Thus, a leftward shift in FIPIE profiles with increasing of MW observed in Figure 3.3 suggests decreased tendency of emulsions to undergo FIPIE, or increased stability of emulsions against FIPIE with an increase in the MW of Pluronics.

**Table 3.2** Pluronics used in analyzing effect of MW of triblock copolymers on FIPIE.

| Set | Pluronic | MW | PEO% | $n_{PEO}$ | $n_{PPO}$ |
|---|---|---|---|---|---|
| 1-1 | L64 | 2,900 | 40% | 2 × 13 | 30 |
| | P84 | 4,200 | 40% | 2 × 19 | 43 |
| | P104 | 5,900 | 40% | 2 × 27 | 61 |
| | | | | | |
| 1-2 | F77 | 6,600 | 70% | 2 × 53 | 34 |
| | F127 | 12,600 | 70% | 2 × 100 | 65 |
| | | | | | |
| 1-3 | F68 | 8,400 | 80% | 2 × 76 | 29 |
| | F88 | 11,400 | 80% | 2 × 103 | 39 |
| | F108 | 14,600 | 80% | 2 × 132 | 50 |

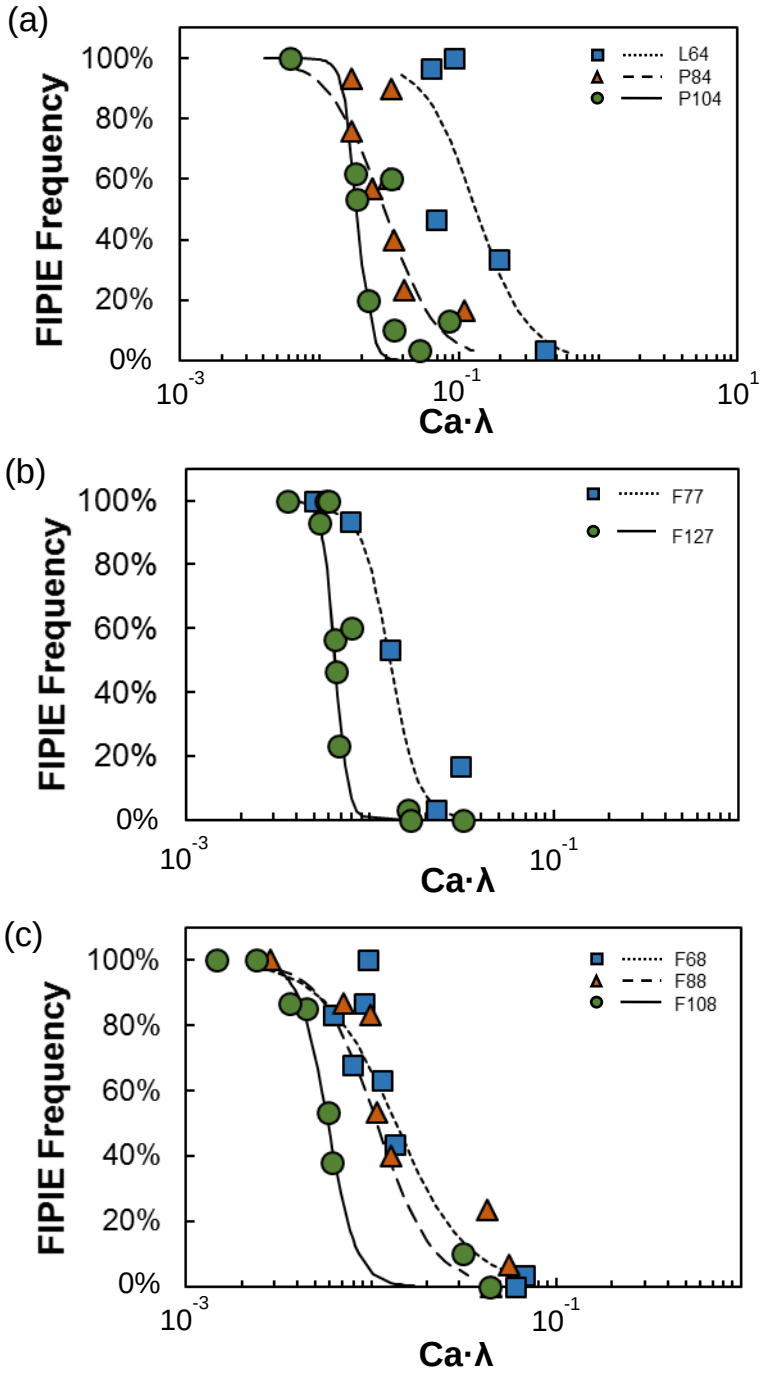


**Figure 3.3** FIPIE frequency of O/W emulsions in PICs as a function of Ca·λ, for sets of Pluronics with constant $n_{PEO}/n_{PPO}$ and increasing MW. (a) Set 1-1: 40% PEO Pluronics with MW in the order of L64<P84<P104; (b) Set 1-2: 70% PEO Pluronics with MW in the order of F77<F127; (c) Set 1-3 80% PEO Pluronics with MW in the order of F68<F88 < F108.

### 3.3.2 Effect of PEO length on FIPIE

We probe the effect of the length of PEO blocks while keeping the length of PPO blocks constant to isolate and analyze the effect of $n_{PEO}$ (length of PEO) on FIPIE using three sets of Pluronics. In the increasing order of $n_{PEO}$, Set 2-1: $n_{PEO}$ = 13, 18, 76: L64 < P65 < F68; Set 2-2: $n_{PEO}$ = 19, 103: P84<F88; Set 2-3: $n_{PEO}$ = 27, 132: P104 <F108 (Table 3.3). The FIPIE profiles shift uniformly leftwards with increase of $n_{PEO}$, indicating that emulsion's tendency to undergo FIPIE decreases with an increase in $n_{PEO}$ (Figure 3.4).

**Table 3.3** Pluronics used in analyzing effect of $n_{PEO}$ of triblock copolymers on FIPIE.

| Set | Pluronic | MW | PEO% | $n_{PEO}$ | $n_{PPO}$ |
|---|---|---|---|---|---|
| 2-1 | L64 | 2,900 | 40% | 2 × 13 | 30 |
| | P65 | 3,400 | 50% | 2 × 18 | 29 |
| | F68 | 8,400 | 80% | 2 × 76 | 29 |
| | | | | | |
| 2-2 | P84 | 4,200 | 40% | 2 × 19 | 43 |
| | F88 | 11,400 | 80% | 2 × 103 | 39 |
| | | | | | |
| 2-3 | P104 | 5,900 | 40% | 2 × 27 | 61 |
| | F108 | 14,600 | 80% | 2 × 132 | 50 |

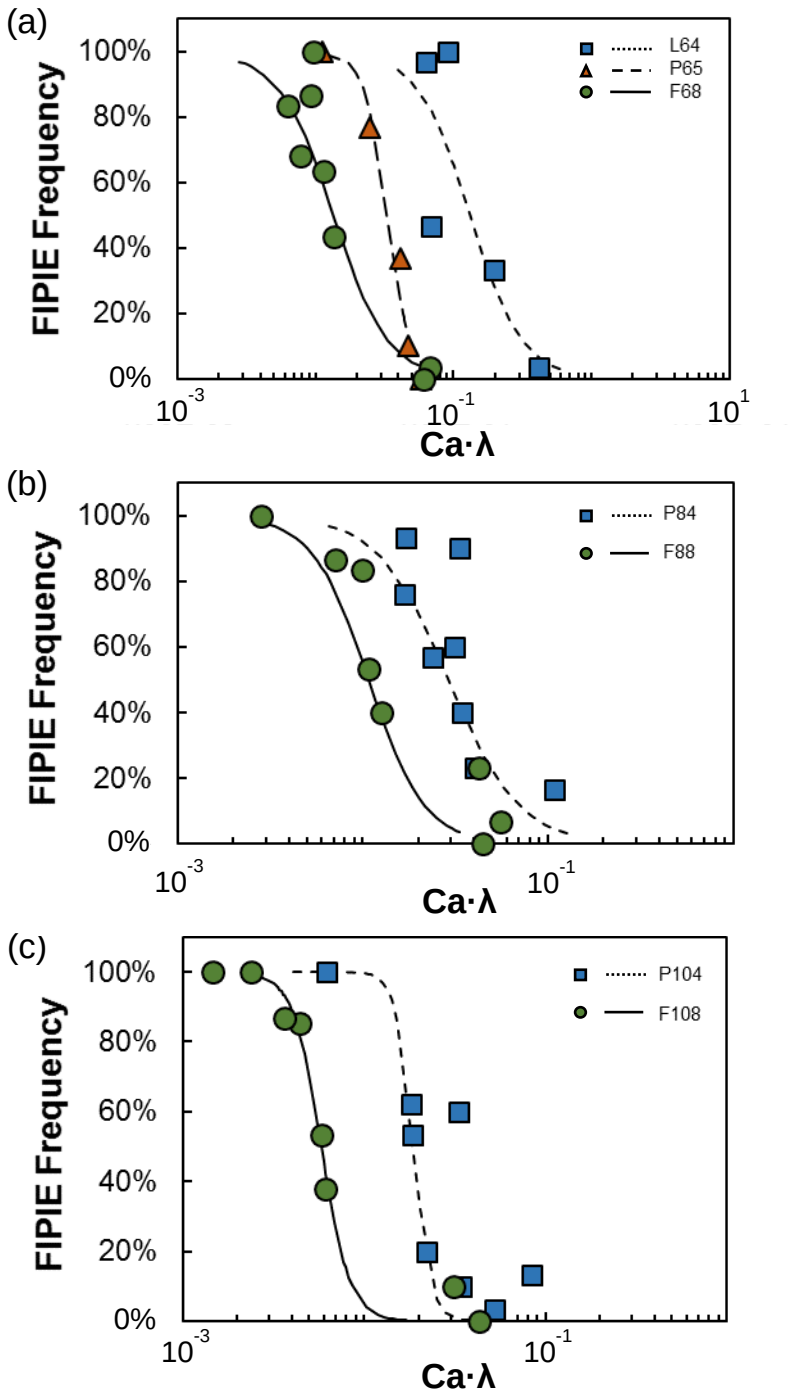


**Figure 3.4** FIPIE frequency of O/W emulsions in PICs as a function of Ca·λ, for sets of Pluronics with constant $n_{PPO}$ and increasing $n_{PEO}$. (a) Set 2-1: $n_{PEO}$ in the order of L64<P65<F68; (b) Set 2-2: $n_{PEO}$ in the order of P84<F88; (c) Set 2-3: $n_{PEO}$ in the order of P104<F108.

### 3.3.3 Effect of PPO length on FIPIE

Here we study the effect of the length of PPO blocks while keeping the length of PEO blocks constant to isolate and analyze the effect of $n_{PPO}$ (length of PPO) on FIPIE using two sets of Pluronics. In the increasing order of $n_{PPO}$, Set 3-1: $n_{PPO}$ = 29, 43, 69: P65 < P84 < P123; Set 3-2: $n_{PPO}$ =39, 65: F88 < F127 (Table 3.4).

Interestingly, the FIPIE frequency profiles for P65 and P84 are quite similar, whereas the P123 stabilized emulsions exhibit dramatic resistance against FIPIE despite their similar $n_{PEO}$; 100% FIPIE cannot be achieved when emulsions are stabilized with P123 even at very low values of $Ca \cdot \lambda$ (Figure 3.5). In the meantime, the Set 3-2 FIPIE profiles shift leftwards with increase of $n_{PPO}$.

**Table 3.4** Pluronics used in analyzing effect of $n_{PPO}$ of triblock copolymers on FIPIE.

| Set | Pluronic | MW | PEO% | $n_{PEO}$ | $n_{PPO}$ |
|---|---|---|---|---|---|
| 3-1 | P65 | 3,400 | 50% | 2 × 18 | 29 |
| | P84 | 4,200 | 40% | 2 × 19 | 43 |
| | P123 | 5,750 | 30% | 2 × 19 | 69 |
| | | | | | |
| 3-2 | F88 | 11,400 | 80% | 2 × 103 | 39 |
| | F127 | 12,600 | 70% | 2 × 100 | 65 |

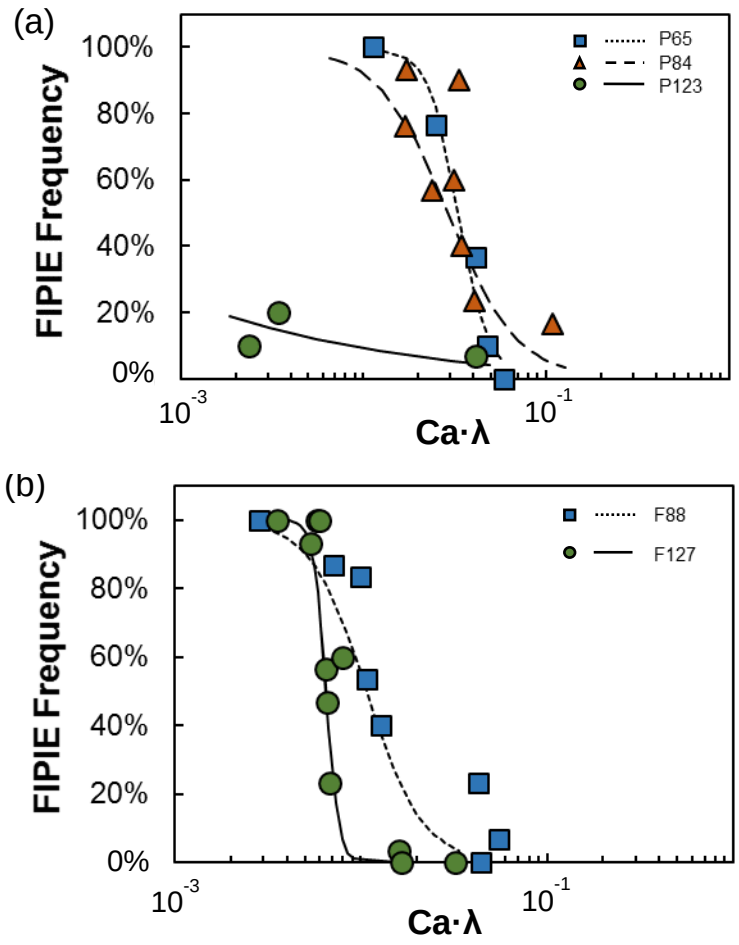


**Figure 3.5** FIPIE frequency of O/W emulsions in PICs as a function of Ca·λ, for sets of Pluronics with constant $n_{PEO}$ and increasing $n_{PPO}$. (a) Set 3-1: $n_{PPO}$ in the order of P65<P84<P123; (b) Set 3-2: $n_{PPO}$ in the order of F88<F127. P123 curve is an aid for the eye rather than a fit to a logistic function.

### 3.3.4 Pluronic steric pressure analysis in the aqueous film

These results show surfactant composition strongly affects the tendency of an emulsion to undergo FIPIE. The FIPIE tendency of Pluronic-stabilized emulsions show consistent negative correlation with $n_{PEO}$ as seen by the leftward shift of FIPIE profiles when an emulsion is stabilized with triblock copolymers with longer PEO blocks. This trend could originate from the conformation of the triblock copolymer at the oil-water interface. Prior studies on the behavior of Pluronics at the oil-water interface have reported that PEO blocks form brush-like layers that stretch into the aqueous phases, providing steric repulsion between approaching oil-water interfaces.[115-116] With an increase in the $n_{PEO}$, the thickness of the resulting brush layer increases, strongly suggesting that the tendency of emulsion droplets to undergo FIPIE depends on the strength of repulsive steric interactions provided by the hydrophilic domain of the copolymer surfactant.

It was previously shown that a critical step that leads to the FIPIE of an emulsion in a tapered channel is the drainage and rupture of an aqueous film between an oil droplet and a wetting layer of oil on the channel surface as the droplet passes through the tapered channel.[102, 111] As the oil droplet is deformed, the aqueous film is thinned and eventually this film destabilizes, leading to film rupture and phase inversion of the emulsion. We hypothesize that the rupture of this aqueous film is correlated with the so-called driving pressure which is the difference between capillary pressure and the disjoining pressure: [117-120]

$$\Delta P = P_{\sigma} - \Pi \qquad (3\text{-}6)$$

where $\Delta P$ is the driving pressure, $P_\sigma$ is the capillary pressure across the fluid interface, and $\Pi$ is the disjoining pressure. The driving pressure determines whether drainage of a fluid film would take place as well as the rate of liquid drainage from the film.

The disjoining pressure, $\Pi$, is a combination of thermodynamic forces that act upon a liquid film, including van der Waals (vdW) attraction, steric repulsion, and electrostatic interaction, and can be expressed as:[51, 121-122]

$$\Pi = \Pi_{vdW} + \Pi_{steric} + \Pi_{elec}. \quad (3\text{-}7)$$

We hypothesize that the tendency of emulsions to undergo FIPIE depends strongly on steric repulsion pressure which decreases driving pressure for thinning of the aqueous film and suppresses the reduction in the film thickness. Electrostatic contribution to the disjoining pressure is likely to be negligible in the current system since Pluronic is a non-ionic surfactant. Steric pressure from a brush layer can be estimated based on the Alexander-de Gennes brush model:[116, 123-124]

$$\Pi_{steric} = \alpha \frac{k_B T}{s^3}\left[\left(\frac{2\delta}{h}\right)^{9/4} - \left(\frac{h}{2\delta}\right)^{3/4}\right] \text{ at } 0 < 2\delta < h \quad (3\text{-}8)$$

$$\Pi_{steric} = 0 \text{ at } 2\delta \geq h$$

where $\alpha$ is empirically fitted parameter, s is the average distance between anchor points of PEO blocks at the water-oil interface, $\delta$ is the brush layer thickness, and h is the thickness of the thin film.

The measurements of the Pluronics brush layer thickness and the amount adsorbed at the PDMS droplet /water interface reported in a prior study are used in our calculation.[125-127] The empirically fitted parameters from prior reports are used.[124, 128] Based on the relative PEO/PPO ratio, $\alpha$ are selected to be 0.02 for L64, P84, P104 (PEO < PPO), and 0.07 for F68, F88, F108 (PEO> PPO). The brush layer thicknesses of P84, F88, P104, and F108 from prior reports on Pluronic adsorption at PDMS droplet/water interface are used (Table 3.5).[126-127] The brush layer thickness of L64 and F68 are extrapolated based on Equation (3-9) and (3-10).[127]

$$< R_g{}^2 > = 2nl^2 \qquad (3\text{-}9)$$

$$\% \text{ Extension} = \frac{\delta_{max}}{R_g{}^2} \times 100\% \qquad (3\text{-}10)$$

The brush layer is formed mainly by the PEO blocks of the Pluronics. $R_g^2$ is an estimate of the end-to-end distance of the PEO blocks, n is the number of PEO units within the blocks, l is the length of one PEO unit (l = 0.396 nm), $\delta_{max}$ is the maximum (plateau) brush layer thickness measured, and % extension is the comparison between $\delta_{max}$ and $Rg^2$ of the PEO block.

Measurements obtained by Barnes[127] indicate the % extension of Pluronic adsorbed at PDMS droplet/water interface depends on the relative sizes of PEO and PPO blocks. Pluronic with long PPO blocks are reported to have full extension of the PEO blocks while full extension is not achieved by Pluronics with PEO blocks longer than PPO blocks (F-series Pluronics). Thus, we extrapolate the % extension of the PEO blocks of

L64 and F68 to be 100% and 48% respectively. The brush layer thicknesses of L64 and F68 are calculated as 4.1, and 11.5 nm and included in Table 3.5.

**Table 3.5** Pluronics' brush layer % extension and thickness.

| | $n_{PEO}$ | %Extension | Measured Brush layer thickness (nm) | Extrapolated %Extension | Calculated Brush layer thickness (nm) |
|---|---|---|---|---|---|
| L64 | 13.2 | | | 100% | 4.1 |
| P84 | 19.1 | 95%[127] | 5.7[127] | | |
| P104 | 26.8 | | 7.0[126] | | |
| | | | | | |
| F68 | 76.4 | | | 48% | 11.5 |
| F88 | 103.6 | 48%[127] | 15.5[127] | | |
| F108 | 132.7 | 49%[127] | 20.6[127] | | |

The average distance between PEO blocks are calculated based on the area per molecule of Pluronic adsorbed at PDMS droplet/water interface. We use the area per molecule values of F88 and F108 reported by Barnes et al.[127] and Prestidge et al.,[125] which they calculated based on the amount of Pluronics adsorbed at the PDMS droplet /water interface. It is reported that the area per Pluronic surfactant depends on its PEO block length.[124, 127-129] By plotting the area per molecule of Pluronics adsorbed at PDMS droplet/water interface as a function of PEO block length ($n_{PEO}$), we estimate the area per molecule for L64, P84, P104, and F68 using the linear relationship shown in Figure 3.6.

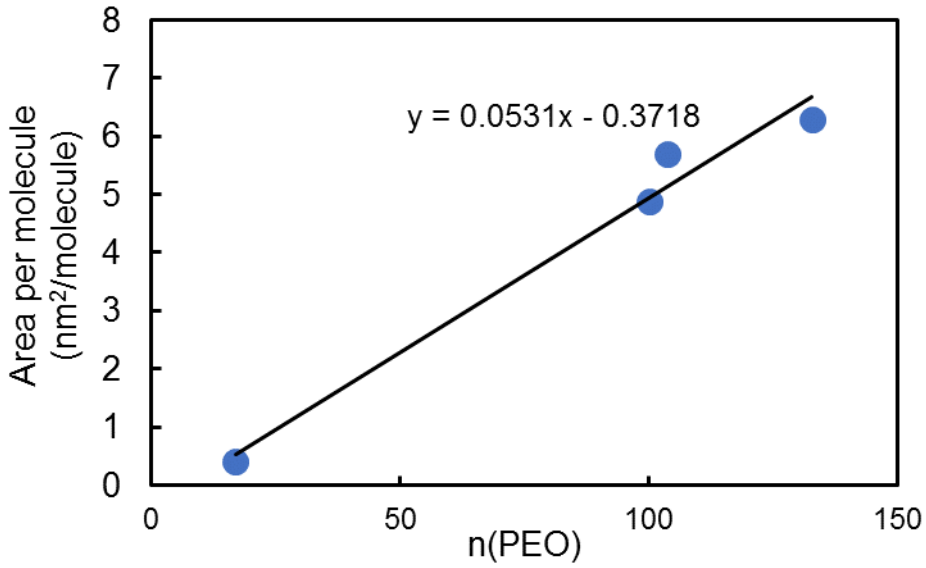


**Figure 3.6** Area per molecule plotted against the length of the PEO for PEO-PPO-PEO copolymers on liquid PDMS droplets.[127]

$$s = \sqrt{\frac{1}{\text{Area per molecule } (\text{nm}^2)}} \qquad (3\text{-}11)$$

The average distance between anchor points of PEO blocks at the oil/water interface are then estimated as the square root of the area per molecule using Equation (3-11).[128] The data is presented in Table 3.6.

**Table 3.6** Pluronics' area per molecule and average distance between anchor points of PEO blocks at the oil-water interface (s).

| | Area per molecule ($nm^2$/molecule) | s (nm) |
|---|---|---|
| L64 | 0.33 | 0.57 |
| P84 | 0.64 | 0.80 |
| P104 | 1.05 | 1.03 |
| | | |
| F68 | 3.69 | 1.92 |
| F88 | 5.70[127] | 2.39 |
| F108 | 6.30[127] | 2.51 |

With these parameters, the steric pressure provided by different triblock copolymer surfactants are calculated as shown in Figure 3.7.

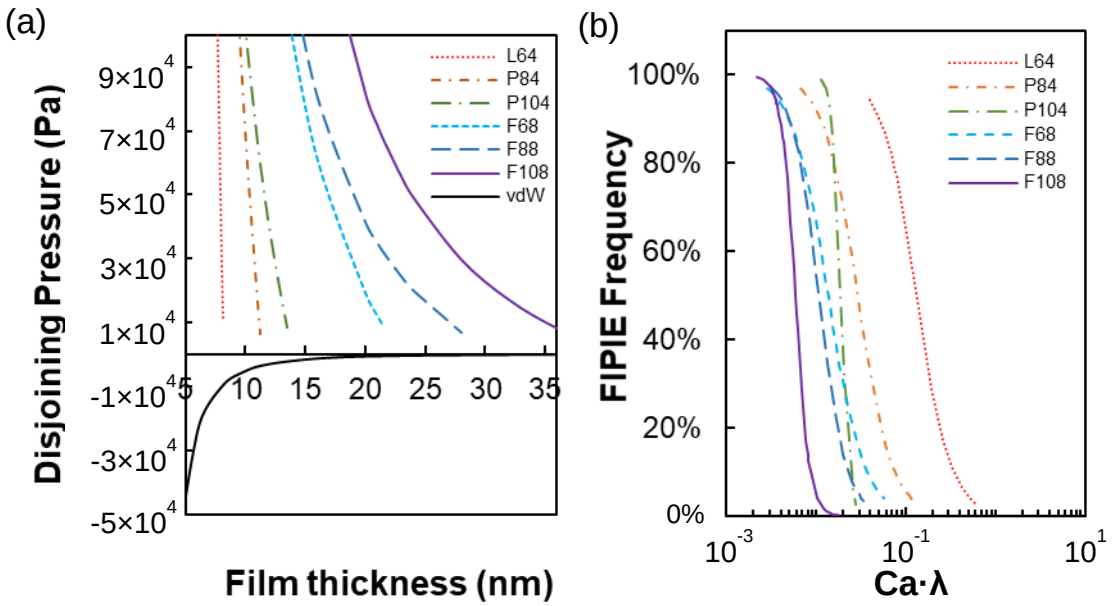

**Figure 3.7** (a) van der Waals (vdW shown in the black solid curve) attraction, steric repulsion of 6 Pluronics, L64, P84, P104, F68, F88, and F108, calculated as a function of aqueous film thickness (b) FIPIE profile of the 6 Pluronics.

In addition, the van der Waals attraction is also estimated, using Hamaker constant (A), and the thickness of the thin film (h), shown in Equation (3-12). We use A = to $1x10^{-19}$ J in our analysis.[51]

$$\Pi_{vdW} = \frac{A}{6\pi h^3} \qquad (3\text{-}12)$$

For a given aqueous film thickness, the vdW attraction stays constant, whereas steric repulsion pressure increases with molecular weight and $n_{PEO}$, lowering the total driving pressure for aqueous film drainage, and increasing the resistance of the emulsion against FIPIE. This trend (Figure 3.7a) is consistent with the resistance of emulsions to undergo FIPIE as summarized in Figure 3.7b, and thus strongly supports the hypothesis that larger Pluronics and longer PEO are able to resist FIPIE by providing stronger steric repulsions between oil droplets and oil layers on the channel surface. The consistency in the FIPIE trend and steric pressures provided by Pluronics offers us an insight into the role of steric repulsions in film rupture in dynamic flow conditions.

The inflection points of the FIPIE profiles also show a power law correlation with the steric repulsion pressures provided by the Pluronics as shown in Figure 3.8a. This trend indicates that while there is a strong inverse correlation between the steric repulsion pressure and the length of PEO in determining the tendency of emulsions to undergo FIPIE, with an increase in the PEO%, the MW effect on FIPIE suppression diminishes.

For the Set 1-1, Pluronics with 40% PEO, the inflection points shifted leftwards by 0.1136 as the MW increases from 2900 Da (L64) to 5900 Da (P104). Comparatively, for the Set 1-3, Pluronics with 80% PEO, the inflection points shifted leftwards by only 0.0077 as the MW increases from 8400 Da (F68) to 14600 Da (F108).

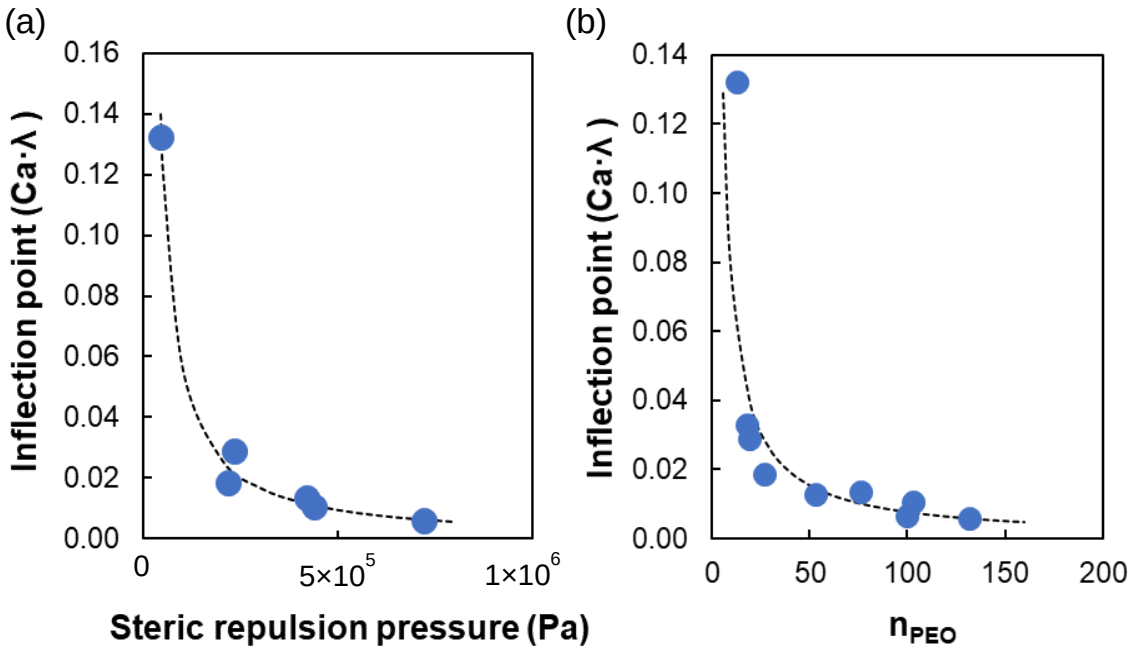


**Figure 3.8** FIPIE profile inflection points plotted as a function of (a) the steric repulsion pressure provided by Pluronics, steric pressures calculated at aqueous film thickness of 8 nm for L64, P84, P104, F68, F88, and F108, and of (b) the $n_{PEO}$ of all Pluronics used in this study except P123.

### 3.3.5 Dilatational elasticity analysis on Pluronics with different PPO block lengths

P123-stabilized emulsions exhibit a unique behavior when they are compared to those stabilized with Pluronics with similar $n_{PEO}$ but different $n_{PPO}$. Emulsions made with P123 show extraordinarily high resistance against FIPIE; FIPIE frequency was suppressed to under 20% for the entire range of $Ca \cdot \lambda$ we explored. While we do not fully understand the mechanism behind such high resistance against FIPIE, one possibility is that the high stability originates from the long PPO block of P123 compared to P84 and P65. The PPO blocks can dwell at the fluid interface thus provide high dilatational elasticity leading to high resistance against rupture of the aqueous film during large deformation of the emulsion interface. Prior studies have in fact shown that emulsions with increased dilatational elasticity have higher emulsion stability, consistent with our results.[130-131]

To test this hypothesis, we use the oscillating pendant drop method to probe the interfacial rheology of Pluronic-covered oil-water interfaces. The dynamic changes of area and IFT of a sinusoidally oscillated pendant drop are recorded (Figure 3.9), from which the storage modulus (E') at the interface can be derived.

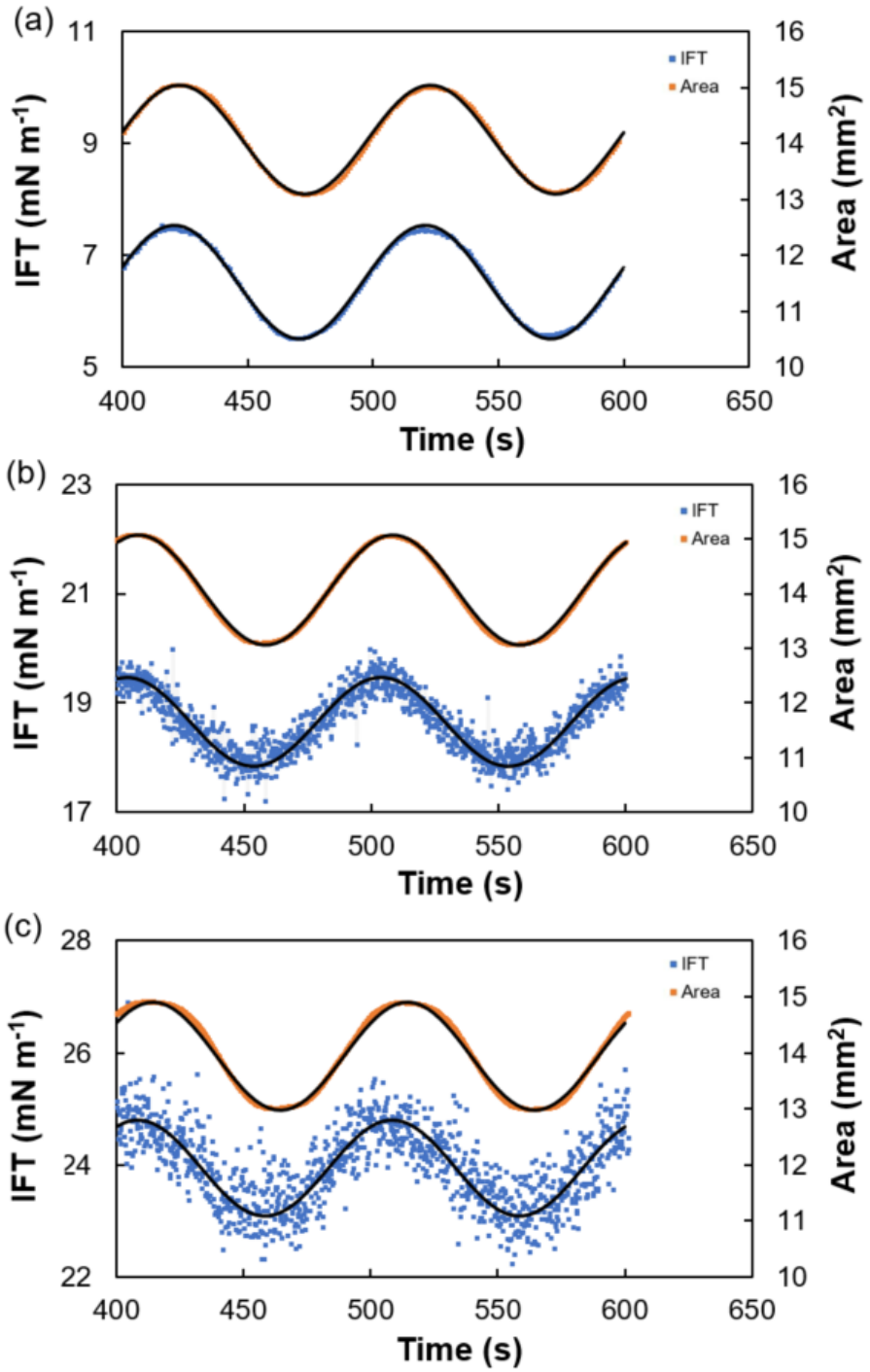


**Figure 3.9** Interfacial area and interfacial tension changes induced by sinusoidally oscillating an LMO oil pendent drop in contact with (a) P123, (b) P84, and (c) P65 aqueous solutions. The concentrations of the Pluronics are kept at 1 μM. The oscillating frequency is 0.01 Hz.

$$\tan\delta = \frac{\zeta}{1+\zeta} \tag{3-13}$$

$$E_o = \frac{\tilde{\gamma}}{\tilde{A}/A} \cdot \sqrt{1 + 2\zeta + 2\zeta^2} \tag{3-14}$$

$$E' = E_o \cdot \frac{1+\zeta}{1 + 2\zeta + 2\zeta^2} \tag{3-15}$$

$$E'' = E_o \cdot \frac{\zeta}{1 + 2\zeta + 2\zeta^2} \tag{3-16}$$

$\delta$ is the phase angle between area and IFT waves. We use the differences between the peaks of area and IFT waves to calculate $\delta$. It can be presented as a function of the dimensionless factor, $\zeta$. The limiting elasticity, $E_o$, is a function of $\tilde{\gamma}$, the amplitude of the interfacial tension oscillation, $\tilde{A}$, the amplitude of the interfacial area oscillation, A, the mean interfacial area, and $\zeta$. The $E'$, and the loss modulus ($E''$) can then be calculated using Equation (3-15) and (3-16).

Our results show the P123 provides the highest storage modulus, 14.22 mN/m, whereas the storage modulus provided by P84 and P65 are 10.29 and 10.88 mN/m respectively (Table 3.7). The phase angle between the area and IFT curves also increase from 7.17$^o$ of P123 to 16.93$^o$ of P84 and 20.45$^o$ of P65, implying the interfaces becoming more viscous and less elastic.

**Table 3.7** Interfacial moduli of P123, P84, and P65 covered oil-water interface.

| | Storage modulus (E' (mN $m^{-1}$)) | Loss modulus (E" (mN $m^{-1}$)) | Phase angle (δ ($^o$)) |
|---|---|---|---|
| P123 | 14.22 | 1.79 | 7.17 |
| P84 | 10.29 | 3.11 | 16.93 |
| P65 | 10.88 | 4.07 | 20.45 |

## 3.4 Conclusions

In this chapter, we provide a comprehensive investigation of the effect of Pluronic composition and molecular weight on the FIPIE of emulsions in a tapered channel. There is a negative correlation between Pluronic $n_{PEO}$ and the tendency of emulsions to undergo FIPIE in a tapered channel. Our results suggest that upon compression, the brush layers formed by the hydrophilic domain of PEO-PPO-PEO copolymer surfactants at the interfaces provide high steric repulsion, suppressing the drainage of the thin aqueous film and coalescence of the oil phases. These effects subsequently hinder FIPIE. We also observe significant suppression of FIPIE by a small molecular weight, high PPO% Pluronic, P123, which we attribute to dilatational elasticity provided by its PPO blocks at

the oil/water interface. We believe the understanding obtained in this work will potentially promote broader application of FIPIE, reducing emulsification energy cost, and enabling continuous processing of emulsions for materials fabrications.[98, 111, 132]

# Chapter 4 Phase Inversion Emulsification via Dynamic Ion Pairing

## 4.1 Introduction

Emulsions are mixtures of two immiscible liquids, one dispersed in the other. They are used in various fields including cosmetic,[133-134] food,[1] and pharmaceutical industries.[135-136] Because of their high interface to volume ratio, products using emulsion with small droplets can efficiently deliver the cargo they contain. In general, a large energy input is necessary to produce emulsions with small droplets using conventional emulsification processes such as mechanical stirring. Studies have shown that of the energy that is used to produce an emulsion, only a very small fraction as low as 0.1 % is used to produce the droplets; most of the energy is dissipated.[11,92] Emulsification is intrinsically a very energy inefficient process. Phase inversion emulsification (PIE), which is a process that generates a target emulsion through switching the dispersed and continuous phases of a precursor emulsion, is a novel emulsification method that can be very energy efficient.[98]

To reduce the energy requirement for emulsification and also to prolong the stability of emulsions, surface active agents (a.k.a., surfactants) are added to the liquid mixtures.[4] Typically, these surfactants are amphiphilic compounds containing both hydrophilic and hydrophobic parts. It has been shown that one method to trigger phase inversion emulsification is to induce a change in the amphiphilic nature of the surfactant. For example, emulsion stabilized by di-block copolymer synthesized using styrene and (2-(dimethylamino)ethyl methacrylate) (DMAEMA) undergoes phase inversion upon

temperature change because DMAEMA is thermosensitive and its hydrophilicity decreases upon temperature increase.[10]

There is a surging consumer demand for replacing various chemical agents used in manufacturing of consumer goods with agents of natural origin, due to both health and environmental considerations.[137] While petrochemical-based materials have been identified as the source of toxicity in various products, such as in detergents,[138-139] natural materials are generally considered better tolerated by the human and animals, and leave less negative impact to the environment as being biodegradable.[25-26] Among the many materials of natural origin, polysaccharides have gained significant interest and is now broadly applied in coating and food processing.[24, 140-141] Among polysaccharides, chitosan is the second most abundant type after cellulose and has functionalities such as antibacterial properties.[142] Composed of β-(1→4)-linked D-glucosamine and N-acetyl-D-glucosamine, chitosan is reported to be hydrophilic and possess only weak surface activity.[143] Modification is needed to increase the amphiphilicity of chitosan so that it can stabilize the oil-water interfaces. A common technique for its modification is Schiff's base reaction, which covalently bonds amine groups of chitosan to aldehydes.[23, 144] Also, no water-in-oil (W/O) emulsions has been stabilized using chitosan as the surfactant.

Ion pairing is a process that binds two molecules that bear opposite charges through electrostatic interaction.[29] In Chapter 2, we have extracted a polyelectrolyte into an organic solvent by ion pairing. Inspired by our prior work, we hypothesize that we can use ion pairs formed by chitosan and an oppositely charged species to stabilize oil-in-water (O/W) emulsions and also to induce PIE and form W/O emulsions. In this study, we use dioctyl sulfosuccinate sodium salt (AOT) as a model agent to form ion pairs with

chitosan. We show that by emulsifying an aqueous solution containing chitosan and toluene containing AOT, both W/O and O/W emulsions can be generated. The emulsion type as well as size of the emulsion droplets are shown to depend on the solution pH and the molar ratio of chitosan and AOT.

## 4.2 Experimental Section

### 4.2.1 Materials

Chitosan (C, degree of deacetylation= 75-85%; MW = 50,000- 190,000 Da), dioctyl sulfosuccinate sodium salt (AOT, purity ≥ 97%), octadecyltrichlorosilane (OTS), and Nile Red (technical grade) were purchased from Sigma-Aldrich. Acetic acid (AA), hydrochloric acid (HCl), sodium hydroxide (NaOH), toluene, were purchased from Fisher. Deionized (DI) water (18.2 mΩ-cm, purified by Barnstead Nanopure System) was used to prepare all aqueous solutions.

### 4.2.2 Emulsion preparation

A chitosan stock solution is made by dissolving 1% w/v chitosan in 1% v/v AA solution and stirred overnight at room temperature.[23] The resulted chitosan stock solution is further diluted to 0.1 %w/v using DI water for emulsion generation. The solution pH is adjusted using HCl and NaOH. The oil phase is prepared by dissolving various amount of AOT in toluene. Emulsions are generated by mixing an equal volume of aqueous and

toluene solutions. 3 mL of aqueous solution containing chitosan and 3mL of toluene containing AOT are added to the same vial. The mixture is first emulsified with a vortex mixer for 30 s, followed by homogenization using a homogenizer (IKA Ultra-Turrax T25 Basic) at 9500 rpm for 1 min. Control emulsions using only chitosan are made by homogenizing aqueous solutions containing chitosan and pure toluene. Control emulsions using only AOT are made by homogenizing DI water and toluene containing AOT.

Fluorescence images are captured using a confocal laser scanning microscope (Olympus Fluo View FV 1000). 0.01 wt% Nile Red is added to the toluene solution for fluorescence imaging. The emulsions are injected into a glass microchannel with a $1.05 \times 1.05$ $mm^2$ square cross section. To image W/O emulsions, glass microchannels are treated with 30 s OTS (1 vol% in toluene) salinization followed by 30 min heat treatment on a hot plate at 150 $^{o}$C.

### 4.2.3 Interface characterization using pendant drops

To characterize the interface between oil and water upon the formation of chitosan/AOT ion pair formation, we use pendant drop tensiometry (Attention Theta). A pendant drop of toluene is formed in the aqueous solution using a U-shape dispensing needle. The curvature of the toluene droplet is recoded and analyzed to obtain interfacial tension (IFT) (OneAttention). The interface is allowed to equilibrate for an hour. The aqueous solutions tested include DI water, 0.1% w/v chitosan aqueous solutions with pH adjusted to 2.5, 4.1, and 6.4. The toluene solutions have AOT concentrations of 0, 0.6mM, and

6mM. Due to solubility of AOT in both water and toluene, the IFT at the toluene-water interface when AOT is present is measured with 0.6 mM and 6mM AOT added to DI water, while toluene is used as the pendent drop.

## 4.3 Results and Discussions

### 4.3.1 Control emulsion by adding either chitosan or AOT

Chitosan is a naturally occurring weak polyelectrolyte (pKa = 6.5).[145-146] With its amine groups protonated, chitosan is positively charged at low pH. To dissolve chitosan in DI water, acetic acid (AA) is often added to facilitate the process. Chitosan is fully protonated at pH 4.[147] It deprotonates with an increase of solution pH and eventually precipitates out of the solution at pH 6.5.[148] The precipitation at such a pH range indicates that the chitosan without any charge is rather hydrophobic and cannot stay hydrated and solubilized in water.

(a) 

(b) 

(c)  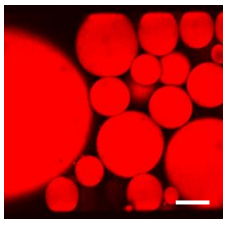

(d)  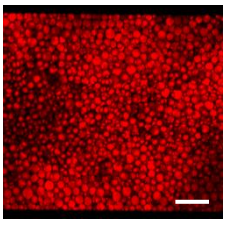

**Figure 4.1** Macroscopic and fluorescence microscopy images of emulsion by emulsifying aqueous solutions containing chitosan at different pHs and toluene: (a) pH 2.5 (b) pH 4.1 (c) pH 5.3 (d) pH 6.4.

As shown in Figure 4.1, chitosan alone cannot stabilize an emulsion when pH of the aqueous solution is at 4.1 or below. This is possibly because chitosan is highly charged and rather hydrophilic under such an acidic condition; thus its surface activity is very low – it stays fully dissolve/hydrated in the water phase. With an increase in the pH of the aqueous solution, chitosan deprotonates and gains surface activity, likely due to the hydrophobic nature of the uncharged glucosamine groups. Stable O/W emulsions are formed and the size of the O/W emulsion droplets decreases with an increase in the aqueous solution pH. The smallest droplet is achieved at pH 6.4 in our study for emulsions made using chitosan alone.

(a)

(b)

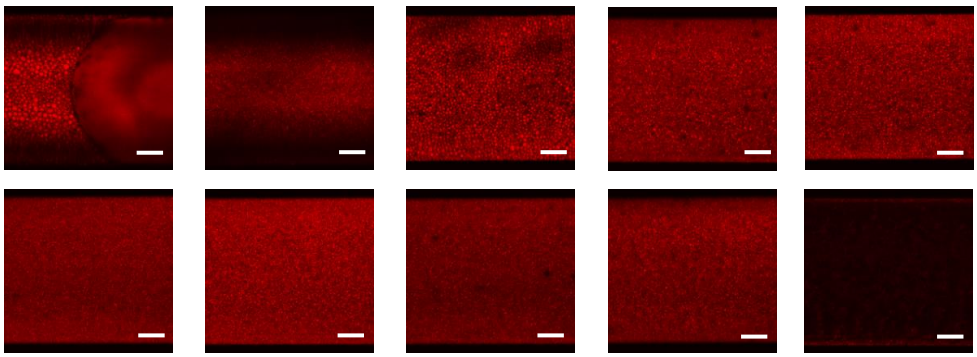

**Figure 4.2** Macroscopic (a) and fluorescence microscopy images (b) of emulsion by emulsifying DI water and toluene containing AOT. AOT : C molar ratio from left to right: (a) 0:1, 0.1:1, 0.2:1, 0.3:1, 0.4:1, 0.5:1, 0.6:1, 0.7:1, 0.8:1, 0.9:1, 1:1 (b) (top) 0.1:1, 0.2:1, 0.3:1, 0.4:1, 0.5:1, (bottom) 0.6:1, 0.7:1, 0.8:1, 0.9:1, 1:1.

Likewise, when a 1:1 oil/water mixture is homogenized with AOT, the emulsions formed are again O/W emulsions. This is consistent with a previous report that the hydrophile-lipophile balance (HLB) number of AOT is 10.2 and forms O/W emulsion,[149] though a fair number of studies also have used AOT to form W/O microemulsions.[150] With an increase in the concentration of AOT, the size of the emulsion droplets decreases. The size of the emulsion droplets minimizes around 3.6 mM AOT concentration and stays mostly unchanged during further AOT concentration increase.

### 4.3.2 Emulsion by Chitosan-AOT ion pairing

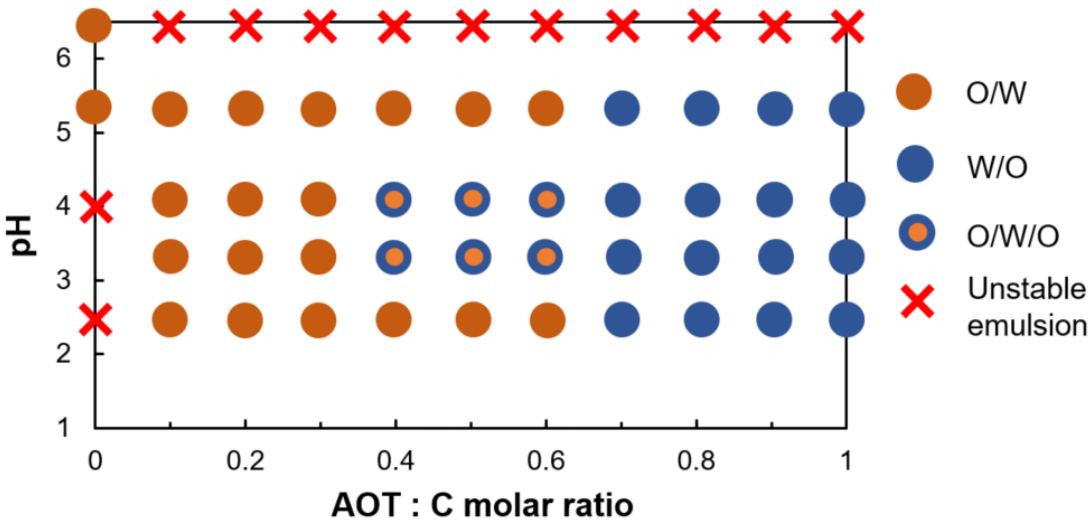

**Figure 4.3** Phase diagram of emulsion made with chitosan-AOT ion pair as a function of both the pH of aqueous solution and AOT concentration presented as the AOT :C molar ratio.

Ion pairing is a technique that relies on the association of oppositely charged substances by electrostatic interaction. The formed ion pairs are reported to have different properties compared to their individual components. For example, ion pairs of oppositely charged polyelectrolyte and surfactant form at low surfactant concentration (below its cmc) are reported to be more surface active than both the polyelectrolyte and surfactant alone.[151] In our study, we find the surface activity of the chitosan-AOT ion pairs can be adjusted by changing solution pH and AOT concentration, which leads to formation of different types of emulsions. The types of the emulsions formed are summarized in the state diagram shown in Figure 4.3. In brief, emulsions cannot be stabilized at pH 6.4 and above. Instead of stabilizing the toluene-water interface, the chitosan and AOT form solid complexes in toluene (Figure 4.8). At lower solution pHs, emulsions are formed and remain stable at least for a month. We also observe that both W/O and O/W emulsions can be produced by changing the solution pH and/or the concentration of AOT. With an increase in the concentration of AOT, W/O emulsions are formed instead of O/W emulsions. The amount of the AOT required to induce phase inversion is smallest at pH 4.1. It is 2.4 mM in toluene, correspond to a 0.4 :1 molar ratio between AOT and the repeat unit of chitosan, glucosamine, in the final emulsion (AOT : C molar ratio = 0.4:1).

### 4.3.3 Effect of AOT concentration on emulsion formation

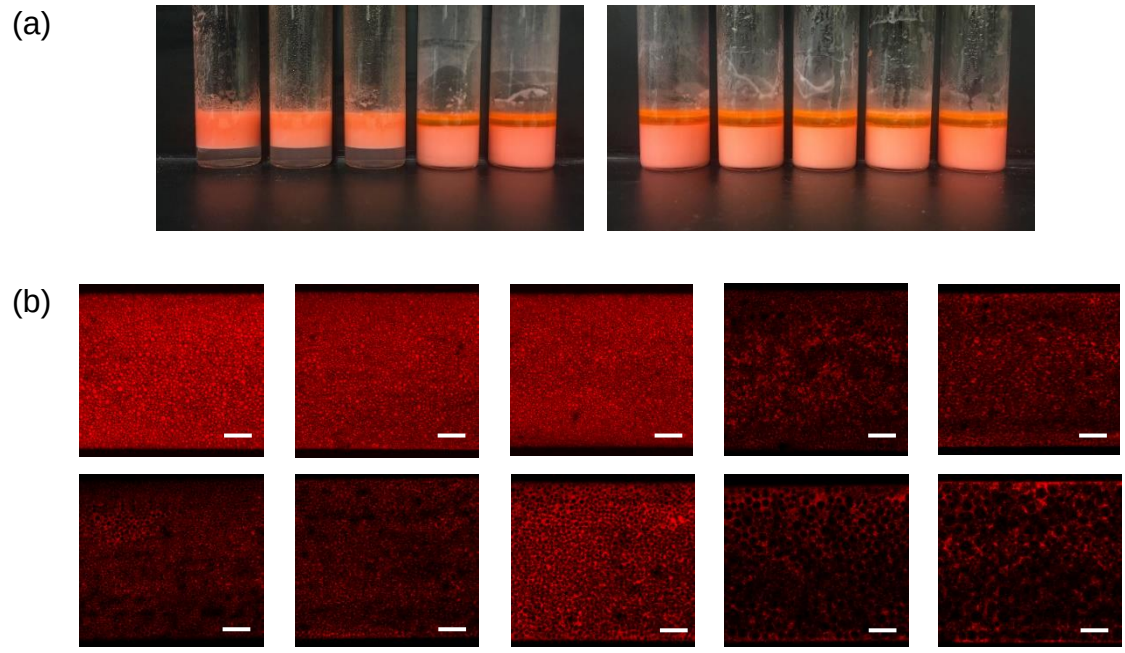


**Figure 4.4** Macroscopic (a) and fluorescence microscopy images (b) of emulsion stabilized by chitosan-AOT ion pair at pH 4.1. AOT : C molar ratio from left to right: (a) 0:1, 0.1:1, 0.2:1, 0.3:1, 0.4:1, 0.5:1, 0.6:1, 0.7:1, 0.8:1, 0.9:1, 1:1 (b) (top) 0.1:1, 0.2:1, 0.3:1, 0.4:1, 0.5:1, (bottom) 0.6:1, 0.7:1, 0.8:1, 0.9:1, 1:1.

The emulsion type, emulsion droplet size, as well as the formation of multiple emulsion droplets are affected by the ratio of AOT and C. To probe the effect of AOT:C ratio, we keep the concentration of chitosan constant at 0.1% w/v, and vary the concentration of AOT such that the AOT:C ratio is varied between 0.1:1 and 1:1. The emulsion made at pH 4.1 is referred to here as a reference (Figure 4.4). With AOT concentration increasing from 0.6 mM (0.1: 1 AOT: C molar ratio) to 1.8 mM (0.3: 1 AOT :C molar ratio), we see a small decrease in the size of O/W emulsion droplets, from ~ 25 μm to ~20 μm. Phase inversion takes place when the AOT concentration increase to 2.4mM (0.4:1 AOT: C

molar ratio). O/W emulsions are formed when the concentration of AOT is higher than 2.4 mM. Oil-in-water-in-oil (O/W/O) multiple emulsion droplets are observed when the concentration of AOT is between 2.4 mM (0.4: 1 AOT: C molar ratio) and 3.6 mM (0.6: 1 AOT :C molar ratio). From 4.2 mM (0.7: 1 AOT :C molar ratio) to 6.0 mM (1: 1 AOT :C molar ratio) AOT concentration, the size of the emulsion droplets are largely affected by the AOT concentration. The size of the emulsion droplets increases from ~25 μm (4.2 mM AOT) to ~ 50 μm (6.0 mM AOT).

We believe the emulsion type as well as the droplet size are affected by changes in the association between chitosan and AOT as the concentration of AOT is changed. Studies have shown that to induce association between a charged polymer and an oppositely charged surfactant, the concentration of the surfactant has to exceed a critical value, which is referred to as its critical aggregation concentration (cac).[151] We believe the cac of AOT in our system is larger than 1.8 mM (0.3:1 AOT :C molar ratio). Below this concentration, the toluene-water interface is stabilized by free AOT molecules. An important distinction we want to address here is the cac is normally used to describe polymer and surfactant association in a bulk liquid medium (e.g., water), while in our study the chitosan and AOT association takes place near the toluene-water interface, thus the exact behavior can likely to be different.

Phase inversion takes place at the AOT concentration of 2.4 mM (0.4:1 AOT :C molar ratio). As more AOT associates with chitosan, the chitosan-AOT ion pairs become more hydrophobic. By analogy to the HLB number of a surfactant, the increase in the association with AOT would decrease the HLB number of the ion pairs formed. In this

case, the chitosan-AOT ion pair's HLB number decreases from above 12 to lower than 8 when the AOT concentration increases from 1.8 mM to 2.4 mM, and the emulsion they form become W/O emulsion.

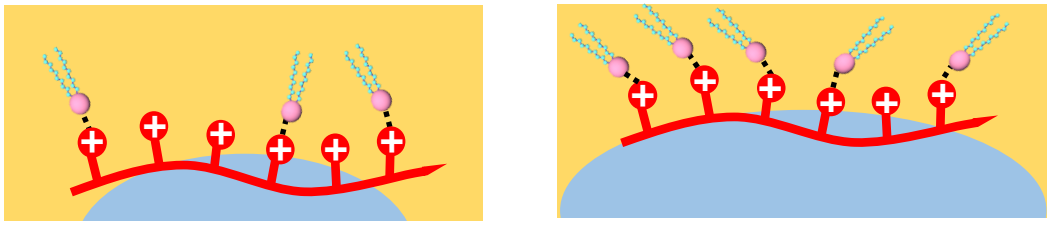


**Figure 4.5** Schematic illustration of chitosan-AOT ion pair and emulsion formation at pH 4.1 and different AOT concentrations: 4.2 mM AOT (0.7:1 AOT :C molar ratio), and 6.0 mM AOT(1:1 AOT :C molar ratio).

In the end, the size of the droplets in emulsions doubled when AOT concentration increases from 4.2 mM (0.7:1 AOT :C molar ratio) to 6.0 mM (1:1 AOT :C molar ratio). As aforementioned, at low AOT concentration, a fair amount of free AOT can be present at the interface. As more AOT associates with chitosan at high AOT concentrations, the properties of the toluene-water interface would be dominated by chitosan-AOT ion pairs. With a further increase in the AOT concentration, chitosan-AOT ion pairs become more hydrophobic due to the larger number of the associated AOT. Consequently, the chitosan-AOT ion pairs lose their surface activity and the size of the emulsion droplets become larger due to coalescence and poor stability (Figure 4.5).

For the multiple emulsion droplets formed between AOT concentration of 2.4 mM (0.4:1 AOT :C molar ratio) and 3.6 mM (0.6:1 AOT :C molar ratio), further investigation is warranted to probe their formation mechanism. In the meantime, the one step formation of the W/O/W multiple emulsions by di-block copolymers through phase inversion has been previously reported.[16] These emulsions are stabilized by the steric repulsion provided by the di-blocks copolymers. Thus, we hypothesize the emulsions in our system can be stabilized in a similar mechanism. Ion pairs generated at intermediate AOT concentration can potentially adsorb to both the inner and outer toluene-water interface, and the steric repulsion they provide stabilize the oil middle phase.

### 4.3.4 Effect of pH on emulsion formation

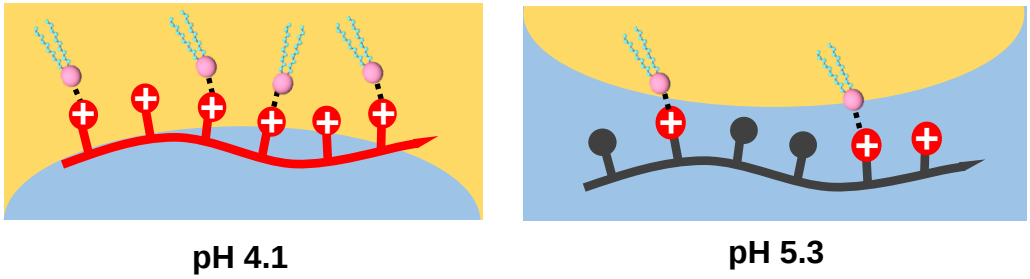


**Figure 4.6** Schematic illustration of chitosan-AOT ion pair and emulsion formation at pH 4.1 and pH 5.3, 3.0 mM AOT concentration.

Emulsion formation is also affected by solution pH because the charge density along the backbone of chitosan is pH-dependent. Between the AOT concentration of 2.4 mM (0.4:1 AOT :C molar ratio) and 3.6 mM (0.6:1 AOT :C molar ratio), O/W emulsions form at the

aqueous solution pH of 5.3, whereas W/O emulsions form at the aqueous solution pH of 3.3 and 4.1. We believe the formation of two opposite types of emulsions is due to different charged states of chitosan under the different pHs. Chitosan is fully protonated at pH 4.[147] Thus, at this highly ionized state, chitosan can undergo ion pairing with a large number of AOT, whereas at pH 5.3, the number of AOT bound to a single chitosan chain will be smaller due to deprotonation of chitosan. Consequently, with same AOT concentration, at pH 4.1, chitosan can associate with more AOT and form more hydrophobic ion pairs. Ultimately this ion pair, due to their hydrophobicity, stabilize W/O emulsions (Figure 4.6).

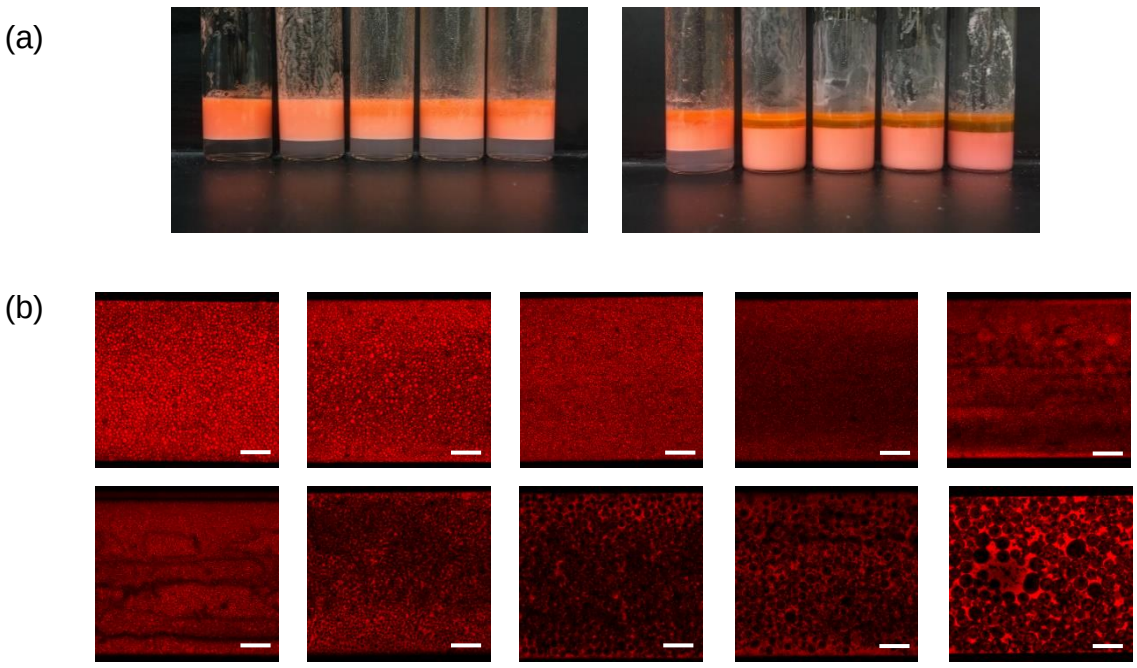


**Figure 4.7** Macroscopic (a) and fluorescence microscopy images (b) of emulsion stabilized by chitosan- AOT ion pair at pH 2.5. AOT : C molar ratio from left to right: (a) 0:1, 0.1:1, 0.2:1, 0.3:1, 0.4:1, 0. 5:1, 0.6:1, 0.7:1, 0.8:1, 0.9:1, 1:1 (b) (top) 0.1:1, 0.2:1, 0.3:1, 0.4:1, 0.5:1, (bottom) 0.6:1, 0.7:1, 0.8:1, 0.9:1, 1:1.

For emulsions made at pH 2.5, PIE take place at the AOT concentration of 4.2 mM (0.7:1 AOT :C molar ratio). The size of the emulsion droplets shows a minimum near the phase inversion boundary, which is the same trends observed for emulsions made at solution pH of 4.1 (Figure 4.7). The high AOT concentration required to induce PIE is not consistent with what we speculated previously. As long as the chitosan is fully protonated, the concentration of AOT required for its PIE should not be different. Such discrepancy can be due to the hydrolysis of chitosan as reported previously in various studies involving chitosan.[23] In the meantime, with the HCl added for the solution pH alteration, more ions are now present in the solution which may interfere with ion pairing between chitosan and AOT due to electrostatic screening.

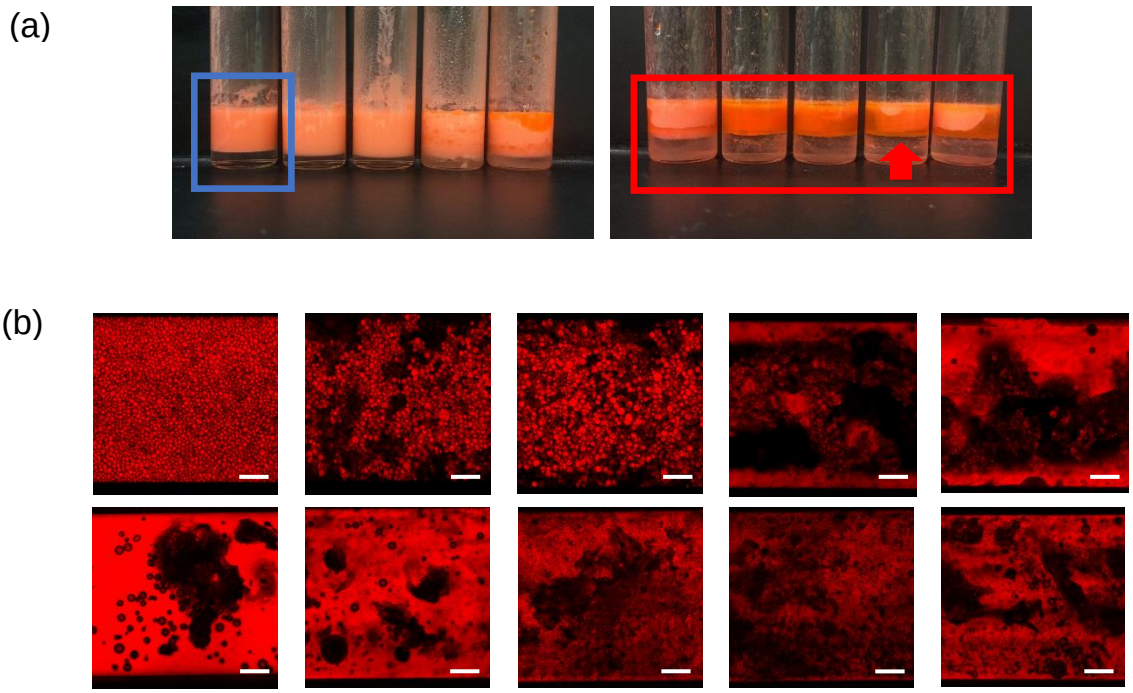

**Figure 4.8** Macroscopic (a) and fluorescence microscopy images (b) of emulsion stabilized, and clusters floating in toluene formed by chitosan- AOT ion pair at pH 6.4. AOT : C molar ratio from left to right: (a) 0:1, 0.1:1, 0.2:1, 0.3:1, 0.4:1, 0.5:1, 0.6:1, 0.7:1, 0.8:1, 0.9:1, 1:1 (b) (top) 0.1:1, 0.2:1, 0.3:1, 0.4:1, 0.5:1, (bottom) 0.6:1, 0.7:1, 0.8:1, 0.9:1, 1:1. Emulsion stabilized by chitosan-AOT ion pair identified with blue frame. Chitosan-AOT aggregate float in toluene identified with red frame.

At pH 6.4, the chitosan and AOT form solid complexes that reside in toluene rather than stabilizing the toluene-water interface from 3.6mM (0.6:1 AOT :C molar ratio), to 6.0 mM (1:1 AOT :C molar ratio) AOT concentration (Figure 4.8, samples identified in red frame). At 0.6 mM AOT concentration (0.1:1 AOT :C molar ratio), the O/W emulsion can be stabilized (Figure 4.8, sample identified in blue frame). However, further increase of the AOT concentration leads to the formation of a network of O/W emulsion droplets. Eventually, AOT and chitosan form clusters and partition into toluene, and the two solutions phase separate.

The hydrophiliciy/hydrophobicity of an ion pair would affect the surface activity of the chitosan-AOT ion pair. We hypothesize that the chitosan- AOT ion pairs formed at pH 6.4 is significantly hydrophobic, which eventually lead to the formation of hydrophobic solid complexes. At low AOT concentrations below 0.6 mM (0.1:1 AOT :C molar ratio), association between AOT and chitosan remains weak, thus O/W emulsion would form. Between 1.2 mM (0.2:1 AOT :C molar ratio) and 3.0mM (0.5:1 AOT :C molar ratio) AOT concentration, we hypothesize chitosan and AOT form coacervates, which lead to the immobilized and connected O/W emulsion droplets. With a further increase of the AOT concentration, the complex formed continue to decrease in its hydrophilicity and eventually the complex solidify and partition into the oil phase (Figure 4.8).

### 4.3.5 pH Responsiveness of Emulsions stabilized with chitosan and AOT ion pairs

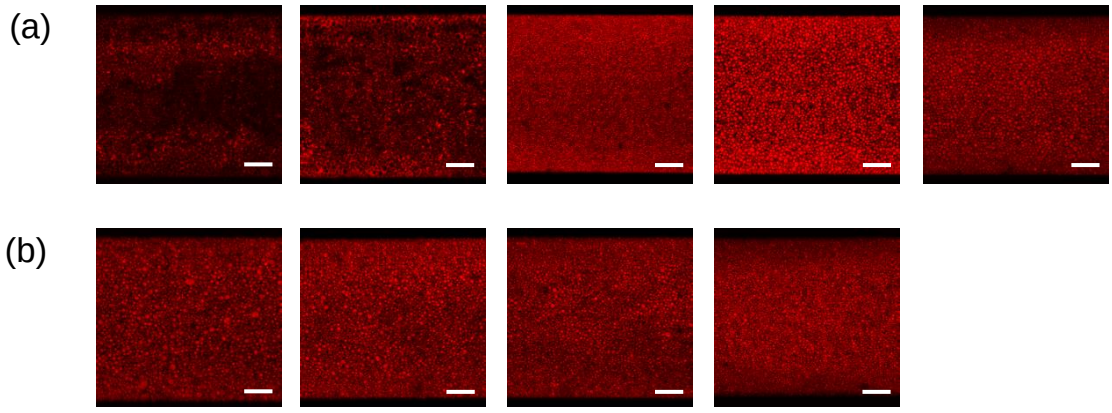


**Figure 4.9** (a) Fluorescence microscopy images of emulsion stabilized by chitosan- AOT ion pair at (i) pH 4.1, 0.5:1 AOT: C molar ratio, following by pH alteration by sequential addition of (ii) 30 µmol NaOH (iii) 30 µmol NaOH (iv) 60 µmol HCl (v) 60 µmol HCl. (b) Fluorescence microscopy images of emulsion stabilized by chitosan- AOT ion pair at (i) pH 5.3, 0.5:1 AOT: C molar ratio, following by pH alteration by sequential addition of (ii) 30 µmol HCl (iii) 30 µmol HCl (iv) 60 µmol HCl.

Results summarized in Figure 4.3 suggest that the solution pH could be a stimulus to trigger phase inversion emulsification *in situ*. In the phase diagram for emulsions made at pH 4.1 and pH 5.3, between AOT concentration of 2.4 mM (0.4:1 AOT :C molar ratio) and 3.6 mM (0.6:1 AOT :C molar ratio), emulsions formed are W/O and O/W emulsions respectively. Thus, it should be possible to induce PIE by changing the emulsion pH between these two states. To test this possibility, HCl and NaOH are added to the emulsions to decrease and increase the solution pH. Shown in Figure 4.9 (a), the W/O emulsion initially formed at pH 4.1 with 3.0 mM AOT undergoes phase inversion to produce an O/W emulsion when the amount of added NaOH is larger than that required

to increase the solution pH from 4.1 to 5.3 (30 μmol NaOH). However, the O/W emulsions, including both the O/W emulsion made at pH 5.3 and the O/W emulsion made through PIE, cannot be induced to undergo phase inversion to form an W/O emulsion, even when added HCl is larger than that needed to decrease the pH of the aqueous solution from 5.3 to 2.5.

**Table 4.1** Acid and base addition for chitosan dissolution and pH adjustment.

| pH adjustment | AA and NaOH addition (mM) | pH |
|---|---|---|
| Original solution (0.1%v/v Acetic acid (AA)) | 17 | 4.1 |
| NaOH addition | 10 | 5.3 |
| Acetic acid (AA) addition | 58 | 4.1 |

We rule out the possibility that the inability of the O/W emulsion to undergo PIE is due to the type of acid added. When acetic acid (AA) is added instead of HCl for pH adjustment, O/W emulsion still cannot be induced to undergo phase inversion. To dissolve chitosan, 0.1% v/v acetic acid is added to the solution. It accounts for an initial 17 mM AA concentration in the solution. Such initial concentration set a high requirement for the amount of NaOH and AA to be added for subsequent pH adjustment (Table 4.1). The presence of a high concentration of free ions in the emulsion can potentially interfere with the chitosan-AOT ion pairing through electrostatic screening.

We hypothesize the reason of why 60 µmol of NaOH is needed to induce PIE of the W/O emulsion is due to the shift of the pKa of chitosan. It has been well documented that the pKa in ionizable groups of weak polyelectrolytes are different from their isolated form in solution, due to the interaction between neighboring groups.[152] Association with oppositely charged species can shift the pKa of polyelectrolytes. Thus, we hypothesize a seemingly excess amount of NaOH needed because the pKa of the chitosan has shifted when it forms chitosan-AOT ion pair.

### 4.3.6 Interfacial properties of chitosan and chitosan-AOT ion pair

The surface activity and interfacial properties of chitosan and chitosan-AOT ion pair is analyzed using pendant drop analysis. This approach enables the direct measurement of interfacial tension (IFT) by balancing the gravitational and the surface tension forces if the interface remains fluid. If a solid-like skin layer develops at the interface, the shape of pendant droplets will indicate the presence of such a layer.

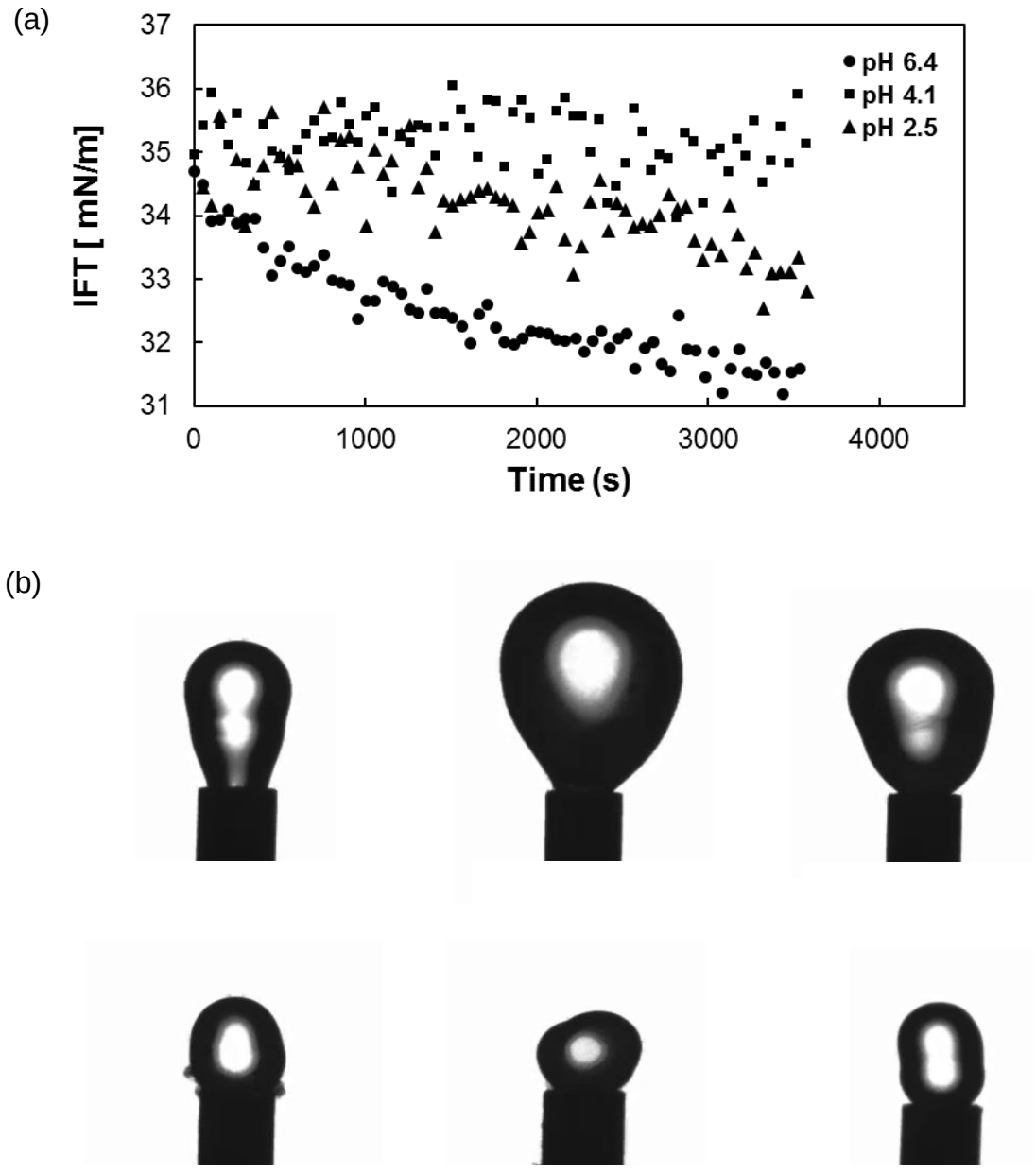


**Figure 4.10** (a) Dynamic interfacial tension at toluene-water interface of 0.1% w/v chitosan at pH 6.4, 4.1, and 2.5 (b)Optical micrographs of chitosan-AOT ion pair deposition at the toluene-water interface, (top) with 0.1:1 AOT :C molar ratio, at different aqueous solution pHs, from left to right: pH 2.5, 4.1, 6.4; (bottom) with 1: 1 AOT :C molar ratio, at different aqueous solution pHs, from left to right: pH 2.5, 4.1, 6.4.

The chitosan concentration in the aqueous phase is kept constant at 0.1% w/v, same as that used in emulsion generation. The different solution pH tested in the experiment are pH 2.5, pH 4.1, and pH 6.4. Without any AOT at pH 4.1, chitosan is hardly surface active. The IFT value barely changes from that of the clean toluene-DI water interface after 1 hr of equilibration. The chitosan is most surface active at pH 6.4. Continuous decrease in IFT value is detected. These measurements are consistent with the observation of the chitosan-only emulsions as shown in Section 4.3.1; chitosan at pH 6.4 alone can stabilize the O/W emulsion, and it cannot do so at pH 4.1. We also notice a mild decrease of IFT by chitosan at pH 2.5. We hypothesize this is due to chitosan hydrolysis. Studies have shown that the glycosidic bonds of chitosan can be cleaved under acidic condition, which leads to its fragmentation.[153-154] Containing mostly hydrophilic sites, including hydroxyl and amine groups, in its backbone, chitosan is rather hydrophilic. Yet, a few acetylated amine groups would impart chitosan mild amphiphilicity.[155] With decrease in the molecular size, the chitosan molecules can adsorb to the interface more compactly. The steric hinderance for the adsorption of chitosan is also lowered compare to its higher molecular weight form. Consequently, we see a mild decrease in the IFT values measured using chitosan at pH 2.5.

Meanwhile, we notice when AOT is present in toluene, the chitosan and AOT form a solid-like skin layer. The rate of the skin layer formation is affected by the AOT concentration in toluene. When the concentration of AOT in the toluene is 0.6 mM (0.1: 1 AOT :C molar ratio), skin layers form within minutes. When the concentration of AOT in the toluene is 6 mM (1: 1 AOT :C molar ratio), the skin layers form within seconds (Figure 4.10).

A study on the adsorption and interfacial properties of the polyelectrolyte-surfactant aggregates, poly(cetytrimethylammonium bromide) (pCTVB), has suggested the surfactants in the aggregates facilitate the transportation of the aggregates to the interface.[17] After the adsorption, the surfactants can either remain in the aggregates or partition into the bulk solution while the polyelectrolytes remain strongly adsorbed at the interface. We believe our system can have a similar mechanism. Because of its solubility in both water and toluene, AOT can first partition into the aqueous solution. After forming ion pair with chitosan, AOT would enhance the diffusion of the chitosan-AOT ion pair as a whole and accelerate its deposition to the toluene-water interface. Because no skin layer is formed during chitosan control IFT measurement, we hypothesize AOT is present in these skin layers too. In the meantime, as the surfactant adsorption kinetics can be governed by two limiting cases, either by the transport of surfactant from bulk to the interface, or by the adsorption/desorption rate of the surfactant at the interface, we acknowledge the fast formation of the solid-like skin layer at the toluene-water interface can also be due to the accelerated adsorption rate of the chitosan-AOT ion pair at the interface. Further investigation is needed to have a thorough understanding of the mechanism of the formation, transport, and interfacial adsorption of the chitosan-AOT ion pairs, as well as the composition of the chitosan-AOT skin layers

## 4.4 Conclusions

In this study, we demonstrate PIE using ion pairs formed between chitosan and AOT. Chitosan and AOT form ion pairs via electrostatic interaction and their binding ratio can be adjusted by changing the pH of the aqueous solution and the AOT concentration in toluene. W/O emulsions are formed at high AOT concentrations, at solution pH range between 2.5 and 5.3. The pH responsiveness test shows W/O-to-O/W emulsion phase inversion, but not the opposite PIE, which may be due to electrostatic screening. Pendant drop characterization of the interface shows rapid formation of chitosan-AOT solid-like skin layers at toluene-water interface. We believe our preliminary results on the chitosan-AOT ion pairs will provide guidance for future work on PIE via polyelectrolyte – surfactant dynamic ion pairing. The ongoing work will include studying emulsion phase inversion using a broader pallet of polyelectrolytes and surfactants as well as to develop better understanding on the structure of the ion pairs formed.

# Chapter 5 Conclusions and Outlooks

## 5.1 Conclusions

In Chapter 1 of this dissertation, the concepts of emulsion and surfactant are introduced, and many benefits of studying the behavior of macromolecules at emulsion interface is discussed. Two approaches, ion pairing and microfluidics, are introduced as ways for modification of hydrophobicity as well as surface activity of macromolecules and detailed approach to study emulsion phenomena, respectively.

Chapter 2 shows that salt-responsive polyelectrolyte microcapsules can be generated in one step with strong polyelectrolytes using SO NICE method. By dissolving a strong polyelectrolyte in an organic medium via ion pairing with an oppositely charged hydrophobic surfactant, W/O/W double emulsions can be used as templates for the generation of polyelectrolyte microcapsules with high encapsulation efficiency and salt responsive properties. This approach potentially widens the pallet of polyelectrolytes that can be used for functional microcapsules via SO NICE.

Chapter 3 provides a comprehensive investigation of the effect of Pluronic composition and molecular weight on the FIPIE of emulsions in a tapered channel. There is a negative correlation between Pluronic $n_{PEO}$ and the tendency of emulsions to undergo FIPIE in a tapered channel. The results suggest that upon compression, the brush layers formed by the hydrophilic domain of PEO-PPO-PEO copolymer surfactants at the interfaces provide high steric repulsion, suppressing the drainage of the thin aqueous film and coalescence

of the oil phases. These effects subsequently hinder FIPIE. Significant suppression of FIPIE by a small molecular weight, high PPO% Pluronic, P123 is observed, which is attributed to the dilatational elasticity provided by its long PPO blocks at the oil/water interface.

Chapter 4 presents PIE using ion pairs formed between chitosan and AOT. Chitosan and AOT form ion pairs via electrostatic interaction and their binding ratio can be adjusted by changing the pH of the aqueous solution and the AOT concentration in toluene. W/O emulsions are formed at high AOT concentrations, at solution pH range between 2.5 and 5.3. The pH responsiveness test shows W/O-to-O/W emulsion phase inversion, but not the opposite PIE, which may be due to electrostatic screening. Pendant drop characterization of the interface shows rapid formation of chitosan-AOT solid-like skin layers at toluene-water interface.

## 5.2 Outlook for Future Research

In our study, the combination of chitosan and AOT is explored as a function of aqueous phase pH and AOT concentration for emulsion generation. We believe the real potential of the application of macromolecule and surfactant association, in this case, ion pairing, extends far beyond what I have demonstrated in this thesis.

One of the advantages of ion pairing is its flexibility and versatility. While individual surfactants are designed with specific HLB and geometries, the properties of ion pairs can

be tuned on a “continuous scale” by associating macromolecules and surfactants at different ratios. The capability to change from a low HLB (lower than 8) to a high HLB (higher than 12) of the ion pair, for example, enables not only phase inversion emulsification, but also delicate adjustment of the curvature of interfaces it stabilizes. Charge density of the polyelectrolyte is one trend that we explored in this thesis. Many other parameters that can affect the ion pairing between the polyelectrolyte and surfactants and the properties of their ion pairs can be utilized; these include but are not limited to molecular weight of polyelectrolytes, chain flexibility of polyelectrolytes, chain length and number of surfactant tails. We believe with the further development of dynamic ion paring, simple materials of natural origin, through simple processes, can generate versatile surfactant systems for emulsion processing.

A better understanding on the structure of polyelectrolyte-surfactant ion pairs will greatly facilitate their application. At the moment, our analysis has included UV-Vis spectroscopy and IFT measurement. More investigation methods are waiting to be explored. Circular dichroism has been widely developed and used in many studies for detecting the conformation of the ion pairs. Dialysis equilibrium is used to characterize the binding isotherm between polyelectrolyte and surfactant. Many other approaches exist including electrical conductivity measurement, viscometry, dynamic light scattering, and solubilization of fluorescence dyes.

Using all-natural ingredients is becoming an important consideration for various industries that manufacture and process emulsions. It is preferable to have minimum modification of the natural materials. Ion pairing natural materials provide an approach to

reduce the necessity for their modification while enriching their applications. In addition, detailed understanding of mechanisms relates to ion pairing would greatly facilitate their adoption in many sectors. We have only explored one natural macromolecule, chitosan, and one petroleum derived surfactant, AOT, in our study. Yet, the type of natural macromolecules including polysaccharides, proteins, and polynucleotides, and the type of natural surfactants, including free fatty acids, amino acids, and phospholipids, extend far beyond.

# Bibliography


1. Lam, R. S.; Nickerson, M. T., Food proteins: a review on their emulsifying properties using a structure-function approach. *Food chemistry* **2013,** *141* (2), 975-84.

2. Schramm, L. L. Emulsions: fundamentals and applications in the petroleum industry; American Chemical Society : Washington D.C., 1992.

3. McClements, D. J., Nanoemulsions versus microemulsions: terminology, differences, and similarities. *Soft Matter* **2012,** *8* (6), 1719-1729.

4. Rosen, M. J.; Kunjappu, J. T. Surfactants and interfacial phenomena ; John Wiley & Sons, 2012.

5. Wennerström, H.; Balogh, J.; Olsson, U., Interfacial tensions in microemulsions. *Colloids and Surfaces A: Physicochemical and Engineering Aspects* **2006,** *291* (1-3), 69-77.

6. Evilevitch, A.; Jönsson, B.; Olsson, U.; Wennerström, H., Molecular Transport in a Nonequilibrium Droplet Microemulsion System. *Langmuir : the ACS journal of surfaces and colloids* **2001,** *17* (22), 6893-6904.

7. Shah, D. O., *Macro- and Microemulsions*. American Chemical Society: 1985; Vol. 272, p 516.

8. Dukhin, S. S.; Sjöblom, J.; Wasan, D. T.; Sæther, Ø., Coalescence coupled with either coagulation or flocculation in dilute emulsions. *Colloids and Surfaces A: Physicochemical and Engineering Aspects* **2001,** *180* (3), 223-234.

9. Kumar, S.; Narsimhan, G.; Ramkrishna, D., Coalescence in Creaming Emulsions. Existence of a Pure Coalescence Zone. *Industrial & Engineering Chemistry Research* **1996,** *35* (9), 3155-3162.

10. Besnard, L.; Marchal, F.; Paredes, J. F.; Daillant, J.; Pantoustier, N.; Perrin, P.; Guenoun, P., Multiple emulsions controlled by stimuli-responsive polymers. *Advanced materials* **2013,** *25* (20), 2844-8.

11. Binks B. P. (Ed.), Modern Aspects of Emulsion Science, The Royal Society of Chemistry, Cambridge, 1998.

12. *Bibette, J., Leal-Calderon, F., Schmitt, V., Poulin, P. Emulsion Science: Basic Principles An Overview, Springer-Verlag: Berlin, 2002*.

13. Wang, J.-H.; Lee, G.-B., Formation of Tunable, Emulsion Micro-Droplets Utilizing Flow-Focusing Channels and a Normally-Closed Micro-Valve. *Micromachines* **2013,** *4* (3), 306-320.

14. Evans, D. F., Wennerstrom, H. F. The Colloidial Domain, Wiley-VCH, 1999.

15. Tcholakova, S.; Denkov, N. D.; Ivanov, I. B.; Campbell, B., Coalescence stability of emulsions containing globular milk proteins. *Advances in colloid and interface science* **2006,** *123-126*, 259-93.

16. Hong, L.; Sun, G.; Cai, J.; Ngai, T., One-step formation of w/o/w multiple emulsions stabilized by single amphiphilic block copolymers. *Langmuir : the ACS journal of surfaces and colloids* **2012,** *28* (5), 2332-6.

17. Davidson, M. L.; Walker, L. M., Interfacial properties of polyelectrolyte-surfactant aggregates at air/water interfaces. *Langmuir : the ACS journal of surfaces and colloids* **2018**.

18. Lee, C. T.; Psathas, P. A.; Johnston, K. P.; deGrazia, J.; Randolph, T. W., Water-in-Carbon Dioxide Emulsions: Formation and Stability. *Langmuir : the ACS journal of surfaces and colloids* **1999,** *15* (20), 6781-6791.

19. Raffa, P.; Wever, D. A.; Picchioni, F.; Broekhuis, A. A., Polymeric Surfactants: Synthesis, Properties, and Links to Applications. *Chemical reviews* **2015,** *115* (16), 8504-63.

20. Alexandridis, P.; Alan Hatton, T., Poly(ethylene oxide)□poly(propylene oxide)□poly(ethylene oxide) block copolymer surfactants in aqueous solutions and at interfaces: thermodynamics, structure, dynamics, and modeling. *Colloids and Surfaces A: Physicochemical and Engineering Aspects* **1995,** *96* (1), 1-46.

21. Pitto-Barry, A.; Barry, N. P. E., Pluronic® block-copolymers in medicine: from chemical and biological versatility to rationalisation and clinical advances. *Polym. Chem.* **2014,** *5* (10), 3291-3297.

22. Locatelli-Champagne, C.; Suau, J. M.; Guerret, O.; Pellet, C.; Cloitre, M., Versatile Encapsulation Technology Based on Tailored pH-Responsive Amphiphilic

Polymers: Emulsion Gels and Capsules. *Langmuir : the ACS journal of surfaces and colloids* **2017,** *33* (49), 14020-14028.

23. Chen, H.; McClements, D. J.; Chen, E.; Liu, S.; Li, B.; Li, Y., In Situ Interfacial Conjugation of Chitosan with Cinnamaldehyde during Homogenization Improves the Formation and Stability of Chitosan-Stabilized Emulsions. *Langmuir : the ACS journal of surfaces and colloids* **2017,** *33* (51), 14608-14617.

24. Mikkonen, K. S.; Parikka, K.; Ghafar, A.; Tenkanen, M., Prospects of polysaccharide aerogels as modern advanced food materials. *Trends in Food Science & Technology* **2013,** *34* (2), 124-136.

25. Lei, L.; He, Z.; Chen, H.; McClements, D. J.; Li, B.; Li, Y., Microstructural, rheological, and antibacterial properties of cross-linked chitosan emulgels. *RSC Advances* **2015,** *5* (121), 100114-100122.

26. Bouyer, E.; Mekhloufi, G.; Rosilio, V.; Grossiord, J. L.; Agnely, F., Proteins, polysaccharides, and their complexes used as stabilizers for emulsions: alternatives to synthetic surfactants in the pharmaceutical field? *International journal of pharmaceutics* **2012,** *436* (1-2), 359-78.

27. Meyer, J. D.; Manning, M. C., Hydrophobic Ion Pairing: Altering the Solubility Properties of Biomolecules. *Pharmaceutical Research* **1998,** *15* (2), 188-193.

28. Georgieva, D.; Schmitt, V.; Leal-Calderon, F.; Langevin, D., On the possible role of surface elasticity in emulsion stability. *Langmuir : the ACS journal of surfaces and colloids* **2009,** *25* (10), 5565-73.

29. Marcus, Y.; Hefter, G., Ion Pairing. *Chemical reviews* **2006,** *106* (11), 4585-4621.

30. Fu, J.; Schlenoff, J. B., Driving Forces for Oppositely Charged Polyion Association in Aqueous Solutions: Enthalpic, Entropic, but Not Electrostatic. *Journal of the American Chemical Society* **2016,** *138* (3), 980-90.

31. Zhang, Y.; Batys, P.; O'Neal, J. T.; Li, F.; Sammalkorpi, M.; Lutkenhaus, J. L., Molecular Origin of the Glass Transition in Polyelectrolyte Assemblies. *ACS central science* **2018,** *4* (5), 638-644.

32. Tagle, L. H.; Diaz, F. R., Polymerization by phase transfer catalysis—5. Polycarbonates from diphenols with aromatic side groups. *European Polymer Journal* **1987,** *23* (2), 109-112.

33. Antonietti, M.; Conrad, J.; Thuenemann, A., Polyelectrolyte-Surfactant Complexes: A New Type of Solid, Mesomorphous Material. *Macromolecules* **1994,** *27* (21), 6007-6011.

34. Powers, M. E.; Matsuura, J.; Brassell, J.; Manning, M. C.; Shefter, E., Enhanced solubility of proteins and peptides in nonpolar solvents through hydrophobic ion pairing. *Biopolymers* **1993,** *33* (6), 927-932.

35. Whitesides, G. M., The origins and the future of microfluidics. *Nature* **2006,** *442* (7101), 368-73.

36. Tice, J. D.; Song, H.; Lyon, A. D.; Ismagilov, R. F., Formation of Droplets and Mixing in Multiphase Microfluidics at Low Values of the Reynolds and the Capillary Numbers. *Langmuir : the ACS journal of surfaces and colloids* **2003,** *19* (22), 9127-9133.

37. Groisman, A.; Quake, S. R., A microfluidic rectifier: anisotropic flow resistance at low Reynolds numbers. *Phys Rev Lett* **2004,** *92* (9), 094501.

38. Ren, K.; Zhou, J.; Wu, H., Materials for Microfluidic Chip Fabrication. *Accounts of chemical research* **2013,** *46* (11), 2396-2406.

39. Brugarolas, T.; Tu, F.; Lee, D., Directed assembly of particles using microfluidic droplets and bubbles. *Soft Matter* **2013**.

40. Bu, M.; Melvin, T.; Ensell, G. J.; Wilkinson, J. S.; Evans, A. G. R., A new masking technology for deep glass etching and its microfluidic application. *Sensors and Actuators A: Physical* **2004,** *115* (2-3), 476-482.

41. McDonald, J. C.; Whitesides, G. M., Poly(dimethylsiloxane) as a Material for Fabricating Microfluidic Devices. *Accounts of chemical research* **2002,** *35* (7), 491-499.

42. Ng, J. M. K.; Gitlin, I.; Stroock, A. D.; Whitesides, G. M., Components for integrated poly(dimethylsiloxane) microfluidic systems. *Electrophoresis* **2002,** *23* (20), 3461-3473.

43. Quake, S. R.; Scherer, A., From Micro- to Nanofabrication with Soft Materials. *Science* **2000,** *290* (5496), 1536.

44. Cosson, S.; Lutolf, M. P., Hydrogel microfluidics for the patterning of pluripotent stem cells. *Scientific reports* **2014,** *4*, 4462.

45. Cheng, S. Y.; Heilman, S.; Wasserman, M.; Archer, S.; Shuler, M. L.; Wu, M., A hydrogel-based microfluidic device for the studies of directed cell migration. *Lab on a chip* **2007,** *7* (6), 763-9.

46. Utada, A.; Fernandez-Nieves, A.; Stone, H.; Weitz, D., Dripping to Jetting Transitions in Coflowing Liquid Streams. *Physical Review Letters* **2007,** *99* (9).

47. Chu, L.-Y.; Utada, A. S.; Shah, R. K.; Kim, J.-W.; Weitz, D. A., Controllable Monodisperse Multiple Emulsions. *Angewandte Chemie* **2007,** *119* (47), 9128-9132.

48. Bremond, N.; Thiam, A.; Bibette, J., Decompressing Emulsion Droplets Favors Coalescence. *Physical Review Letters* **2008,** *100* (2).

49. Rosenfeld, L.; Fan, L.; Chen, Y.; Swoboda, R.; Tang, S. K. Y., Break-up of droplets in a concentrated emulsion flowing through a narrow constriction. *Soft Matter* **2014,** *10* (3), 421-430.

50. Gai, Y.; Khor, J. W.; Tang, S. K. Y., Confinement and viscosity ratio effect on droplet break-up in a concentrated emulsion flowing through a narrow constriction. *Lab on a chip* **2016,** *16* (16), 3058-3064.

51. Chen, H.; Dong, E.; Li, J.; Stone, H. A., Adhesion of moving droplets in microchannels. *Applied Physics Letters* **2013,** *103* (13), 131605.

52. Shui, L.; van den Berg, A.; Eijkel, J. C., Interfacial tension controlled W/O and O/W 2-phase flows in microchannel. *Lab on a chip* **2009,** *9* (6), 795-801.

53. Windbergs, M.; Zhao, Y.; Heyman, J.; Weitz, D. A., Biodegradable core-shell carriers for simultaneous encapsulation of synergistic actives. *Journal of the American Chemical Society* **2013,** *135* (21), 7933-7.

54. Zhao, Q.; Han, B.; Wang, Z.; Gao, C.; Peng, C.; Shen, J., Hollow chitosan-alginate multilayer microcapsules as drug delivery vehicle: doxorubicin loading and in vitro and in vivo studies. *Nanomedicine : nanotechnology, biology, and medicine* **2007,** *3* (1), 63-74.

55. Bysell, H.; Mansson, R.; Hansson, P.; Malmsten, M., Microgels and microcapsules in peptide and protein drug delivery. *Adv Drug Deliv Rev* **2011,** *63* (13), 1172-85.

56. Hirech, K., Microencapsulation of an insecticide by interfacial polymerisation. *Powder Technology* **2003,** *130* (1-3), 324-330.

57. Yang, Z.; Peng, Z.; Li, J.; Li, S.; Kong, L.; Li, P.; Wang, Q., Development and evaluation of novel flavour microcapsules containing vanilla oil using complex coacervation approach. *Food chemistry* **2014,** *145*, 272-7.

58. Datta, S. S.; Abbaspourrad, A.; Amstad, E.; Fan, J.; Kim, S. H.; Romanowsky, M.; Shum, H. C.; Sun, B.; Utada, A. S.; Windbergs, M.; Zhou, S.; Weitz, D. A., 25th anniversary article: double emulsion templated solid microcapsules: mechanics and controlled release. *Advanced materials* **2014,** *26* (14), 2205-18.

59. Martins, I. M.; Barreiro, M. F.; Coelho, M.; Rodrigues, A. E., Microencapsulation of essential oils with biodegradable polymeric carriers for cosmetic applications. *Chemical Engineering Journal* **2014,** *245*, 191-200.

60. Tekin, R.; Bac, N.; Erdogmus, H., Microencapsulation of Fragrance and Natural Volatile Oils for Application in Cosmetics, and Household Cleaning Products. *Macromolecular Symposia* **2013,** *333* (1), 35-40.

61. Doring, G.; Flume, P.; Heijerman, H.; Elborn, J. S.; Consensus Study, G., Treatment of lung infection in patients with cystic fibrosis: current and future strategies. *Journal of cystic fibrosis : official journal of the European Cystic Fibrosis Society* **2012,** *11* (6), 461-79.

62. Gao, P.; Nie, X.; Zou, M.; Shi, Y.; Cheng, G., Recent advances in materials for extended-release antibiotic delivery system. *The Journal of antibiotics* **2011,** *64* (9), 625-34.

63. Loira-Pastoriza, C.; Todoroff, J.; Vanbever, R., Delivery strategies for sustained drug release in the lungs. *Adv Drug Deliv Rev* **2014,** *75*, 81-91.

64. Tostanoski, L. H.; Chiu, Y.-C.; Andorko, J. I.; Guo, M.; Zeng, X.; Zhang, P.; Royal, W.; Jewell, C. M., Design of Polyelectrolyte Multilayers to Promote Immunological Tolerance. *ACS nano* **2016,** *10* (10), 9334-9345.

65. Zhu, Z.; Zhuo, R., Controlled release of carboxylic-containing herbicides by starch-g-poly(butyl acrylate). *Journal of Applied Polymer Science* **2001,** *81* (6), 1535-1543.

66. Sun, C.; Shu, K.; Wang, W.; Ye, Z.; Liu, T.; Gao, Y.; Zheng, H.; He, G.; Yin, Y., Encapsulation and controlled release of hydrophilic pesticide in shell cross-linked nanocapsules containing aqueous core. *International journal of pharmaceutics* **2014,** *463* (1), 108-14.

67. Khot, L. R.; Sankaran, S.; Maja, J. M.; Ehsani, R.; Schuster, E. W., Applications of nanomaterials in agricultural production and crop protection: A review. *Crop Protection* **2012,** *35*, 64-70.

68. Vergaro, V.; Scarlino, F.; Bellomo, C.; Rinaldi, R.; Vergara, D.; Maffia, M.; Baldassarre, F.; Giannelli, G.; Zhang, X.; Lvov, Y. M.; Leporatti, S., Drug-loaded polyelectrolyte microcapsules for sustained targeting of cancer cells. *Adv Drug Deliv Rev* **2011,** *63* (9), 847-64.

69. Gao, C.; Mohwald, H.; Shen, J. C., Enhanced biomacromolecule encapsulation by swelling and shrinking procedures. *Chemphyschem : a European journal of chemical physics and physical chemistry* **2004,** *5* (1), 116-20.

70. Hu, S.-H.; Tsai, C.-H.; Liao, C.-F.; Liu, D.-M.; Chen, S.-Y., Controlled Rupture of Magnetic Polyelectrolyte Microcapsules for Drug Delivery. *Langmuir : the ACS journal of surfaces and colloids* **2008,** *24* (20), 11811-11818.

71. De Geest, B. G.; De Koker, S.; Sukhorukov, G. B.; Kreft, O.; Parak, W. J.; Skirtach, A. G.; Demeester, J.; De Smedt, S. C.; Hennink, W. E., Polyelectrolyte microcapsules for biomedical applications. *Soft Matter* **2009,** *5* (2), 282-291.

72. Kaufman, G.; Nejati, S.; Sarfati, R.; Boltyanskiy, R.; Loewenberg, M.; Dufresne, E. R.; Osuji, C. O., Soft microcapsules with highly plastic shells formed by interfacial polyelectrolyte-nanoparticle complexation. *Soft Matter* **2015,** *11* (38), 7478-82.

73. Kaufman, G.; Boltyanskiy, R.; Nejati, S.; Thiam, A. R.; Loewenberg, M.; Dufresne, E. R.; Osuji, C. O., Single-step microfluidic fabrication of soft monodisperse polyelectrolyte microcapsules by interfacial complexation. *Lab on a chip* **2014,** *14* (18), 3494-7.

74. Kim, M.; Yeo, S. J.; Highley, C. B.; Burdick, J. A.; Yoo, P. J.; Doh, J.; Lee, D., One-Step Generation of Multifunctional Polyelectrolyte Microcapsules via Nanoscale Interfacial Complexation in Emulsion (NICE). *ACS nano* **2015,** *9* (8), 8269-8278.

75. Kim, M.; Doh, J.; Lee, D., pH-Induced Softening of Polyelectrolyte Microcapsules without Apparent Swelling. *ACS Macro Letters* **2016,** *5* (4), 487-492.

76. Peyratout, C. S.; Dahne, L., Tailor-made polyelectrolyte microcapsules: from multilayers to smart containers. *Angewandte Chemie* **2004,** *43* (29), 3762-83.

77. Delcea, M.; Mohwald, H.; Skirtach, A. G., Stimuli-responsive LbL capsules and nanoshells for drug delivery. *Adv Drug Deliv Rev* **2011,** *63* (9), 730-47.

78. Lee, H.; Jeong, Y.; Park, T. G., Shell Cross-Linked Hyaluronic Acid/Polylysine Layer-by-Layer Polyelectrolyte Microcapsules Prepared by Removal of Reducible Hyaluronic Acid Microgel Cores. *Biomacromolecules* **2007,** *8* (12), 3705-3711.

79. Shum, H. C.; Lee, D.; Yoon, I.; Kodger, T.; Weitz, D. A., Double Emulsion Templated Monodisperse Phospholipid Vesicles. *Langmuir : the ACS journal of surfaces and colloids* **2008,** *24* (15), 7651-7653.

80. Monteillet, H.; Hagemans, F.; Sprakel, J., Charge-driven co-assembly of polyelectrolytes across oil–water interfaces. *Soft Matter* **2013,** *9* (47), 11270.

81. Lengsfeld, C. S.; Pitera, D.; Manning, M.; Randolph, T. W., Dissolution and Partitioning Behavior of Hydrophobic Ion-Paired Compounds. *Pharmaceutical Research* **2002,** *19* (10), 1572-1576.

82. Paradkar, V. M.; Dordick, J. S., Mechanism of extraction of chymotrypsin into isooctane at very low concentrations of aerosol OT in the absence of reversed micelles. *Biotechnology and bioengineering* **1994,** *43* (6), 529-540.

83. Wang, H.; Singh, V.; Behrens, S. H., Image Charge Effects on the Formation of Pickering Emulsions. *The journal of physical chemistry letters* **2012,** *3* (20), 2986-90.

84. Messina, R., Image charges in spherical geometry: Application to colloidal systems. *The Journal of chemical physics* **2002,** *117* (24), 11062-11074.

85. Bae, J.; Russell, T. P.; Hayward, R. C., Osmotically driven formation of double emulsions stabilized by amphiphilic block copolymers. *Angewandte Chemie* **2014,** *53* (31), 8240-5.

86. Hayward, R. C.; Utada, A. S.; Dan, N.; Weitz, D. A., Dewetting Instability during the Formation of Polymersomes from Block-Copolymer-Stabilized Double Emulsions. *Langmuir : the ACS journal of surfaces and colloids* **2006,** *22* (10), 4457-4461.

87. Shum, H. C.; Zhao, Y. J.; Kim, S. H.; Weitz, D. A., Multicompartment polymersomes from double emulsions. *Angewandte Chemie* **2011,** *50* (7), 1648-51.

88. Varona, S.; Kareth, S.; Martín, Á.; Cocero, M. J., Formulation of lavandin essential oil with biopolymers by PGSS for application as biocide in ecological agriculture. *The Journal of Supercritical Fluids* **2010,** *54* (3), 369-377.

89. Yukuyama, M. N.; Ghisleni, D. D. M.; Pinto, T. J. A.; Bou-Chacra, N. A., Nanoemulsion: process selection and application in cosmetics – a review. *International Journal of Cosmetic Science* **2015,** *38* (1), 13-24.

90. Petela, R., Generation of oil emulsion for stirred tank processes. *Fuel* **1994,** *73* (4), 557-562.

91. Sadurni, N.; Solans, C.; Azemar, N.; Garcia-Celma, M. J., Studies on the formation of O/W nano-emulsions, by low-energy emulsification methods, suitable for pharmaceutical applications. *European journal of pharmaceutical sciences : official journal of the European Federation for Pharmaceutical Sciences* **2005,** *26* (5), 438-45.

92. Karcher, V.; Perrechil, F. A.; Bannwart, A. C., INTERFACIAL ENERGY DURING THE EMULSIFICATION OF WATER-IN-HEAVY CRUDE OIL EMULSIONS. *Brazilian Journal of Chemical Engineering* **2015,** *32*, 127-137.

93. Sajjadi, S., Nanoemulsion Formation by Phase Inversion Emulsification: On the Nature of Inversion. *Langmuir : the ACS journal of surfaces and colloids* **2006,** *22* (13), 5597-5603.

94. Yang, Z. Z.; Xu, Y. Z.; Zhao, D. L.; Xu, M., Preparation of waterborne dispersions of epoxy resin by the phase-inversion emulsification technique. 1. Experimental study on the phase-inversion process. *Colloid and Polymer Science* **2000,** *278* (12), 1164-1171.

95. Salager, J. L.; Forgiarini, A.; Marquez, L.; Pena, A.; Pizzino, A.; Rodriguez, M. P.; Rondon-Gonzalez, M., Using emulsion inversion in industrial processes. *Advances in colloid and interface science* **2004,** *108-109*, 259-72.

96. Bouchama, F.; van Aken, G. A.; Autin, A. J. E.; Koper, G. J. M., On the mechanism of catastrophic phase inversion in emulsions. *Colloids and Surfaces A: Physicochemical and Engineering Aspects* **2003,** *231* (1-3), 11-17.

97. Perazzo, A.; Preziosi, V.; Guido, S., Phase inversion emulsification: Current understanding and applications. *Advances in colloid and interface science* **2015,** *222*, 581-99.

98. Kumar, A.; Li, S.; Cheng, C.-M.; Lee, D., Recent Developments in Phase Inversion Emulsification. *Industrial & Engineering Chemistry Research* **2015,** *54* (34), 8375-8396.

99. Akay, G., Flow-induced phase inversion in the intensive processing of concentrated emulsions. *Chemical Engineering Science* **1998,** *53* (2), 203-223.

100. Bremond, N.; Domejean, H.; Bibette, J., Propagation of drop coalescence in a two-dimensional emulsion: a route towards phase inversion. *Phys Rev Lett* **2011,** *106* (21), 214502.

101. Zhang, Y.; van Nieuwkasteele, J. W.; Qiang, M.; Tsai, P. A.; Lammertink, R. G., Spatial Site-Patterning of Wettability in a Microcapillary Tube. *ACS applied materials & interfaces* **2016,** *8* (17), 10657-60.

102. Man, J.; Li, Z.; Li, J.; Chen, H., Phase inversion of slug flow on step surface to form high viscosity droplets in microchannel. *Applied Physics Letters* **2017,** *110* (18), 181601.

103. Meng, Q.; Zhang, Y.; Li, J.; Lammertink, R. G.; Chen, H.; Tsai, P. A., Altering Emulsion Stability with Heterogeneous Surface Wettability. *Scientific reports* **2016,** *6*, 26953.

104. Fendler Janos, H., The colloidal domain: Where physics, chemistry, biology, and technology meet. By D. Fennell Evans and Hakån Wennerström. VCH Publishers, New York 1994, XXXII, 515 pp., hardcover, $65.00, DM 980, ISBN 1–56081–525–6. *Advanced materials* **1996,** *8* (3), 260-260.

105. de Folter, J. W.; Hutter, E. M.; Castillo, S. I.; Klop, K. E.; Philipse, A. P.; Kegel, W. K., Particle shape anisotropy in pickering emulsions: cubes and peanuts. *Langmuir : the ACS journal of surfaces and colloids* **2014,** *30* (4), 955-64.

106. Bates, C. M.; Bates, F. S., 50th Anniversary Perspective: Block Polymers—Pure Potential. *Macromolecules* **2016,** *50* (1), 3-22.

107. Dickinson, E., Milk protein interfacial layers and the relationship to emulsion stability and rheology. *Colloids and Surfaces B: Biointerfaces* **2001,** *20* (3), 197-210.

108. Faraudo, J.; Bresme, F., Origin of the short-range, strong repulsive force between ionic surfactant layers. *Phys Rev Lett* **2005,** *94* (7), 077802.

109. Binks, B. P., Particles as surfactants—similarities and differences. *Current Opinion in Colloid & Interface Science* **2002,** *7* (1), 21-41.

110. Kozlov, M. Y.; Melik-Nubarov, N. S.; Batrakova, E. V.; Kabanov, A. V., Relationship between Pluronic Block Copolymer Structure, Critical Micellization Concentration and Partitioning Coefficients of Low Molecular Mass Solutes. *Macromolecules* **2000,** *33* (9), 3305-3313.

111. Kumar, A.; Li, S.; Cheng, C. M.; Lee, D., Flow-induced phase inversion of emulsions in tapered microchannels. *Lab on a chip* **2016,** *16* (21), 4173-4180.

112. Brugarolas, T.; Gianola, D. S.; Zhang, L.; Campbell, G. M.; Bassani, J. L.; Feng, G.; Lee, D., Tailoring and Understanding the Mechanical Properties of Nanoparticle-Shelled Bubbles. *ACS applied materials & interfaces* **2014**.

113. Utada, A. S.; Lorenceau, E.; Link, D. R.; Kaplan, P. D.; Stone, H. A.; Weitz, D. A., Monodisperse Double Emulsions Generated from a Microcapillary Device. *Science* **2005,** *308* (5721), 537.

114. Gai, Y.; Khor, J. W.; Tang, S. K., Confinement and viscosity ratio effect on droplet break-up in a concentrated emulsion flowing through a narrow constriction. *Lab on a chip* **2016,** *16* (16), 3058-64.

115. Gotchev, G.; Kolarov, T.; Khristov, K.; Exerowa, D., Electrostatic and steric interactions in oil-in-water emulsion films from Pluronic surfactants. *Advances in colloid and interface science* **2011,** *168* (1-2), 79-84.

116. Exerowa, D.; Platikanov, D., Thin liquid films from aqueous solutions of non-ionic polymeric surfactants. *Advances in colloid and interface science* **2009,** *147-148*, 74-87.

117. Liu, Z.; Chan, S. T.; Faizi, H. A.; Roberts, R. C.; Shum, H. C., Droplet-based electro-coalescence for probing threshold disjoining pressure. *Lab on a chip* **2015,** *15* (9), 2018-24.

118. Steinhaus, B.; Spicer, P. T.; Shen, A. Q., Droplet Size Effects on Film Drainage between Droplet and Substrate. *Langmuir : the ACS journal of surfaces and colloids* **2006,** *22* (12), 5308-5313.

119. Karakashev, S. I.; Manev, E. D., Hydrodynamics of thin liquid films: Retrospective and perspectives. *Advances in colloid and interface science* **2015,** *222*, 398-412.

120. Manev, E. D.; Nguyen, A. V., Critical thickness of microscopic thin liquid films. *Advances in colloid and interface science* **2005,** *114-115*, 133-46.

121. Cosima, S.; Regine von, K., Disjoining pressure in thin liquid foam and emulsion films—new concepts and perspectives. *Journal of Physics: Condensed Matter* **2003,** *15* (27), R1197.

122. Vance, B., Forces and structure in thin liquid soap films. *Journal of Physics: Condensed Matter* **1999,** *11* (19), R215.

123. Sedev, R.; Exerowa, D., DLVO and non-DLVO surface forces in foam films from amphiphilic block copolymers. *Advances in colloid and interface science* **1999,** *83* (1), 111-136.

124. Manor, O.; Chau, T. T.; Stevens, G. W.; Chan, D. Y.; Grieser, F.; Dagastine, R. R., Polymeric stabilized emulsions: steric effects and deformation in soft systems. *Langmuir : the ACS journal of surfaces and colloids* **2012,** *28* (10), 4599-604.

125. Prestidge, C. A.; Barnes, T.; Simovic, S., Polymer and particle adsorption at the PDMS droplet-water interface. *Advances in colloid and interface science* **2004,** *108-109*, 105-118.

126. Barnes, T. J.; Prestidge, C. A., PEO−PPO−PEO Block Copolymers at the Emulsion Droplet−Water Interface. *Langmuir : the ACS journal of surfaces and colloids* **2000,** *16* (9), 4116-4121.

127. Barnes, T., Emulsion Droplets of Controlled Deformability: Electrokinetics, Colloid Stability and Polymer Adsorption. Ph.D. Thesis, University of South Australia, Mawson Lakes, SA, Australia. **2003**.

128. Musoke, M.; Luckham, P. F., Interaction forces between polyethylene oxide-polypropylene oxide ABA copolymers adsorbed to hydrophobic surfaces. *Journal of colloid and interface science* **2004,** *277* (1), 62-70.

129. Miano, F.; Bailey, A.; Luckham, P. F.; Tadros, T. F., Adsorption of poly(ethylene oxide)—poly(propylene oxide) ABA block copolymers on carbon black and the rheology of the resulting dispersions. *Colloids and Surfaces* **1992,** *68* (1), 9-16.

130. Neumann, B.; Vincent, B.; Krustev, R.; Müller, H.-J., Stability of Various Silicone Oil/Water Emulsion Films as a Function of Surfactant and Salt Concentration. *Langmuir : the ACS journal of surfaces and colloids* **2004,** *20* (11), 4336-4344.

131. Powell, K. C.; Damitz, R.; Chauhan, A., Relating emulsion stability to interfacial properties for pharmaceutical emulsions stabilized by Pluronic F68 surfactant. *International journal of pharmaceutics* **2017,** *521* (1-2), 8-18.

132. Akay, G., Sustainable Ammonia and Advanced Symbiotic Fertilizer Production Using Catalytic Multi-Reaction-Zone Reactors with Nonthermal Plasma and Simultaneous Reactive Separation. *ACS Sustainable Chemistry & Engineering* **2017,** *5* (12), 11588-11606.

133. Bernardo, F. P.; Saraiva, P. M., Integrated process and product design optimization: a cosmetic emulsion application. In *Computer Aided Chemical Engineering*, Puigjaner, L.; Espuña, A., Eds. Elsevier: 2005; Vol. 20, pp 1507-1512.

134. Yorgancioglu, A.; Bayramoglu, E. E., Production of cosmetic purpose collagen containing antimicrobial emulsion with certain essential oils. *Industrial Crops and Products* **2013,** *44*, 378-382.

135. Sadurní, N.; Solans, C.; Azemar, N.; García-Celma, M. J., Studies on the formation of O/W nano-emulsions, by low-energy emulsification methods, suitable for pharmaceutical applications. *European Journal of Pharmaceutical Sciences* **2005,** *26* (5), 438-445.

136. Friedman, D. I.; Schwarz, J. S.; Weisspapir, M., Submicron emulsion vehicle for enhanced transdermal delivery of steroidal and nonsteroidal antiinflammatory drugs. *Journal of Pharmaceutical Sciences* **1995,** *84* (3), 324-329.

137. McClements, D. J.; Gumus, C. E., Natural emulsifiers - Biosurfactants, phospholipids, biopolymers, and colloidal particles: Molecular and physicochemical basis of functional performance. *Advances in colloid and interface science* **2016,** *234*, 3-26.

138. Liwarska-Bizukojc, E.; Miksch, K.; Malachowska-Jutsz, A.; Kalka, J., Acute toxicity and genotoxicity of five selected anionic and nonionic surfactants. *Chemosphere* **2005,** *58* (9), 1249-53.

139. Pettersson, A.; Adamsson, M.; Dave, G., Toxicity and detoxification of Swedish detergents and softener products. *Chemosphere* **2000,** *41* (10), 1611-1620.

140. Park, S.; Kim, H. H.; Yang, S. B.; Moon, J. H.; Ahn, H. W.; Hong, J., A Polysaccharide-Based Antibacterial Coating with Improved Durability for Clear Overlay Appliances. *ACS applied materials & interfaces* **2018,** *10* (21), 17714-17721.

141. Schmitt, C.; Turgeon, S. L., Protein/polysaccharide complexes and coacervates in food systems. *Advances in colloid and interface science* **2011,** *167* (1-2), 63-70.

142. Aider, M., Chitosan application for active bio-based films production and potential in the food industry: Review. *LWT - Food Science and Technology* **2010,** *43* (6), 837-842.

143. Babak, V.; Lukina, I.; Vikhoreva, G.; Desbrières, J.; Rinaudo, M., Interfacial properties of dynamic association between chitin derivatives and surfactants. *Colloids and Surfaces A: Physicochemical and Engineering Aspects* **1999,** *147* (1), 139-148.

144. Chen, H.; Hu, X.; Chen, E.; Wu, S.; McClements, D. J.; Liu, S.; Li, B.; Li, Y., Preparation, characterization, and properties of chitosan films with cinnamaldehyde nanoemulsions. *Food Hydrocolloids* **2016,** *61*, 662-671.

145. Fu, J.; Ji, J.; Yuan, W.; Shen, J., Construction of anti-adhesive and antibacterial multilayer films via layer-by-layer assembly of heparin and chitosan. *Biomaterials* **2005,** *26* (33), 6684-92.

146. Keresztessy, Z.; Bodnár, M.; Ber, E.; Hajdu, I.; Zhang, M.; Hartmann, J. F.; Minko, T.; Borbély, J., Self-assembling chitosan/poly-γ-glutamic acid nanoparticles for targeted drug delivery. *Colloid and Polymer Science* **2009,** *287* (7), 759-765.

147. Wang, Q. Z.; Chen, X. G.; Liu, N.; Wang, S. X.; Liu, C. S.; Meng, X. H.; Liu, C. G., Protonation constants of chitosan with different molecular weight and degree of deacetylation. *Carbohydrate polymers* **2006,** *65* (2), 194-201.

148. Boddohi, S.; Killingsworth, C. E.; Kipper, M. J., Polyelectrolyte Multilayer Assembly as a Function of pH and Ionic Strength Using the Polysaccharides Chitosan and Heparin. *Biomacromolecules* **2008,** *9* (7), 2021-2028.

149. Han, D. H.; Lee, S. Y.; Hong, W. H., Separation of intracellular proteins from Candida utilis using reverse micelles in a spray column. *Biotechnology Techniques* **1994,** *8* (2), 105-110.

150. Kawai, T.; Hamada, K.; Shindo, N.; Kon-no, K., Formation of AOT Reversed Micelles and W/O Microemulsions. *Bulletin of the Chemical Society of Japan* **1992,** *65* (10), 2715-2719.

151. Friberg, S. E., Interactions of Surfactants with Polymers and Proteins. E.D.Goddard and K.P. Ananthapadmanabhan (eds.), CRC Press, Boca Raton, FL, 1993, pp. 1-427, $169.95. *Journal of Dispersion Science and Technology* **1994,** *15* (3), 399-399.

152. Mafe, S., Estimation of pKa shifts in weak polyacids using a simple molecular model: effects of strong polybases, hydrogen bonding and divalent counterion binding. *Chemical Physics* **2004,** *296* (1), 29-35.

153. Il'ina, A. V.; Varlamov, V. P., Hydrolysis of Chitosan in Lactic Acid. *Applied Biochemistry and Microbiology* **2004,** *40* (3), 300-303.

154. Einbu, A.; Grasdalen, H.; Varum, K. M., Kinetics of hydrolysis of chitin/chitosan oligomers in concentrated hydrochloric acid. *Carbohydrate research* **2007,** *342* (8), 1055-62.

155. Wang, X. Y.; Heuzey, M. C., Chitosan-Based Conventional and Pickering Emulsions with Long-Term Stability. *Langmuir : the ACS journal of surfaces and colloids* **2016,** *32* (4), 929-36.